QUANTISATION ON SPACELIKE HYPERSURFACES IN CURVED SPACETIMES

by

AMJAD PERVEZ

A THESIS

SUBMITTED IN PARTIAL FULFILLMENT OF

THE REQUIREMENTS FOR THE DEGREE OF

DOCTOR OF PHILOSOPHY

IN THE

DEPARTMENT OF MATHEMATICS

QUAID-I-AZAM UNIVERSITY

ISLAMABAD, PAKISTAN

1993

DEDICATED TO

BABA JI

My Parents

My Wife, Brothers, Sisters

My Baby Faiza Amjad

ACKNOWLEDGEMENT

I am most grateful to Almighty Allah, the most Beneficent the Merciful for enabling to me complete the work presented here.

I am extremely obliged to my supervisor, Professor Asghar Qadir, who introduced me to the field of General Relativity. It is due to his able guidance, patience, stimulation and innumerable suggestions that I was able to complete this work. I am also most grateful to Professor D.N.Page for his comments on some work done here. My thanks are also due to A.A.Siddiqui and my other colleagues.

I would like to thank the Pakistan Science Foundation for full financial support under the project PSF/RES/C-QU/Maths.(16). Finally, I thank the Third World Academy of Sciences for assistance under the project TWAS RG MP 890-065 in providing some of the computational facilities and literature used in this thesis.

June, 1993 AMJAD PERVEZ

ABSTRACT

Canonical quantisation on spacelike hypersurfaces to determine the vacuum expectation value of the number operator is discussed here. A brief review of canonical quantisation in different frames is explained in the first chapter.

The foliation of the Schwarzschild spacetime by three different spacelike hypersurfaces is presented in the second chapter. Two of them, constant mean extrinsic curvature and free-fall spacelike hypersurfaces, provide a complete unambiguous foliation of the spacetime while the spacelike hypersurfaces of constant Kruskal-Szekeres time do not. We use the connected spacelike hypersurfaces of constant Kruskal- Szekeres time hypersurfaces only to set up the procedure of canonical quantisation. For the vacuum expectation value of the number operator we use the Bogoluibov transformations and coefficients. A complete discussion of quantisation of scalar fields on the three spacelike hypersurfaces is given in the third chapter. Chapter four consists of a summary of the results obtained and some questions for further investigation.

CONTENTS

	Acknowledgements	iii
	Abstract	iv
	Contents	v
CHAPTER ONE	Introduction	1
	1.1 Black Holes	9
	1.2 Quantisation in Minkowski Spacetime	14
	1.3 Quantisation in Linearly Accelerated Frame	18
	1.4 Hawking Radiations from Black Hole	24
	1.5 Problems with Hawking's Radiation	32
CHAPTER TWO	Foliation of the Schwarzschild Spacetime	38
	2.1 Foliation of the Schwarzschild Spacetime by CKST Hypersurfaces	38
	2.2 K-Surfaces	45
	2.3 ψN-Hypersurfaces	53
CHAPTER THREE	Quantisation of Scalar Fields on Spacelike Hypersurfaces	63
	3.1 The Scalar Field Equation in KS Coordinates	63
	3.2 Quantisation on Spacelike Hypersurfaces	65
	3.3 Quantisation on Spacelike Hypersurfaces of CKST	72

3.4 Quantisation on Spacelike
Hypersurfaces of CMEC 85
3.5 Quantisation on ψN-Hypersurfaces 112
CHAPTER FOUR Conclusion 121
Appendices 126
Appendix A 126
Appendix B 131
Appendix C 133
REFERENCES 135

CHAPTER ONE

INTRODUCTION

At the turn of this century there was one consistent fundamental physical theory (classical physics). With the advent of Einstein there emerged two theories: Relativity and Quantum theory[1]; which seem to be mutually inconsistent. General Relativity (GR) is applicable for high accelerations and the Quantum theory (QT) for sufficiently small sizes and energy/mass changes. Though, up to now, there have not been any situations directly observed where both effects are significant, it is still necessary that these theories of the day, if fundamental, must be made consistent. As a step in this direction, Fulling[2] and Hawking[3] tried to perform some calculations without developing such a consistent theory. This work proved to be pivotal in the development of the theory of quantum fields in curved spacetimes and greatly increased the attention given to this subject by others.

Fulling's[2] was the original novel idea. Instead of trying to quantise GR itself, why not quantise fields in other metrics than the usual, flat, Minkowski spacetime? The simplest attempt would be to quantise a massless scalar field from the point of view of a linearly accelerated

observer. He found an ambiguity in the procedure. The expectation value (EV) of the number operator[4] defined by the accelerated observer in the inertial vacuum was different from that in the Minkowski vacuum. In general it turned out to be fractional. He regarded this result as an indication that the quantisation procedure was inapplicable in general. This calculation will be reviewed and discussed in more detail in §.1.3.

Hawking[5] quantised a massless scalar field in a Schwarzschild background. He found that the Schwarzschild vacuum appears non-empty to a Minkowski observer, corresponding to the observer at infinity, far away from the black hole (BH). He concluded that there was radiation coming from the surface of the Schwarzschild BH. Already, Bekenstein[6] had suggested that entropy could be assigned to a BH. Hawking found black body radiation coming from the BH at a temperature proportional to the surface gravity of the BH. This seemed to fit very well with Bekenstein's proposal. This calculation will be reviewed and discussed in more detail in §.1.4.

Another view was proposed by Padmanabhan[7]. He argued that the energy calculated by Fulling should not be regarded as radiation but as the response of the detector to acceleration. This proposal would suggest that the analysis by Hawking again gives the response of the

detection device to the acceleration associated with a fixed frame in the presence of a gravitational source. This interpretation would avoid various odd features[8] of Hawking radiation, to be discussed in §.1.5. For completeness it should be mentioned that the matter was also very thoroughly investigated by Unruh[9], who had not reached the same conclusion as Padmanabhan.

The observer-dependence of Hawking radiation is a source of worry for believing it to be a genuine physical effect. If it disappears in some frame and appears in another, according to some observers the BH should never evaporate while according to others it could evaporate arbitrarily fast. *How fast or slow* it disappears can be expected to be observer-dependent, but not *whether* it does so. Ofcourse there is no rigorous calculation demonstrating that Hawking radiation disappears in any frame. It can be naively argued that a freely falling observer sees a Minkowski spacetime around him and hence should see no Hawking radiation. This is not necessarily a valid argument. QT being non-local, the fact that the spacetime is *locally* Minkowski cannot be used to deduce that there will be no effects of the spacetime curvature. More concretely, the wave functions to be used are defined over all space and not only at a point. As such, it is necessary to actually perform the calculation and check whether there

will be Hawking radiation in a free fall frame or not. The procedure we adopt here is that used by Fulling[2]. Ideally we should have used the more flexible path integral formalism of Dirac[10] and Feynmann[11], but that has been left for subsequent investigation. The usual canonical quantisation procedure is simpler and more transparent. It also connects with other work done on observer-dependent quantisation. As such it seems preferable for use initially.

Following the procedure of Fulling various frames in Minkowski spacetime were investigated[12]. A generic feature appeared to be that there was no change in the EV of the number operator for those frames in which there is no event horizon, while a change was found in all cases where there is an event horizon.

Floyd and Penrose[13] demonstrated that while classical black holes (BHs) can not emit any energy some energy *can* be extracted from the environs a rotating BH. A particle sent into the ergosphere of the BH with an angular momentum opposite to that of the hole could come out with more energy than it takes in. This is achieved by the particle emitting a part which locally appears to have positive energy but from far away appears to have negative energy. This mechanism for energy extraction can also be understood in terms of an analogue of the Casimir effect[14], in which

two conducting plates brought close together attract each other with a force proportional to the inverse fourth power of the distance between them. (The Casimir effect is explained as being due to vacuum polarisation.)

Misner[15] argued that certain modes of the fields (in the quantum mechanical sense) are amplified by carrying away some rotational energy of the BH. He called this phenomenon "superradiance". It is the wave mechanical analogue of the Penrose[13] process. A qualitative explanation and prediction of this effect was given by Zel'dovich[16]. He and Starobinsky[17] argued that in a quantum field theory there should be spontaneous creation of particles in these superradiant modes. This expectation was confirmed by Unruh[9] by explicit calculations. Hawking showed that Unruh's result for a pre-existing BH is consistent with a limiting case of his, (Hawking's) results. Gibbons[18] performed a similar calculation to Unruh's for a charged BH.

Letaw and Pfautsch[19] demonstrated that for rotating coordinates the vacuum expectation value (VEV) of the number operator remains zero while the superradiant modes are modified. As such they disproved the conjecture that superradiance gives the same effect as the change of VEV of the number operator. It is possible that the superradiance effect is related to the response of the detector to

acceleration, as argued by Padmanabhan[7]. This conjecture would need to be investigated more thoroughly. In this thesis we will restrict our attention to the modification of the VEV of the number operator, leaving the phenomenon of superradiance for later investigation.

Hawking used null hypersurfaces in the quantisation procedure. We will quantise scalar fields (even allowing massive fields) on spacelike hypersurfaces (SHs) which are complete and foliate the spacetime. These hypersurfaces are smooth and pass through the event horizon. We use Kruskal-Szekeres (KS) coordinates[20] which avoid the coordinate singularity at the event horizon for the Schwarzschild metric. The SH of constant KS time (CKST) are the simplest[21] for calculational purposes. However, the set we consider does not completely foliate the spacetime. We consider only the CKST hypersurfaces which do not hit the singularity at $r = 0$. In the region $-1 < v < 1$, the hypersurfaces are complete and pass through the event horizon avoiding the singularity. Notice that they are asymptotically flat in that their mean extrinsic curvature (MEC) and intrinsic curvature scalar tend to zero as r tends to infinity. In §.2.1 we will discuss the foliation of the spacetime by the SH of CKST while §.3.3 deals with the quantisation of massive scalar fields on those hypersurfaces which lie inside the region $-1 < v < 1$. The

quantisation procedure shows that the VEV of the number operator remains zero. This is not to say that the VEV of the number operator quantised on the hypersurfaces for $|v| \geq 1$ must be zero.

Brill, Cavallo and Isenberg[22] numerically demonstrated that K-surfaces (surfaces of constant MEC) foliate the Schwarzschild spacetime and asymptotically tend to hyperboloids, avoiding the singularity at r = 0. Also, K-surfaces must be flat at the throat of the Einstein-Rosen bridge[23]. This foliation of the spacetime is particularly adapted to studying radiation problems and the regions for large curvature in a more general asymptotically flat spacetime. K-surfaces are also interesting because these hypersurfaces have constant York time[24], which advances steadily from one hypersurface to the next. These hypersurfaces are determined[25] by a variational principle and will be discussed in §.2.2. In §.3.4 the scalar fields have been quantised on K-surfaces of the Schwarzschild geometry in KS coordinates. The quantisation procedure shows[26] that the VEV of the number operator remains zero.

The next example we consider is designed to test the conjecture that there will be no change in the VEV of the number operator seen by freely falling observers. It has been separately argued[27] that there is a physically

'preferred' frame, called the pseudo-Newtonian (ψN) frame, corresponding to an observer falling freely from infinity. The ψN-hypersurfaces correspond to the rest frames of a special class of freely falling observers[28] on whose geodesics the "energy at infinity" equals the "rest mass at infinity" and there is no angular momentum at infinity. The ψN-hypersurface is defined to be orthogonal to the geodesic of such observers at every point. The description of this hypersurface in Schwarzschild coordinates breaks down at r=2m. Ofcourse the hypersurface described must pass through the horizon even though its description in Schwarzschild coordinates breaks down there. For the quantisation of the scalar fields on ψN-hypersurfaces the requirement is that they provide a complete foliation of the spacetime. It has been verified[29] that these hypersurfaces have zero Riemanian curvature everywhere! The MEC tend to infinity at the singularity only. These hypersurfaces provide a complete foliation of the Schwarzschild spacetime by hypersurfaces that run into the singularity. A complete discussion of the foliation will be given in §.2.3. The usual quantisation procedure which will be discussed in §.3.5, shows that the VEV of the number operator remains zero.

A review of the earlier work introducing BHs and quantisation in Minkowski spacetime is provided in the rest

of this chapter. Chapter four contains a brief summary and discussion of the work.

1.1. Black Holes

An object from which not even light can escape but which can pull in the other objects (due to its gravitational attraction) is called a BH. It can be seen that in the Schwarzschild solution of Einstein's equations, $r = 2m$ is the distance at which the escape velocity becomes the velocity of light. Notice that the Schwarzschild metric becomes singular at $r = 0$ and $r = 2m$. The former is an essential singularity and the latter a coordinate singularity. $r = 2m$ is called the Schwarzschild radius. By calculating the curvature invariants,

$$R_1 = R_{\mu\nu}{}^{\mu\nu},$$
$$R_2 = R_{\mu\nu}{}^{\rho\pi} R_{\rho\pi}{}^{\mu\nu}, \qquad (1.1.1)$$

etc., where $R^{\mu}{}_{\nu\rho\pi}$ the Riemanian tensor, it can be verified that there is no essential singularity at $r = 2m$, and R_1, R_2, ... remain finite there. Hence it is called a coordinate singularity. At $r = 0$ the Schwarzschild metric displays an essential singularity, in that the second and third curvature invariants become infinite there.

Kruskal and Szekeres[20] independently developed a better behaved coordinate system. This coordinate system changes (t,r) to (v,u), while θ and ϕ are unchanged. These

coordinates avoid the problem of a coordinate singularity at r = 2m. There are four regions of the (v,u) plane, which could be denoted by I, II, III and IV (see Fig.1.) i.e.

$$\text{I}\quad\begin{cases}(r \geq 2m,\ u \geq 0)\\ u = (r/2m - 1)^{1/2}\, exp(r/4m)\, cosh(t/4m)\\ v = (r/2m - 1)^{1/2}\, exp(r/4m)\, sinh(t/4m)\end{cases},$$

$$\text{II}\quad\begin{cases}(r \leq 2m,\ v \geq 0)\\ u = (1 - r/2m)^{1/2}\, exp(r/4m)\, sinh(t/4m)\\ v = (1 - r/2m)^{1/2}\, exp(r/4m)\, cosh(t/4m)\end{cases}, \qquad (1.1.2)$$

$$\text{III}\quad\begin{cases}(r \geq 2m,\ u \leq 0)\\ u = -(r/2m - 1)^{1/2}\, exp(r/4m)\, cosh(t/4m)\\ v = -(r/2m - 1)^{1/2}\, exp(r/4m)\, sinh(t/4m)\end{cases},$$

$$\text{IV}\quad\begin{cases}(r \leq 2m,\ v \leq 0)\\ u = -(1 - r/2m)^{1/2}\, exp(r/4m)\, sinh(t/4m)\\ v = -(1 - r/2m)^{1/2}\, exp(r/4m)\, cosh(t/4m)\end{cases}.$$

For the inverse transformations, t, r given by

$$t = \begin{cases}4m\ tan^{-1}(v/u), & \text{(in regions I and III)}\\ 4m\ tan^{-1}(u/v), & \text{(in regions II and IV)}\end{cases}, \qquad (1.1.3)$$

and

$$u^2 - v^2 = (r/2m - 1)exp(r/2m), \qquad (1.1.4)$$

in all regions. Notice that in KS coordinate system, the singularity at r = 0 is located at

$$v^2 - u^2 = 1, \qquad (1.1.5)$$

and hence there are actually two spacelike singularities at

$$v = \pm\,(1 + u^2), \qquad (1.1.6)$$

corresponding to r = 0, one (−) a past singularity and the

other (+) a future singularity.

Notice that $r \geq 2m$ is given by $u^2 \geq v^2$ i.e. there are two exterior regions; both $u \geq +|v|$ and $u \leq -|v|$ correspond to $r \geq 2m$. Similarly, $r \leq 2m$ is given by $v^2 \geq u^2$ showing

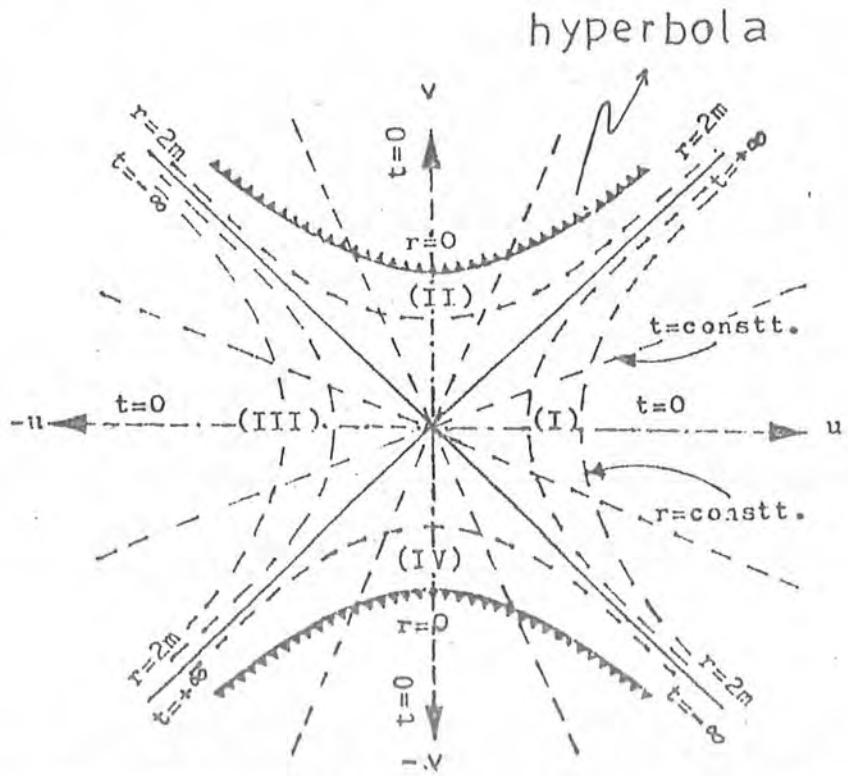

Figure 1. The Schwarzschild geometry represented in KS coordinates. Four disjoint Schwarzschild coordinate patches give regions I, II, III and IV of the Schwarzschild geometry, whereas a single connected KS coordinate system suffices. In the u,v-plane, curves of constant r are hyperbolae with asymptotes $u = \pm v$, while curves of constant t are straight lines through the origin.

two interior regions; both $v \geq +|u|$ and $v \leq -|u|$ correspond to $r \leq 2m$.

Nevertheless the sphere $r = 2m$ is physically very special. It is a null surface in that all vectors on the surface are null vectors and a geodesics with a null tangent vector lying on this surface will continue to lie on it. It is a trapped surface in that all regions interior to this surface have geodesics that cannot emerge out. It is also a red shift horizon (on account of the infinite red shift at $r = 2m$) and hence it is an event horizon.

For asymptotically flat spacetimes the asymptotic forms of the fields at infinity can be examined. Penrose[30] developed a powerful mathematical technique for studying the asymptotic properties of spacetime. This technique is a conformal transformation of spacetime, which brings infinity to a finite value and thereby converts asymptotic calculations at infinity to finite calculations. This technique also provides rigorous definitions of several types of infinity (timelike, null and spacelike) that one encounters in asymptotically flat spacetime.

In visualizing the asymptotic structure of spacetime, here we considered the KS coordinates that attribute finite coordinate values to infinity. We will replace[31] the KS coordinates (v,u,θ,ϕ) for the Schwarzschild background by new coordinates (ψ,ξ,θ,ϕ)

$$\left.\begin{aligned} v + u &= \tan\left(\frac{\psi + \xi}{2}\right), \\ v - u &= \tan\left(\frac{\psi - \xi}{2}\right), \end{aligned}\right\} \tag{1.1.7}$$

and

$$\left.\begin{aligned} v^2 - u^2 &= \left(1 - \frac{r}{2m}\right)\exp\left(\frac{r}{2m}\right) \\ &= \tan\left(\frac{\psi + \xi}{2}\right)\ \tan\left(\frac{\psi - \xi}{2}\right)\ . \end{aligned}\right\} \tag{1.1.8}$$

The resulting coordinate diagram (see Fig.2.) depicts clearly the causal connections between the horizons, the singularities and various regions of infinity.

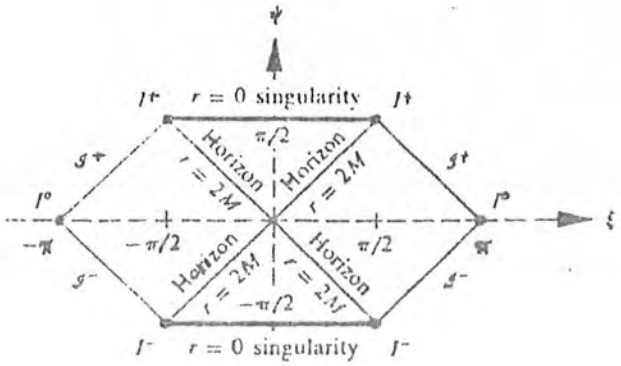

Figure 2. Schwarzschild spacetime as depicted in the ψ, ξ, θ, ϕ coordinates of Eqs.(1.1.7) and (1.1.8). This diagram should be compared with the KS coordinate diagram (Fig.1). This is called the Penrose diagram for the Schwarzschild geometry. Here the points I^- and I^+ are past and future time-like infinity respectively, while I^o is spacelike infinity. The edges $\mathscr{I}^-$ and $\mathscr{I}^+$ are past and future null infinity, respectively.

1.2. Quantisation in Minkowski Spacetime

The usual quantisation procedure adapted is for a scalar field Φ with the Lagrangian[32] density

$$\mathcal{L} = \frac{1}{2}\sqrt{|g|}(g^{\mu\nu}\Phi_{,\mu}\Phi_{,\nu} - M^2\Phi^2), \quad \mu,\nu=0,1,2,\ldots n \tag{1.2.1}$$

where "$,\mu$" denotes partial differentiation relative to x^{μ}, M is the mass of the quantised field, $g_{\mu\nu}$ are the metric coefficients, $g = \det(g_{\mu\nu})$ and it, therefore, satisfies the Klein-Gordon (KG) equation[4]

$$(\Box + M^2)\,\Phi = 0, \tag{1.2.2}$$

where the operator $\Box$ is

$$\Box \equiv \frac{1}{\sqrt{|g|}}\,\frac{\partial}{\partial x^{\mu}}\left(g^{\mu\nu}\sqrt{|g|}\,\frac{\partial}{\partial x^{\nu}}\right). \tag{1.2.3}$$

In this section, we will discuss quantisation in Minkowski spacetime. For Minkowski spacetime in n-dimensional cartesian coordinates, one solution mode of Eq.(1.2.2) is

$$U_k(t,x) = A\,\exp(ik\cdot x - i\omega t), \tag{1.2.4}$$

where

$$\omega = \sqrt{M^2+k_1^2+k_2^2+\ldots+k_n^2}\,, \quad -\infty < k_i < \infty, \quad (i=1,2,\ldots,n)$$

and A is a constant of integration. It can be obtained from the normalisation condition

$$(\psi_1,\psi_2) = -i\int_{\Sigma}\psi_2(x)\overleftrightarrow{f^{\mu}}\psi_2^{*}(x)\;d\Sigma_{\mu}, \tag{1.2.5}$$

where

$$\overleftrightarrow{f^{\mu}} = g^{\mu\nu}\sqrt{|g|}\,\frac{\overrightarrow{\partial}}{\partial x^{\nu}} - \frac{\overleftarrow{\partial}}{\partial x^{\nu}}\,g^{\mu\nu}\sqrt{|g|}\,, \tag{1.2.6}$$

$d\Sigma_{\mu} = n_{\mu}\,d\Sigma$ with n^{μ} a future-directed unit vector orthogonal

to the SH Σ, $d\Sigma$ is the volume element in Σ and '*' denotes the complex conjugate. Using Eq.(1.2.5) for Minkowski spacetime, Eq.(1.2.4) reduces to

$$U_k(t,x) = \frac{1}{\sqrt{2\omega\ (2\pi)^{n-1}}}\ exp(ik\cdot x - i\omega t). \qquad (1.2.7)$$

The solution given by Eq.(1.2.7) satisfies the orthonormality conditions

$$\left.\begin{aligned}(U_k,\ U_{k'}) &= \delta^{n-1}_{kk'}\ ,\\ (U_k,\ U^{*}_{k'}) &= 0\ .\end{aligned}\right\} \qquad (1.2.8)$$

$\delta^{n-1}_{kk'}$ being the $(n-1)$-dimensional Kronecker delta, $\delta_{k_1k'_1}\delta_{k_2k'_2}\delta_{k_3k'_3}\cdots\delta_{k_{n-1}k'_{n-1}}$.

For canonical quantisation, the scalar field Φ is treated as an operator with the following equal time commutation relations

$$\left.\begin{aligned}[\Phi(t,x),\ \Pi(t,x')] &= i\ \delta^{n-1}(x-x'),\\ [\Phi(t,x),\ \Phi(t,x')] &= 0 = [\Pi(t,x),\ \Pi(t,x')],\end{aligned}\right\} \qquad (1.2.9)$$

$\delta^{n-1}(x-x')$ being the $(n-1)$-dimensional Dirac delta function, where $\Pi(t,x)$ is the canonically conjugate momentum defined by

$$\Pi(t,x) = \frac{\partial L}{\partial(\partial_o\Phi)} = \sqrt{|g|}\ g^{oo}\partial_o\Phi\ , \qquad (1.2.10)$$

where ∂_μ stands for $\partial/\partial x^\mu$ in general and ∂_o for $\partial/\partial x^o$ in particular. For the Minkowski spacetime, the field modes (1.2.7) and their respective complex conjugates form a complete orthonormal basis with scalar product (1.2.5), so Φ may be expanded as

$$\Phi(t,x) = \sum_k [a_k\, U_k(t,x) + a_k^\dagger\, U_k^*(t,x)], \qquad (1.2.11)$$

where $a_k^\dagger$ is the Hermitian conjugate of a_k . The equal time commutation relations for Φ and Π are then equivalent to

$$\left.\begin{aligned} &[a_k,\ a_{k'}] = 0 = [a_k^\dagger,\ a_{k'}^\dagger], \\ &[a_k,\ a_{k'}^\dagger] = \delta_{kk'}. \end{aligned}\right\} \qquad (1.2.12)$$

The operator a_k reduces the number of quanta in mode k by one, while $a_k^\dagger$ increases this number by one. Thus a_k and $a_k^\dagger$ are referred to as annihilation and creation operators respectively.

Now, consider a second complete orthonormal set of modes $\bar{U}_j(t,x)$. The field Φ may be expanded in this set also as

$$\Phi(t,x) = \sum_j [\bar{a}_j\, \bar{U}_j(t,x) + \bar{a}_j^\dagger\, \bar{U}_j^*(t,x)], \qquad (1.2.13)$$

such that $\bar{a}_j^\dagger$ and $\bar{a}_j$ satisfies the relations (1.2.12). Since both sets of modes $U_k(t,x)$ and $\bar{U}_j(t,x)$ are complete, therefore the new mode $\bar{U}_j(t,x)$ can be expanded in terms of the old mode $U_k(t,x)$ as

$$\bar{U}_j(t,x) = \sum_k [\alpha_{jk}\, U_k(t,x) + \beta_{jk}\, U_k^*(t,x)]. \qquad (1.2.14)$$

Similarly,

$$U_k(t,x) = \sum_j [\alpha_{jk}^*\, \bar{U}_j(t,x) - \beta_{jk}\, \bar{U}_j^*(t,x)]. \qquad (1.2.15)$$

where α_{jk} and β_{jk} are known as the Bogoluibov coefficients and the relations (1.2.14) and (1.2.15) are Bogoluibov transformations such that

$$\left.\begin{aligned} \sum_k (\alpha_{ik}\,\alpha^*_{jk} - \beta_{ik}\,\beta^*_{jk}) &= \delta_{ij}\ , \\ \sum_k (\alpha_{ik}\,\beta_{jk} - \beta_{ik}\,\alpha_{jk}) &= 0\ . \end{aligned}\right\} \qquad (1.2.16)$$

Now, by using Eqs.(1.2.8) and (1.2.14) the Bogoluibov coefficients can be evaluated as

$$\alpha_{kk'} = (\bar{U}_k,\ U_{k'}),\quad \beta_{kk'} = -(\bar{U}_k,\ U^*_{k'}). \qquad (1.2.17)$$

By equating the expansions (1.2.11) and (1.2.13) and using Eqs.(1.2.14) and (1.2.15), one obtains

$$a_k = \sum_j [\alpha_{jk}\,\bar{a}_j + \beta^*_{jk}\,\bar{a}^\dagger_j], \qquad (1.2.18)$$

$$\bar{a}_j = \sum_k [\alpha^*_{jk}\,a_k - \beta^*_{jk}\,a^\dagger_k]. \qquad (1.2.19)$$

From Eq. (1.2.18), it follows that in general $\beta_{jk} \neq 0$, because the modes $U_k(t,x)$ and $\bar{U}_j(t,x)$ are different. Infact, the VEV of the number operator $N = \sum N_k = \sum a^\dagger_k a_k$ for the $U_k(t,x)$-mode particles in the new vacuum state $|\bar{0}\rangle$ is

$$\langle\bar{0}|N|\bar{0}\rangle = \sum_j |\beta_{jk}|^2, \qquad (1.2.20)$$

which means that the vacuum of $\bar{U}_j(t,x)$ modes contains $\sum_j |\beta_{jk}|^2$ particles in the $U_k(t,x)$ mode.

For the Minkowski spacetime, Eqs. (1.2.17) give

$$\alpha_{kk'} = \delta_{kk'}\ ,\ \beta_{kk'} = 0. \quad (\forall\ k,\ k') \qquad (1.2.21)$$

Thus Eq.(1.2.20) gives a zero VEV of the number operator, i.e. $\bar{U}_j(t,x)$ modes does not contain any particles in the $U_k(t,x)$ modes.

1.3. Quantisation in Linearly Accelerated Frame

The procedure Fulling[2] adopted was first to consider a Riemanian manifold of dimension n=s+1 with metric tensor $g_{ab}(a,b=0,1,2,\ldots,n)$. The components g_{ab} are independent of the time coordinate x^0 and $g_{0j} = 0$, $(j=1,2,\ldots,s)$. For the static metric Eq.(1.2.2) can be solved by separation of variables. On substituting with $t = x^0$, $x = (x^1,x^2,\ldots,x^s)$

$$\Phi(t,x) = \psi_j(x)\ exp(\pm iE_j t) \tag{1.3.1}$$

into Eq.(1.2.2) one obtains the eigenvalue equation

$$\begin{aligned} |g|^{-1/2} g_{00}\partial_l(|g|^{1/2} g^{lk}\partial_k\psi_j) + g_{00}M^2\psi_j &\equiv K\psi_j \\ &= E_j^2\psi_j, \end{aligned} \tag{1.3.2}$$

where the differential operator K is Hermitian with respect to the scalar product,

$$(F_1, F_2) = \int |g|^{1/2} g^{00} F_1^*(x)\ F_2(x)\ d^s x \tag{1.3.3}$$

and is positive. Thus all E_j^2 are positive. If a solution of Eq.(1.2.2) is uniquely determined throughout the region covered by the coordinate system by the values of $\Phi(t,x)$ and $\Pi(t,x)$ on any given hypersurface t = constant, then K will be essentially self adjoint, where $\Pi(t,x)$ is given by Eq.(1.2.10).

Fulling classified the numbers in the spectrum as the point spectrum σ_p or continuous spectrum σ_c (or both) that correspond to a set of generalized eigenfunctions. Thus an arbitrary function defined by Eq.(1.3.3) can be expanded as

$$F(x) = \int d\mu(E_j)\ \hat{f}(E_j)\ \psi_j(x)\ , \tag{1.3.4}$$

where $\psi_j(x)$ be the solution of Eq.(1.3.2), μ is a measure such that Eq.(1.3.2) becomes

$$(F_1,F_2) = \int d\mu(E_j)\ \hat{f}_1^*(E_j)\ \hat{f}_2(E_j)\ ,$$
$$= \int d\mu(E_j)\ \hat{f}_1^*(j)\ \hat{f}_2(j) \qquad (E_j = j), \qquad (1.3.5)$$

and for the normalisation of eigenfunctions

$$d\mu(j) \equiv \sum_{j\in\sigma_p} + \int_{\sigma_c} dj\ .$$

Thus Eqs.(1.3.3) and (1.3.5) leads to the orthonormality conditions such that

$$\left.\begin{aligned} &\int d^3x\,|g|^{1/2}\,g^{00}\,\psi_j^*(x)\,\psi_k(x) = \delta(j,k)\ , \\ &\int d\mu(j)\,\psi_j^*(x)\,\psi_j(y) = (|g|^{1/2}\,g^{00})^{-1}\delta(x-y), \end{aligned}\right\} \qquad (1.3.6)$$

where

$$\int d\mu(k)\,\delta(j,k)\,\hat{f}(k) = \hat{f}(j)\ .$$

The general solution of Eq.(1.2.2) is therefore,

$$\Phi(t,x) = \int \frac{d\mu(j)}{(2E_j)^{1/2}} [a_j\psi_j(x)\exp(-iE_jt) + a_j^\dagger\psi_j(x)\exp(-iE_jt)], \qquad (1.3.7)$$

where a_j and $a_j^\dagger$ are the annihilation and creation operators satisfying the relations (1.2.12). The number operator has the natural interpretation as the observable "number of particles in the state j". Fulling pointed out that a crucial element in this whole construction is unambiguous division of the solutions of Eq.(1.2.2) into positive frequency and negative frequency functions, with temporal behavior of the type $\exp(-E_jt)$ and $\exp(+E_jt)$, respectively. But single particle wave functions are restricted to have

positive frequency.

Fulling applied the above general quantisation procedure to two-dimensional spacetime. He considered $x^0 = v$ $(-\infty < v < \infty)$ and $x^1 = z$ $(0 < z < \infty)$ with the metric coefficients

$$g_{oo} = z^2, \; g_{11} = -1, \; g_{o1} = 0. \tag{1.3.8}$$

Therefore, Eq.(1.3.2) reduces to the form

$$(z^2\frac{d^2}{dz^2} + z\frac{d}{dz} - M^2z^2 + E_j^2)\psi_j(z) = 0, \tag{1.3.9}$$

which is a Bessel equation, whose solution is given by Titchmarsch[33]. The spectrum of E_j^2 extends from 0 to $+\infty$. The normalised solutions of Eq.(1.3.9) are

$$\psi_j(z) = \pi^{-1}\{2j \sinh(\pi j)\}^{1/2} K_{ij}(Mz), \tag{1.3.10}$$

where K_{ij} is the Macdonald (modified Bessel) function of imaginary order.

The expansion of the field $\Phi(v,z)$ in annihilation and creation operators is

$$\Phi(v,z) = \int_o^\infty \frac{dj}{(2j)^{1/2}} \psi_j(z)[a_j exp(-ijv) + a_j^\dagger exp(+ijv)], \tag{1.3.11}$$

and the canonically conjugate momentum

$$\Pi(v,z) = \frac{1}{z}\frac{\partial\Phi}{\partial v}. \tag{1.3.12}$$

Eqs.(1.3.6), (1.3.11) and (1.3.12) yields

$$a_j = 2^{-1/2}[j^{1/2}\int_o^\infty \frac{dz}{z} \psi_j(z) \Phi(0,z) + ij^{-1/2}\int_o^\infty dz \; \psi_j(z) + \Pi(0,z)]. \tag{1.3.13}$$

The spacetime with the metric defined by Eq.(1.3.8), is merely the flat spacetime in the unusual coordinates

$$z = \pm \sqrt{x^2 - t^2} \quad , \quad v = \tanh^{-1}(x/t),$$

or

$$t = z \sinh v, \quad x = z \cosh v. \tag{1.3.14}$$

This spacetime can be identified with the region $\{(t,x);\ |t| < x\}$ in two-dimensional Minkowski spacetime (see Fig.3.). The coordinates v, z are called Rindler[34] coordinates and this region is called the Rindler wedge. Rindler argued that this system of coordinates is very similar to the relation between Schwarzschild and KS coordinates for the space surrounding an isolated point mass. Translation in the coordinate v, with z fixed, corresponds to a homogeneous Lorentz transformation in (t,x) space. It is easy to see geometrically that the classical problem should be well-posed for initial data on any v = constant hypersurface.

For $u = \ln z$, Eq.(1.3.9) becomes

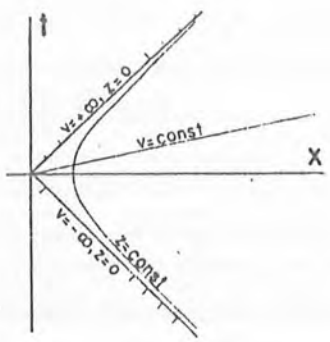

Figure 3. This digram shows that the Rindler coordinates in the Minkowski spacetime gives the flat space.

$$-\frac{d^2\psi_j}{du^2} + exp(2u)\ \psi_j = j^2\psi_j \ , \qquad (1.3.15)$$

where $\psi_j = \psi_j\{exp(u)\}$. This equation was solved numerically (see Fig.4.) in a way consistent with the transcription of path in Cartesian coordinates into the Rindler system (see Fig.5.). It is a physically reasonable description of free particles for large j.

Fulling considered the relativistic theory of free particles. The expansion of the free field at t = 0 and its conjugate momentum are

$$\left.\begin{aligned}\Phi(0,x) &= \int_0^\infty \frac{dk}{(4\pi\omega_k)^{1/2}}\,[\bar{a}_k exp(i\omega_k x) + \bar{a}_k^\dagger exp(-i\omega_k x)]\,,\\ \Pi(0,x) &= \int_0^\infty \frac{-i\ dk}{(4\pi\omega_k^{-1})^{1/2}}[\bar{a}_k exp(i\omega_k x) - \bar{a}_k^\dagger exp(-i\omega_k x)]\,,\end{aligned}\right\} \qquad (1.3.16)$$

where $\omega_k = \sqrt{k^2+M^2}$ and $\bar{a}_k$ and $\bar{a}_k^\dagger$ are the new annihilation and creation operators. The conjugate momentum defined relative to the two coordinate systems are related by

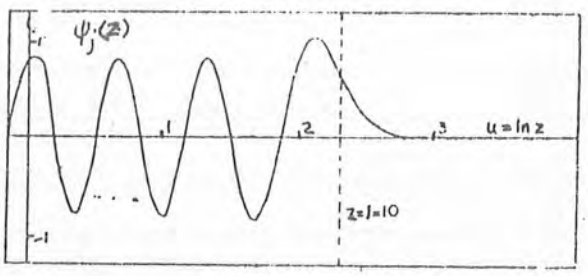

Figure 4. The eigenfunction $\psi_j(z)$ are shown in this diagram. Notice that for $j > 10$, this function tends to zero as $u = \ln z$ tends to infinity.

$$\Pi(0,z) = \frac{1}{z}\frac{\partial\Phi(0,z)}{\partial v} = \frac{\partial\Phi(0,x)}{\partial t} = \Pi(0,x). \qquad (1.3.17)$$

Eqs.(1.3.13) and (1.3.16) gives

$$a_j = \int_{-\infty}^{\infty} dk\ U(E_j,\omega_k)\bar{a}_k + \int_{-\infty}^{\infty} dk\ V(E_j,\omega_k)\bar{a}_k^{\dagger}\ , \qquad (1.3.18)$$

where

$$\left.\begin{aligned} U(E_j,\omega_k) &= [2\pi\omega_k\{1-exp(-2\pi j)\}]^{-1/2} \\ &\quad \times \left(\frac{\sqrt{k^2+M^2}+k}{M}\right)^{ij} = U(j,k), \\ V(E_j,\omega_k) &= [2\pi\omega_k\{exp(2\pi j)-1\}]^{-1/2} \\ &\quad \times \left(\frac{\sqrt{k^2+M^2}+k}{M}\right)^{ij} = V(j,k). \end{aligned}\right\} \qquad (1.3.19)$$

Fulling pointed out that the kernel V(j,k) does not vanish, so that a_j includes creation operator $\bar{a}_k^{\dagger}$. Also, a

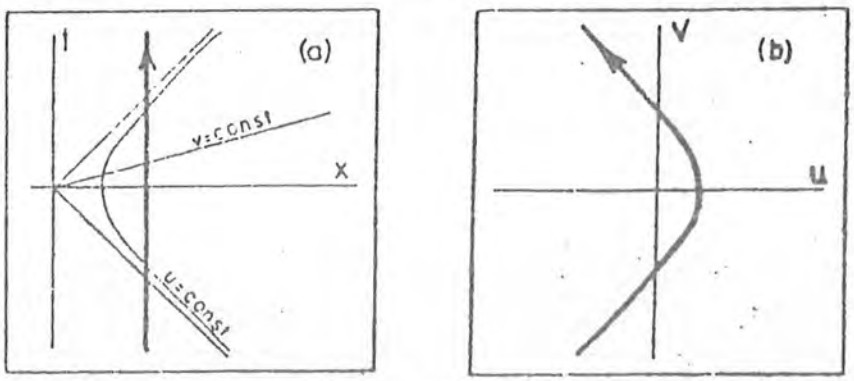

Figure 5. The trejectory of a free particle in flat space is presented in both: (a) Cartesian coordinates and (b) Rindler coordinates. In Cartesian coordinates the incident wave packet is consistent with the straight particle path while in the Rindler coordinate the packet incident from the left (large negative u) scatters and returns to the left.

vector which is annihilated by $\bar{a}_k$ is not annihilated by a_j and vice versa. He concluded that the vacuum of the Rindler space is not an ordinary vacuum of the free field, and hence the notion of a particle is completely different in both spaces. Thus the ambiguity affects the definition of the energy momentum tensor, the principle observable of the system in a gravitational context. These observations have serious implications for the quantum field theory of matter near the horizon of the Schwarzschild solution.

1.4. Hawking Radiation From Black Hole

The quantisation of fields in curved spacetimes background leads to some counter-intuitive results. It is necessary to explain what led to their being taken seriously. For this purpose it is necessary to give a brief explanation of BH thermodynamics. The idea of thermodynamics in the context of BHs was first considered by Greif[35], but he did not make a concrete proposal in BH physics. Later, Carter[36] re-derived the result of Christodolou[37] that the irreducible mass of a Kerr BH is unchanged by considering reversible transformations for BHs. He demonstrated the possibilities inherent in the use of thermodynamic arguments in BH physics. Christodolou's result implies that the BH area increases in most processes and it supports the conjecture of the Floyd and Penrose[13].

Hawking[38] has given a general proof that the BH surface area can not decrease in any process by a radically different approach from Christodolou. Hawking shows that for a system of several BHs, the area of each individual BH can not decrease. Further, when two BHs merge, the area of the resulting BH can be greater but not smaller than the sum of the initial areas. The limitation of non-decreasing surface area of a BH is reminiscent of the second law of thermodynamics. Noting that the BH area can not decrease and basing his arguments on "information loss" in absorption by BHs, Bekenstein[6] proposed an identification of the BH area with entropy. The arguments showed that even though entropy may appear to decrease if thermal energy is absorbed from its surroundings by a BH, there is an increase in the area which cancels the maximum decrease obtainable. Corresponding to this entropy there has to be a 'temperature' for the BH which is proportional to the surface gravity of the BH.

Hawking[5] considered a non-rotating uncharged BH, which is represented by the Schwarzschild metric

$$ds^2=(1-\frac{2m}{r})dt^2-(1-\frac{2m}{r})^{-1}dr^2-r^2(d\theta^2+\sin^2\theta d\phi^2), \qquad (1.4.1)$$

where the apparent singularities at r = 2m are fictitious, arising merely from a bad choice of coordinates. A global structure of the analytically extended Schwarzschild solution can be described by a Penrose diagram[39] (see

Fig.2.).

Most of the Penrose diagram is not, infact, relevant to a BH formed by collapse, since the metric is that of the Schwarzschild solution only in the region outside the collapsing matter and only in the asymptotic region. In the case of exactly spherical collapse the metric is exactly the Schwarzschild metric every where out side the surface of the collapsing object which is represented by a timelike geodesic in the Penrose diagram (see Fig.6.). Inside the object the metric is completely different, the past event horizon, the past $r = 0$ singularity and the other asymptotically flat region do not exist and are replaced by the collapsing surface.

For the massless scalar field operator Φ, the wave equation is

$$\Phi_{;ab}\, g^{ab} = 0, \qquad (a,b=0,1,2,3), \tag{1.4.2}$$

where ";a" denotes covariant differentiation relative to x^a. The operator Φ can be expressed as

$$\Phi(t,x) = \sum_i [a_i\, f_i + a_i^{\dagger}\, f_i^{*}], \tag{1.4.3}$$

where $\{f_i\}$ are the solutions of Eq.(1.4.2) on $\mathscr{I}^-$ and form a complete family satisfying the orthonormality conditions

$$\frac{i}{2}\int_S (f_i\, f_{j;a} - f_j\, f_{i;a})\, d\Sigma^a = \delta_{ij}, \tag{1.4.4}$$

for a suitable surface S. This surface contain only positive frequencies coming from a_i and $a_i^{\dagger}$ on $\mathscr{I}^-$.In the region outside the event horizon and on future null

infinity $\mathscr{I}^+$, the operator Φ can be expressed in the form

$$\Phi(t,x) = \sum_i [b_i\ p_i + b_i^\dagger\ p_i^* + c_i\ q_i + c_i^\dagger\ q_i^*], \qquad (1.4.5)$$

where $\{p_i\}$ are the solutions of the wave equation which are purely outgoing, $\{q_i\}$ are the rest of the solutions b_i, $b_i^\dagger$ c_i, $c_i^\dagger$ are the corresponding annihilation and creation operators. These solutions satisfy the orthonormality condition (1.4.4), where S is taken to be the union of $\mathscr{I}^+$ and the event horizon. Notice that the choice of $\{q_i\}$ does not affect the calculation of emission of particles to $\mathscr{I}^+$. Since $\{f_i\}$ and $\{f_i^*\}$ form the complete basis, therefore,

$$p_i = \sum_j [\alpha_{ij}\ f_j + \beta_{ij}\ f_j^*], \qquad (1.4.6)$$

$$q_i = \sum_j [\gamma_{ij}\ f_j + \eta_{ij}\ f_j^*], \qquad (1.4.7)$$

where α_{ij}, β_{ij}, γ_{ij} and η_{ij} are the Bogoluibov coefficients. The Bogoluibov transformations lead to

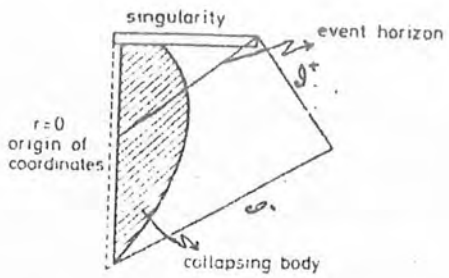

Figure 6. Only the region of the Schwarzschild solution outside the collapsing body is relevant for a BH formed by gravitational collapse. Inside the body the solution is completely different and is not given by this diagram.

corresponding relations between the operators

$$b_i = \sum_j [\alpha^*_{ij}\ a_j - \beta^*_{ij}\ a^\dagger_j], \tag{1.4.8}$$

$$c_i = \sum_j [\gamma^*_{ij}\ a_j - \eta^*_{ij}\ a^\dagger_j]. \tag{1.4.9}$$

The initial vacuum state $|0\rangle$, the state containing no incoming particles on $\mathscr{I}^-$, is denoted by

$$a_i|0\rangle = 0 \quad \text{for all } i. \tag{1.4.10}$$

Since β_{ij} is not zero, in general, the initial vacuum state will not appear to be a vacuum state to an observer at $\mathscr{I}^+$. Thus the VEV of the number operator for the ith outgoing mode is

$$\langle \underline{0}|b^\dagger_i\ b_i|\underline{0}\rangle = \sum_j |\beta_{ij}|^2 . \tag{1.4.11}$$

In order to determine the number of particles created by the gravitational field and emitted to infinity one simply has to calculate β_{ij}, which depends only on the surface gravity of the BH. For the asymptotic form, Hawking considered the ingoing and outgoing solutions as

$$f_{\omega' lm} = (2\pi)^{-1/2}\ \frac{F_{\omega'}(r)}{r(\omega')^{1/2}}\ exp(i\omega' v)\ Y_{lm}(\theta,\phi), \tag{1.4.12}$$

$$p_{\omega lm} = (2\pi)^{-1/2}\ \frac{P_{\omega}(r)}{r(\omega)^{1/2}}\ exp(i\omega u)\ Y_{lm}(\theta,\phi), \tag{1.4.13}$$

where v, u are the usual advanced and retarded coordinates and $Y_{lm}(\theta,\phi)$ are the associated Legendre functions. Also, Eq.(1.4.6) can be written in the form

$$p_\omega = \int_0^\infty (\alpha_{\omega\omega'}\ f_{\omega'} + \beta_{\omega\omega'}\ f^*_{\omega'})\ d\omega', \tag{1.4.14}$$

dropping suffices l, m for simplicity.

To calculate $\alpha_{\omega\omega'}$ and $\beta_{\omega\omega'}$, Hawking considered a solution p_ω propagating backward from $\mathscr{I}^+$ on the event horizon. Let a part $p_\omega^{(1)}$ of p_ω be scattered by the static Schwarzschild field outside the collapsing body and end up on $\mathscr{I}^-$ with the frequency ω and the remainder, $p_\omega^{(2)}$, enter the collapsing body where it will be partly scattered and partly reflected through the centre, eventually emerging at $\mathscr{I}^-$. For the latter part, the retarded time u goes to infinity on the event horizon and the surface of constant phase p_ω pile up near the event horizon (see Fig.7.).

Hawking calculated $p_\omega^{(2)}$ on $\mathscr{I}^-$ as

$$p_\omega^{(2)} \sim \begin{cases} 0, & \text{for } v>v_0 \\ \dfrac{P_\omega^-}{r(2\pi\omega)^{1/2}} \exp\left[-\dfrac{i\omega}{\varkappa}\left\{\log\left(\dfrac{v_0-v}{D_0}\right)\right\}\right], & \text{for } v<v_0 \end{cases} \qquad (1.4.15)$$

where $\varkappa = 1/4m$ is the surface gravity for the Schwarzschild BH , D_0 be constant and $P_\omega^- = P_\omega(2m)$ is the radial function on the past event horizon. For a large value of ω', the Fourier transform of $p_\omega^{(2)}$ gives

$$\alpha^{(2)}_{\omega\omega'} \approx \frac{P_\omega\{(D_0)^{\frac{i\omega}{\varkappa}}\}}{2\pi} \exp\{i(\omega-\omega')v_0\}\left(\frac{\omega'}{\omega}\right)^{1/2} \Gamma\left(1-\frac{i\omega}{\varkappa}\right)(-i\omega')^{-1+\frac{i\omega}{\varkappa}},$$

$$\beta^{(2)}_{\omega\omega'} \approx -i\,\alpha^{(2)}_{\omega(-\omega')}.$$

These equations give

$$|\alpha^{(2)}_{\omega\omega'}| \approx \exp\left(\frac{\pi\omega}{\varkappa}\right) |\beta^{(2)}_{\omega\omega'}| . \qquad (1.4.16)$$

Hawking noticed that actually $p_\omega^{(2)}$ is not given by Eq.(1.4.15) at early advanced time, which means that the singularity in $\alpha_{\omega\omega'}$ occurs at $\omega = \omega'$ and not at $\omega' = 0$. However, Eq.(1.4.16) is still valid for large ω'.

The EV of the total number of created particle at $\mathscr{I}^-$ in the frequency range ω to $\omega + d\omega$ is

$$\int_0^\infty |\beta_{\omega\omega'}|^2 d\omega' .$$

Since $|\beta_{\omega\omega'}|^2$ goes like $(\omega')^{-1/2}$ at large ω', therefore, this integral diverges. This is normally interpretted as an infinite number of particles created and steadily emitted at a rate for an infinite time. So that the total number of particles is Γ W, where

$$W = \{exp(\frac{2\pi\omega}{\kappa})-1\}^{-1},$$

$$\Gamma = \int_0^\infty [|\alpha^{(2)}_{\omega\omega'}|^2 - |\beta^{(2)}_{\omega\omega'}|^2] d\omega' . \qquad (1.4.17)$$

Hawking again noticed that for late retarded times, the function Γ enters the collapsing body which is almost the same as the fraction of the wave-packet that would have crossed the event horizon had the collapsing body been replaced by the exterior Schwarzschild solution. Thus the

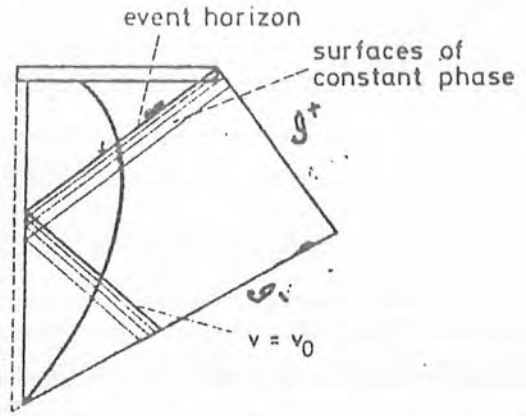

Figure 7. The solution p_ω of the wave equation has an infinite number of cycles near the event horizon and near the surface $v = v_0$.

factor Γ is also the same as the fraction of a similar wave-packet coming from $\mathscr{I}^-$ which would have crossed the future event horizon and have been absorbed by the BH. The relation between emission and absorption cross-section is, therefore, exactly that for a body with temperature of $\varkappa/2\pi$.

Similarly, for q_ω from Eq.(1.4.7), Hawking found for large ω'

$$|\gamma^{(2)}_{\omega\omega'}| \approx exp(\frac{\pi\omega}{\varkappa}) \ |\eta^{(2)}_{\omega\omega'}| \ . \qquad (1.4.18)$$

The number of particles crossing the event horizon in a wave-packet at late time would be $(1 - \Gamma)W$. For a given frequency ω, the absorption fraction Γ goes to zero as the angular quantum number l increases. Thus it might seem that each wave-packet of high l value would contain W particles and that the total rate of particles and energy crossing the event horizon would be infinite. This calculation would be inconsistent with the result[5] that an observer crossing the event horizon sees only a finite energy density of order m^{-4}. The reason for this discrepancy seems to be that the wave-packets $\{p_\omega\}$ and $\{q_\omega\}$ provide a complete basis of the wave equation only in the region outside the event horizon and not on the event horizon itself.

The continuation of the Hawking process seems to imply that the hole will evaporate away ever faster. Its ultimate fate cannot be decided within the context of the

present theory, for when T ~ 1/m the hole is shrinking at a rate comparable with the frequency of the radiation. Thermal equilibrium no longer applies, nor is the notion of a fixed background spacetime a good approximation. It has been conjectured[40] that the end result of the Hawking evaporation process is explosive disappearance of a naked singularity or perhaps a Plank mass object.

1.5. Problems With Hawking Radiation

The interpretation of Hawking's calculations as actual, physical, radiation is counter-intuitive. By definition, a BH does not emit radiation. It is generally argued that it is a classical BH that does not radiate and a quantum BH does. However, this argument does not reduce the problem of being counter-intuitive. Fluctuations of the BH surface could be expected, but this tunneling out of particles seems unreasonable. From this point of view we would like to present some arguments that question the usual interpretation of Hawking's and Fulling's calculations.

The first point is that the calculations depend on the nature of the vacuum around the BH. In other words, had a Dirac field been chosen instead of a scalar field, the definition of vacuua would be modified. In that case, there would be some different radiation, though possibly still

with a Planckian spectrum. The same would be true for the more physically relevant case of the electromagnetic vacuum. Allowing for all possible fields does not seem feasible[41]. However, the matter that went into the BH would have lost its identity. It cannot, therefore, dictate the nature of the vacuum about the BH. As such the hole would have to radiate in all possible field modes and not only in all frequency modes for a given field. It is not clear that such a result is calculable. Even if it is, it is not clear that it would give any reasonable agreement with BH thermodynamics, which was the original reason for taking the physical interpretation.

Fulling had already pointed out[2] that using his procedure the number operator would have a fractional EV, which does not seem to make any sense since the field under consideration is quantised. He, therefore, referred to his results as demonstrating as ambiguity in quantisation in curved spacetime. This point has been largely neglected in the literature but is extremely important. There could be the viewpoint that this fractional value is an indication that the result is an artifact of the Mathematics and does not represent a physical reality. For example, it could be that a complete Quantum Relativistic treatment would give no radiation and the apparent radiation just arises due to neglecting the Quantum Gravity component in an expansion.

There are various strange features of Hawking radiation that are brought out by some thought experiments[8] based on the properties of the BHs and of geodesics in their vicinity. Note that they are not paradoxes in the logical sense as they can all be explained. However, the explanations are counter-intuitive and infact themselves bring out the strange nature the radiation is required to have.

One property of geodesics near a BH is that an object falling in the BH would not be seen to cross its surface but to 'fade away' as it approached it. The reason for this property is that there is an infinite red-shift of light emitted from the surface of the BH and consequently time-intervals are infinitely expand, from the point of view of a distant observer.

Imagine a mini BH with an observer on one side of it and an assistant of his on the other side (see Fig.8.). Assuming that such a BH does radiate, the mass of the BH is taken to be such that the temperature of BH surface is $3^{\circ}K$. (Remember that there is a cosmic microwave background radiation at about $2.7^{\circ}K$). The assistant throws a stone into the hole. This stone emits its own radiation as it falls into the hole (on account of its high acceleration) and loses about 1% of its rest-mass. The mass of the stone is taken to be such that after its energy loss it is just

adequate to reduce the BH mass to the background temperature of 2.7°K. From the point of view of the observer a microwave source is seen standing out from the background. Then, as the stone falls into the hole the source gets "switched off". Thus the distant observer "sees" the stone fall into the hole.

The explanation of this apparent paradox is that the calculation involves taking asymptotic limits. Thus the effect of the stone falling into the hole is seen infinitely far in the future as required by the properties of the geodesics in the vicinity of a BH. However, this means that the BH can never be seen to form if it start forming at some finite time in the past. Since the universe had a finite start (the big bang) only a BH left over from

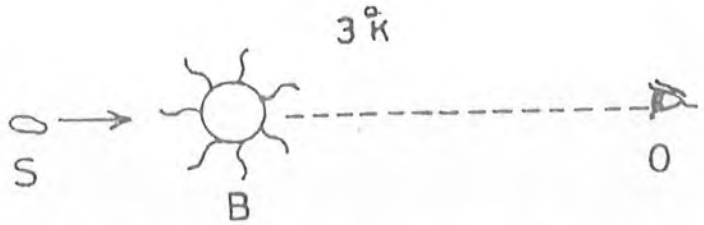

Figure 8. A stone S, thrown into a BH B, radiating at a temperature just above the cosmic background radiation from one side can 'switch off' the radiation as seen by an 'observer at infinity' O, on the other side. The opposite sides are taken to ensure no 'contamination' by radiation from the falling stone.

the big bang itself could radiate. In that case it may be more appropriate to think of it as a "white hole" or a part of the "big bang" occurring now.

Imagine two 'emulsion plates', one much larger than the other, in the vicinity of a BH. The smaller one is fixed in the geometrical shadow of the larger one which is falling freely towards the hole (see Fig.9.). These two plates can be regarded as observers. Since the freely falling observer sees no radiation, the freely falling plate will not show any 'tracks' of radiation (supposedly) the fixed plate will show radiation tracks despite the fact that it lay in the geometrical shadow of the larger plate.

The resolution of the paradox is that the radiation is produced non-locally at the smaller screen due to the

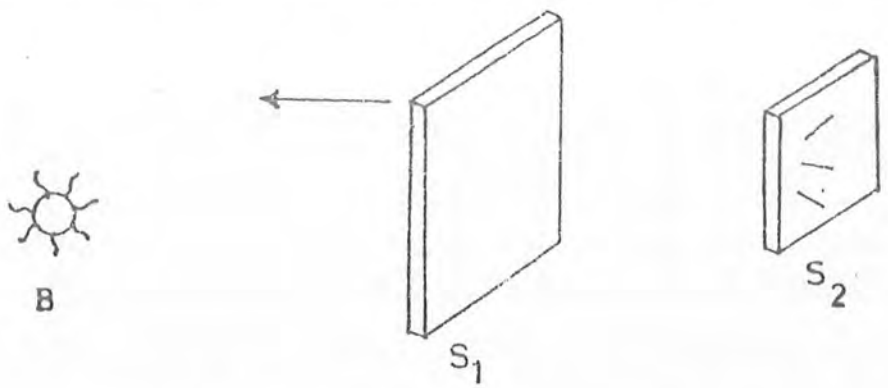

Figure 9. A freely falling screen, S_1, will not record the radiation from BH B, but the screen S_2, in the geometrical shadow of S_1, will record the radiation.

curvature of spacetime caused by the BH. Thus the radiation is a direct interaction between the hole and the detector (the emulsion plate) with no energy travelling, in a causal sense, from the hole to the detector. It is a spontaneous extraction of energy from the hole by the detector. This calls forcibly to mind Padmanabhan's argument[7] that the apparent radiation seen by the accelerated detector is simply its response to the acceleration.

CHAPTER TWO

FOLIATION OF THE SCHWARZSCHILD SPACETIME

There has been much work on obtaining 3+1 splits (foliation) of the Schwarzschild spacetime[22,31,42] on the basis of physical significance or Mathematical convenience. These foliations are best understood in terms of Penrose's compactified representations of the spacetime, often referred to as Penrose diagrams[31,39]. In this chapter we will discuss the foliation of the Schwarzschild spacetime by the SH which may run into the singularity.

2.1. Foliation of The Schwarzschild Spacetime by CKST Hypersurfaces

The Schwarzschild line element (1.4.1) in KS coordinates (v,u) is

$$ds^2 = f^2(dv^2 - du^2) - r^2\,(d\theta^2 + \sin^2\theta\, d\phi^2), \qquad (2.1.1)$$

where f^2 is given by

$$f^2 = \frac{32m^3}{r}\exp(-\frac{r}{2m}) \qquad (2.1.2)$$

and r is given as an implicit function of u and v given by Eq.(1.1.4), where v plays the role of time and u of the distance parameter.

A sequence of the SH of CKST, $v = v_o$, are the simplest for calculational purposes, but those that avoid the singularity do not completely foliate the spacetime

(see Fig.2.1). There are many SH, which do hit the singularity. In the region $|v_o| < 1$, the hypersurfaces are non-singular. We consider only these hypersurfaces. Notice that all these hypersurfaces pass through the throat of the Einstein- Rosen bridge[23] including r = m/2.

The MEC of a hypersurface, K, is given by[32]

$$K = - n^{\mu}{}_{;\mu} , \quad (\mu = 0,1,2,3) \qquad (2.1.3)$$

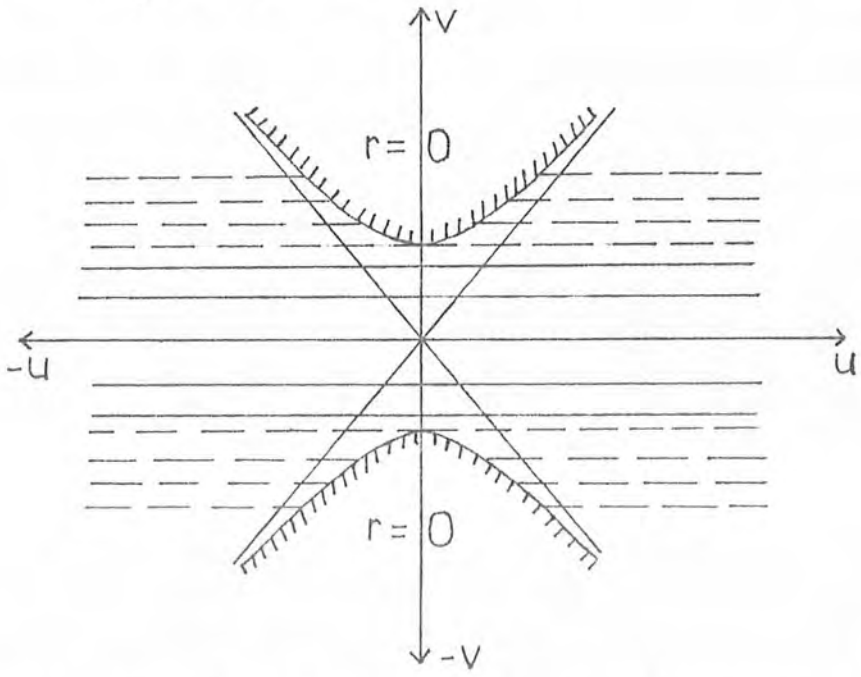

Figure 2.1a. The SH of CKST, $v = v_o$, are shown in the KS diagram. The dotted lines are for $|v_o| \geq 1$, the hypersurfaces, which make the foliation of the spacetime incomplete and they do not avoid the singularity from both ends of u. The other lines are the hypersurfaces, which are smooth in the region $|v_o| < 1$. Notice that all these hypersurfaces pass through the event horizon.

where n^{μ} is the unit normal to the hypersurfaces. Here

$$n^{\mu} = (f^{-1}, 0, 0, 0). \tag{2.1.4}$$

Therefore, Eq.(2.1.3) can be written as

$$-K = n^{o}{}_{,o} + (\ell n\sqrt{|g|})_{,o}\, n^{o}. \tag{2.1.5}$$

In KS coordinates from Eqs.(1.1.4), (2.1.1) and (2.1.4), we have

$$\ell n\sqrt{|g|} = 2\ell nf + 2\ell nr + \ell n(\sin\theta), \tag{2.1.6}$$

and

$$n^{o} = \sqrt{\frac{r}{32m^{3}}}\, exp(\frac{r}{4m}). \tag{2.1.7}$$

The total differential of Eq.(1.1.4) gives

$$r_{,o} = -\frac{8m^{2}}{r}\, v_{o}\, exp(-\frac{r}{2m}). \tag{2.1.8}$$

Now, by differentiating Eqs.(2.1.6) and (2.1.7) with respect to 'v', we get

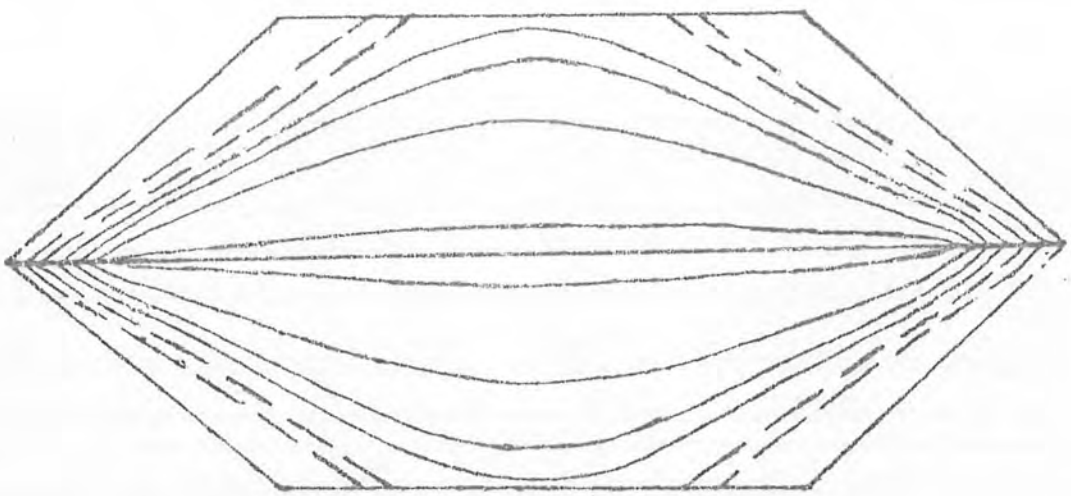

Figure 2.1b. In the Penrose diagram the SH of CKST, $v = v_{o}$, are shown by using the compactified KS coordinates (ψ,ξ).

$$(\ln\sqrt{|g|})_{,o} = (1-\frac{r}{2m})\frac{r_{,o}}{r}, \qquad (2.1.9)$$

$$n^{o}_{,o} = (1+\frac{r}{2m})\frac{r_{,o}}{8m}(2mr)^{-1/2}\exp(\frac{r}{4m}). \qquad (2.1.10)$$

Thus, inserting Eqs.(2.1.7)-(2.1.10) into Eq.(2.1.5), we have

$$K = v_o\sqrt{\frac{2m}{r}}\,(\frac{3}{2r}-\frac{1}{4m})\,\exp(-\frac{r}{4m}). \qquad (2.1.11)$$

The mean intrinsic curvature of the hypersurface is simply the Ricci scalar of the 3-geometry i.e.

$$R = G^{ij}R_{ij} \qquad (i,j = 1,2,3), \qquad (2.1.12)$$

where G^{ij} the inverse of the metric tensor for the purely spatial line element

$$d\sigma^2 = f^2\,du^2 + r^2\,(d\theta^2 + \sin^2\theta\,d\phi^2), \qquad (2.1.13)$$

and R_{ij} is the corresponding Ricci tensor defined by

$$R_{ij} = \Gamma^{k}_{ij,k} - (\ln\sqrt{|G|})_{,ij} + (\ln\sqrt{|G|})_{,k}\,\Gamma^{k}_{ij} - \Gamma^{k}_{il}\,\Gamma^{l}_{kj}, \qquad (2.1.14)$$

with the Christoffel symbol

$$\Gamma^{l}_{kj} = \frac{1}{2}G^{il}(G_{jl,k} + G_{kl,j} - G_{jk,l}). \qquad (2.1.15)$$

Also Eq.(2.1.3) provides

$$r_{,1} = \frac{8m^2u}{r}\exp(-\frac{r}{2m}), \qquad (2.1.16)$$

where u is given by the relation

$$u^2 = v_o^2 + (\frac{r}{2m}-1)\exp(\frac{r}{2m}). \qquad (2.1.17)$$

Now, Eqs.(2.1.13) and (2.1.16) give

$$\left.\begin{aligned} G_{11,1} &= -\frac{128m^4u}{r^2}(1+\frac{2m}{r})\exp(-\frac{r}{m}),\\ G_{22,1} &= 16m^2u\exp(-\frac{r}{2m}),\\ G_{33,1} &= G_{22,1}\sin^2\theta,\\ G_{33,2} &= 2r^2\sin\theta\cos\theta, \end{aligned}\right\} \qquad (2.1.18)$$

and

$$\ell n\sqrt{|G|} = \ell nf + 2\ell nr + \ell n(\sin\theta). \tag{2.1.19}$$

Using Eqs.(2.1.13), (2.1.15), and (2.1.18), the non-zero Christoffel symbols become

$$\left.\begin{aligned}
&\Gamma^1_{11} = -\frac{2mu}{r}\left(1+\frac{2m}{r}\right)\exp\left(-\frac{r}{2m}\right),\\
&\Gamma^1_{22} = -\frac{ru}{4m} = \operatorname{cosec}^2\theta\ \Gamma^1_{33},\\
&\Gamma^2_{12} = \Gamma^3_{13} = \frac{8m^2u}{r^2}\exp\left(-\frac{r}{2m}\right),\\
&\Gamma^2_{33} = -\sin\theta\cos\theta,\ \Gamma^3_{23} = \cot\theta,
\end{aligned}\right\} \tag{2.1.20}$$

and Eqs.(2.1.16) and (2.1.19) give

$$\left.\begin{aligned}
&\left(\ell n\sqrt{|G|}\right)_{,1} = \frac{2mu}{r}\left(\frac{6m}{r}-1\right)\exp\left(-\frac{r}{2m}\right),\\
&\left(\ell n\sqrt{|G|}\right)_{,2} = \cot\theta.
\end{aligned}\right\} \tag{2.1.21}$$

From Eq.(2.1.14), the non-zero Ricci tensors are

$$\left.\begin{aligned}
R_{11} &= \{\Gamma^1_{11}-\left(\ell n\sqrt{|G|}\right)_{,1}\}_{,1}\\
&\quad -\{\Gamma^1_{11}-\left(\ell n\sqrt{|G|}\right)_{,1}\}\Gamma^1_{11}-(\Gamma^2_{12})^2-(\Gamma^3_{13})^2,\\
R_{22} &= \Gamma^1_{22,1}-\left(\ell n\sqrt{|G|}\right)_{,22}\\
&\quad -\{2\Gamma^2_{12}-\left(\ell n\sqrt{|G|}\right)_{,1}\}\Gamma^1_{22}-(\Gamma^3_{23})^2,\\
R_{33} &= R_{22}\sin^2\theta.
\end{aligned}\right\} \tag{2.1.22}$$

Now, Eqs.(2.1.16), (2.1.20) and (2.1.21) yield

$$\left.\begin{aligned}
&\Gamma^1_{11}-\left(\ell n\sqrt{|G|}\right)_{,1} = -2\,\Gamma^2_{12},\\
&\Gamma^2_{12,1} = \left\{\frac{1}{u}-\frac{r}{2m}\left(1+\frac{4m}{r}\right)\Gamma^2_{12}\right\}\Gamma^2_{12},\\
&\Gamma^1_{22,1} = -\frac{r}{4m}\left(1+u\Gamma^2_{12}\right),\\
&\left(\ell n\sqrt{|G|}\right)_{,22} = -\operatorname{cosec}^2\theta.
\end{aligned}\right\} \tag{2.1.23}$$

Putting Eqs.(2.1.23) into Eqs.(2.1.22), the Ricci tensor components take the form

$$\left.\begin{aligned} R_{11} &= \frac{f^2}{r^2}\{v_o^2\ (1+\frac{2m}{r})exp(-\frac{r}{2m}) - \frac{2m}{r}\}, \\ R_{22} &= \frac{m}{r} + \frac{v_o^2}{2}(1-\frac{2m}{r})exp(-\frac{r}{2m}) = R_{33}cosec^2\theta. \end{aligned}\right\} \qquad (2.1.24)$$

Hence from Eqs.(2.1.12), (2.1.13) and (2.1.24), the Ricci scalar becomes

$$R = 2\ (v_o/r)^2\ exp(-\frac{r}{2m}). \qquad (2.1.25)$$

Next, the Riemanian curvature tensor R^i_{jkl} is defined by

$$R^i_{jkl} = \Gamma^i_{jl,k} - \Gamma^i_{jk,l} + \Gamma^i_{mk}\ \Gamma^m_{jl} - \Gamma^i_{ml}\ \Gamma^m_{jk}. \qquad (2.1.26)$$

Therefore,

$$\left.\begin{aligned} R^1_{212} &= \Gamma^1_{22,1} + (\Gamma^1_{11} - \Gamma^2_{12})\Gamma^1_{22}, \\ R^1_{313} &= \Gamma^1_{33,1} + (\Gamma^1_{11} - \Gamma^3_{13})\Gamma^1_{33}, \\ R^2_{121} &= -\Gamma^2_{12,1} + (\Gamma^1_{11} - \Gamma^2_{12})\Gamma^2_{12}, \\ R^2_{323} &= \Gamma^2_{33,2} + \Gamma^2_{12}\Gamma^1_{33} - \Gamma^2_{33}\Gamma^3_{32}, \\ R^3_{131} &= -\Gamma^3_{13,1} + (\Gamma^1_{11} - \Gamma^3_{13})\Gamma^3_{13}, \\ R^3_{232} &= -\Gamma^3_{23,2} - (\Gamma^3_{23})^2 + \Gamma^3_{13}\Gamma^1_{22}. \end{aligned}\right\} \qquad (2.1.27)$$

Thus, by substituting Eqs.(2.1.20) and (2.1.23) into Eqs.(2.1.27), we get

$$\left.\begin{aligned} R^1_{212} &= v_o^2\ (\frac{1}{2} + \frac{m}{r})exp(-\frac{r}{2m}) - \frac{m}{r}\ , \\ R^1_{313} &= R^1_{212}sin^2\theta, \\ R^2_{121} &= \frac{f^2}{2r^2}\{v_o^2\ (1 + \frac{2m}{r})exp(-\frac{r}{2m}) - \frac{2m}{r}\}, \\ R^2_{323} &= \frac{2m}{r}\{1 - v_o^2\ exp(-\frac{r}{2m})\}sin^2\theta\ , \\ R^3_{131} &= R^2_{121},\ R^3_{232} = R^2_{323}\ cosec^2\theta. \end{aligned}\right\} \qquad (2.1.28)$$

Also, Eqs.(2.1.13) and (2.1.28) yield

$$\left.\begin{aligned} R^{12}{}_{12} &= \frac{1}{2r^2}\{v_o^2\ (1+\frac{2m}{r})\,exp(-\frac{r}{2m}) - \frac{2m}{r}\}, \\ R^{19}{}_{19} &= R^{21}{}_{21} = R^{31}{}_{31} = R^{12}{}_{12}\ , \\ R^{29}{}_{29} &= \frac{2m}{r^9}\{1- v_o^2\ exp(-\frac{r}{2m})\} = R^{92}{}_{92}\ . \end{aligned}\right\} \qquad (2.1.29)$$

By substituting Eqs.(2.1.25) and (2.1.29) into Eqs.(1.1.1), the curvature invariants for the SH of CKST become

$$\left.\begin{aligned} R_1 &= R, \\ R_2 &= \frac{12m^2}{r^6}P^2(r) - \frac{4mv_o^2}{r^5}P(r) + \frac{v_o^4}{r^4}\,exp(-\frac{r}{m}), \end{aligned}\right\} \qquad (2.1.30)$$

where

$$P(r) = 1- v_o^2 exp(-\frac{r}{2m}). \qquad (2.1.31)$$

Notice that K, R_1 and R_2 are finite for $r\neq 0$, $|v_o| < \infty$ and all tend to zero as $r \longrightarrow \infty$, but all tend to infinity at the singularity. Also, all curvatures tend to infinity as $|v_o|$ tend to infinity. Further, notice that for $|v_o| < 1$ the hypersurfaces are connected and non-singular, but for $|v_o| \geq 1$ the hypersurfaces hit the singularity from "both ends" of u, where the SH of CKST are not connected.

All the SH of CKST pass through the event horizon. There is an ambiguity in the definition of these hypersurfaces for $|v_o| \geq 1$, in that the hypersurfaces which enter into the singularity, r = 0, for u > 0 are not necessarily those that come out from the singularity for u < 0. It is necessary to mention here that the picture derived from Minkowski space, that the left side is obtained from the right by rotation does not hold here. This creates difficulties for the procedure of canonical

quantisation of scalar fields, as it is not clear what is the hypersurface on which the wave function is to be normalised. As such we will not quantise scalar fields with the asymptotic limits $|v_o| \longrightarrow \infty$. To set up the quantisation procedure we quantise scalar fields on the complete SH of CKST in §.3.3.

2.2. K-Surfaces

In this section, for completeness, we reproduce the work of Brill, Cavallo and Isenberg[22]. They provided a complete foliation of the Schwarzschild spacetime by SH of CMEC (K-surfaces). In §.3.4 we will quantise the scalar fields on the K-surfaces.

The variational principle[25] provides a convenient way to derive the equation of K-surfaces. Let the spacelike surface S be described by[22]

$$t = t(r,\theta,\phi), \tag{2.2.1}$$

and choose a surface $t = 0$ for S_1, then the variational principle gives

$$\delta I = 0, \tag{2.2.2}$$

with

$$\begin{aligned} I &= A(S)+K(S,S_1) \\ &= \int_S n^\mu \, d^3S_\mu + K\int_V d^4V, \end{aligned} \tag{2.2.3}$$

where A(S) is the three-dimensional area of S, S_1 is a fixed hypersurface, $V(S,S_1)$ is the four-dimensional volume bounded by S and S_1, n^μ is the unit normal vector to S and

S_1 and K corresponds to the mean curvature. For the Schwarzschild metric Eqs.(2.2.2) and (2.2.3) become

$$\delta\int\{\Sigma + K\sqrt{B(r)C(r)}\ t\}^{1/2}\ r^2 sin\theta\ drd\theta d\phi = 0, \qquad (2.2.4)$$

where

$$\Sigma^2 \equiv -B\ t_{,1}^2 - \frac{BC}{r^2}\{t_{,2}^2 + (\frac{t_{,3}}{sin\theta})^2\} + C \qquad (2.2.5)$$

is positive for the SH and

$$B(r) = \frac{1}{C(r)} = 1 - \frac{2m}{r}\ . \qquad (2.2.6)$$

The variational equation obtained from Eq.(2.2.4) by varying t is

$$-Kr^2\sqrt{BC} = (Br^2 t_{,1}/\Sigma)_{,1} + (BCt_{,3}/\Sigma)_{,3}/sin^2\theta + (BCsin\theta\ t_{,2}/\Sigma)_{,2}/sin\theta\ . \qquad (2.2.7)$$

For spherical symmetry $t \equiv t(r)$, therefore, Eq.(2.2.7) takes the form

$$(\frac{dt^*}{dr^*})^2 = \frac{(H-J)^2}{(H-J)^2+Br^4}\ , \qquad (2.2.8)$$

where

$$\frac{dt^*}{dr^*} = \sqrt{\frac{B}{C}}\ \frac{dt}{dr}\ , \qquad (2.2.9)$$

$$J = K\int^r \sqrt{B(x)C(x)}\ x^2\ dx, \qquad (2.2.10)$$

and H is a constant of integration.

Now, for the region inside the horizon, the spherically symmetric spacelike surface S is described by $r = r(t)$ and the variational principle given by Eq.(2.2.2) with Eq.(2.2.3), in terms of the Lagrangian gives[22]

$$0 = \delta\int Ldt = \delta\int[r^2\{C\ (\dot{r})^2 - B)\}^{1/2} - J]dt, \qquad (2.2.11)$$

where L is the Lagrangian. Since L is time independent, the Hamiltonian

$$H = \dot{r}\,\frac{\partial L}{\partial \dot{r}} - L\ , \tag{2.2.12}$$

is conserved. Therefore,

$$H = B\,r^2\{C\,(\dot{r})^2 - B)\}^{-1/2} + J = \text{constant}. \tag{2.2.13}$$

Eq.(2.2.13) can be re-written as

$$(\frac{dr^*}{dt^*})^2 - B\,r^4(H-J)^{-2} = 1, \tag{2.2.14}$$

where

$$\frac{dr^*}{dt^*} = \sqrt{\frac{C}{B}}\,\frac{dr}{dt}\ . \tag{2.2.15}$$

Notice that both the solutions, given by Eqs.(2.2.8) and (2.2.14), are equivalent. Thus either Eq.(2.2.8) or Eq.(2.2.14) can be used to solve for K-surfaces, both inside and outside the horizon. Eq.(2.2.14) is particularly used[22] for a qualitative discussion, because it is analogous to the energy conservation law for a particle of unit energy. Thus the equation for K in Schwarzschild coordinates is

$$(\frac{dr}{dt})^2 = (1-\frac{2m}{r})^2\{1 + r^3(r-2m)(H-\frac{K}{3}r^3)^{-2}\}. \tag{2.2.16}$$

Now, in KS coordinates, given by Eq.(1.1.2), we have

$$\left.\begin{aligned}\frac{du}{dr} &= \frac{ru}{4m(r-2m)} + \frac{v}{4m}\,\frac{1}{dr/dt}\ ,\\ \frac{dv}{dr} &= \frac{rv}{4m(r-2m)} + \frac{u}{4m}\,\frac{1}{dr/dt}\ .\end{aligned}\right\} \tag{2.2.17}$$

Also, Eq.(2.2.16) can be re-written as

$$\frac{dr}{dt} = \frac{(r-2m)A}{rE}\ , \tag{2.2.18}$$

where

$$E = H - \frac{K}{3}\,r^3, \qquad A^2 = E^2 + r^3(r-2m). \tag{2.2.19}$$

Inserting Eq.(2.2.18) into Eqs.(2.2.17), we have

$$\frac{du}{dr} = \frac{r(Au+Ev)}{4mA(r-2m)}, \tag{2.2.20}$$

and

$$\frac{dv}{dr} = \frac{r(Av+Eu)}{4mA(r-2m)}. \tag{2.2.21}$$

Thus the equation of K-surfaces in KS coordinates becomes

$$\frac{dv}{du} = \frac{(Av+Eu)}{(Au+Ev)} . \tag{2.2.22}$$

The K-surfaces plotted in Fig.2.2 were obtained by numerical integration of Eq.(2.2.16), or equivalently Eq.(2.2.22), for different values of H and K = 2. To fix the sign of A we demand that K be the divergence of the future pointing normal (or convergence of the past pointing normal). This rule[22] about the sign of A leads to a smooth surface through the turning point, where A = 0, and implies that A switches sign at this point.

For each fixed value of K there exist values H_+=0.77871 and H_-=-1/6 such that all surfaces with $H<H_-$ and $H>H_+$ have one and only one singularity while those with $H_-<H<H_+$ contain either two singularities or none at all. From the explicit form of A^2, we see that the constant values $r_\pm$ corresponding to $H_\pm$ must satisfy $0<r_-<0.75<r_+<1$. Further, we find that for K>0 all nonsingular surfaces ($H_-<H<H_+$) which intersect the region u>0 have minimum r greater than r_+, while the nonsingular, K>0, surfaces intersecting u<0 have minimum r greater than r_-.

For the intrinsic curvature, from Eq.(2.1.1) and (2.2.22), the spatial line element is given by

$$d\sigma_K^2 = F^2\, du^2 + r^2\,(d\theta^2 + \sin^2\theta\, d\phi^2), \qquad (2.2.23)$$

where

$$F = \frac{4mr(r-2m)}{Au+Ev}. \qquad (2.2.24)$$

Now, from Eq.(2.2.23)

$$\left.\begin{aligned} G_{11,1} &= 2FF_{,1} = 2FF_{,r}\,\frac{1}{du/dr}, \\ G_{22,1} &= 2rr_{,1},\ G_{33,1} = G_{22,1}\sin^2\theta, \end{aligned}\right\} \qquad (2.2.25)$$

and $G_{33,2}$ is the same as given in Eq.(2.1.18). Also, from Eqs.(2.2.19), (2.2.20), (2.2.24) and (2.2.25), we have

$$\left.\begin{aligned} E_{,1} &= -KAF,\ A_{,1} = F(2r-3m-KE), \\ G_{11,1} &= 2FF_{,1},\ G_{22,1} = 2\frac{FA}{r}, \\ G_{33,1} &= G_{22,1}\sin^2\theta,\ G_{33,2} = 2r^2\sin\theta\cos\theta. \end{aligned}\right\} \qquad (2.2.26)$$

Inserting Eqs.(2.2.23) and (2.2.26) into Eq.(2.1.15), the

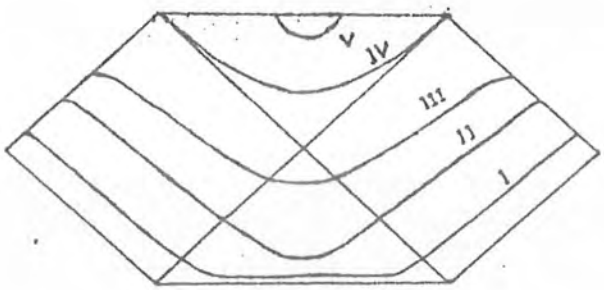

Figure 2.2. The solutions of differential equation given by Eq.(2.2.17) or Eq.(2.2.23) are shown in the Penrose digram for K = 2 and different values of H i.e.

I	II	III	IV	V
H: -1/6	-1/12	1/2	1/6	-1/2.

non-zero Christoffel symbols become

$$\left.\begin{aligned}
&\Gamma^1_{11} = F^{-1}F_{,1}\ ,\\
&\Gamma^1_{22} = -F^{-1}\frac{A}{r} = \Gamma^1_{33}\csc^2\theta\ ,\\
&\Gamma^2_{12} = \Gamma^3_{13} = \frac{AF}{r^3}\ ,\\
&\Gamma^2_{33} = -\sin\theta\cos\theta,\ \Gamma^3_{23} = \cot\theta.
\end{aligned}\right\} \qquad (2.2.27)$$

Further, from Eq.(2.2.23)

$$\ln\sqrt{|G|} = \ln F + 2\ln r + \ln(\sin\theta). \qquad (2.2.28)$$

Therefore, from Eqs.(2.2.20), (2.2.27) and (2.2.22), we have

$$\left.\begin{aligned}
&(\ln\sqrt{|G|})_{,1} = \Gamma^1_{11} + \frac{2A}{r^3}F\ ,\\
&(\ln\sqrt{|G|})_{,2} = \cot\theta,\\
&\Gamma^1_{11} - (\ln\sqrt{|G|})_{,1} = -2\,\Gamma^2_{12},\\
&\Gamma^2_{12,1} = \frac{F^2}{r^3}(2r-3m-KE) + \frac{A}{r^3}F_{,1} - 3\frac{A^2F^2}{r^6} = \Gamma^3_{13,1},\\
&\Gamma^1_{22,1} = \frac{A^2}{r^4} + \frac{AF^{-2}}{r}F_{,1} - \frac{(2r-3m-KE)}{r},\\
&(\ln\sqrt{|G|})_{,22} = -\csc^2\theta.
\end{aligned}\right\} \qquad (2.2.29)$$

Putting Eqs.(2.2.27) and (2.2.29) into Eqs.(2.1.22), the Ricci tensor components take the form

$$\left.\begin{aligned}
&R_{11} = 2\frac{F^2}{r^6}\{2A^2 - r^3(2r-3m-KE)\},\\
&R_{22} = 1 + \frac{1}{r^4}\{A^2 - r^3(2r-3m-KE)\},
\end{aligned}\right\} \qquad (2.2.30)$$

Also, by substituting Eqs.(2.2.27), (2.2.28), (2.2.29) into Eqs.(2.1.27), the Riemanian curvature tensor becomes

$$
\left.
\begin{aligned}
R^{1}_{212} &= \frac{2A^2}{r^4} - \frac{2r-3m-KE}{r}\,, \\
R^{1}_{313} &= R^{1}_{212}\sin^2\theta, \\
R^{2}_{121} &= \frac{F^2}{r^2} R^{1}_{212} = R^{3}_{131}, \\
R^{2}_{323} &= \left(1-\frac{A^2}{r^4}\right)\sin^2\theta\,, \\
R^{3}_{232} &= R^{2}_{323}\,\mathrm{cosec}^2\theta.
\end{aligned}
\right\} \qquad (2.2.31)
$$

Hence by putting Eqs.(2.2.19), (2.2.23), (2.2.24) (2.2.30) and (2.2.31) into Eqs.(1.1.1), the curvature invariants are

$$
\left.
\begin{aligned}
R_1 &= R = 6P(r)Q(r), \\
R_2 &= 2\,P^2(r)S(r) - 24\,\frac{mH}{r^6}\,P(r) + 12\frac{m^2}{r^6}\,,
\end{aligned}
\right\} \qquad (2.2.32)
$$

where

$$
P(r) = \frac{H}{r^3} - \frac{K}{3}\,, \quad Q(r) = \frac{H}{r^3} + \frac{K}{3}\,, \qquad (2.2.33)
$$

and

$$
S(r) = \frac{9H^2}{r^6} + \frac{2KH}{3r^3} + \frac{K^2}{3}\,. \qquad (2.2.33)
$$

Thus for finite values of K and H, the curvature invariants asymptotically go to zero. R_1 and R_2 tend to infinity at the singularity. This gives the complete foliation[24] depicted in Fig.2.3.

Each K-surface is non-singular and passes through the throat of the Einstein-Rosen bridge. The K-surfaces are more complicated than the SH of CKST, in calculations. Notice that the K-surfaces are ambiguity-free as opposed to the SH of CKST, which we could not determine how to continue $|v| > 1$ to the maximal extension.

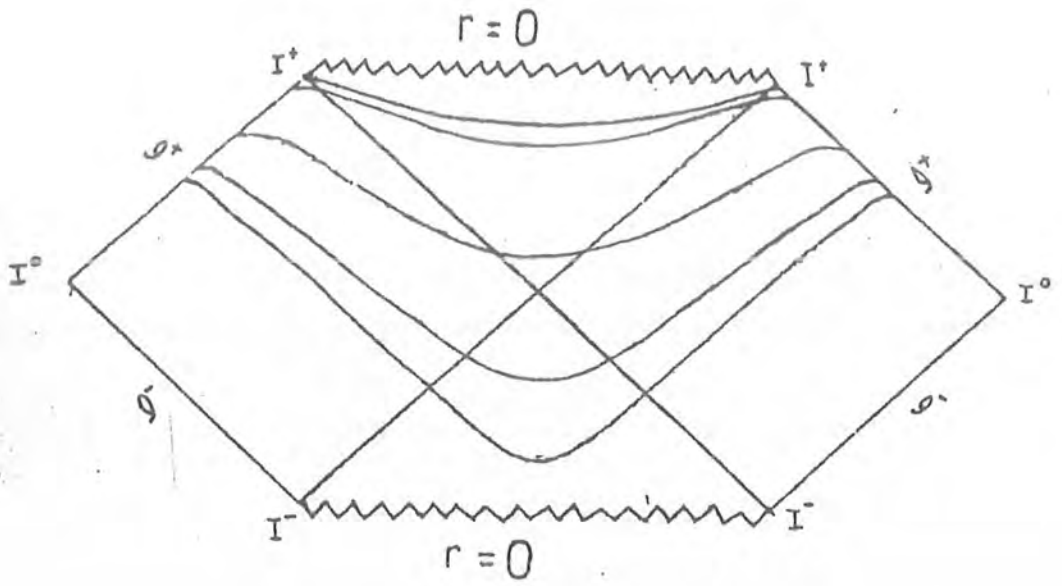

Figure 2.3. Foliation of the Schwarzschild-Kruskal-Szekeres spacetime by K-surfaces in a Penrose diagram is shown. Only a few typical surfaces are shown. Whereas there is some arbitrariness (e.g., in the location of the throat) for the surfaces in the past of r=1.5m all surfaces in the future of r=1.5m must be of the r=const. type. Namely, since the future r=0 singularity corresponds to collapse (converging) normals, surfaces with K<0 must lie to the future of surfaces with K>0. However[22], from the concavity of K-surfaces in the asymptotic region it is known that K-surfaces which emerge from the horizon reach $\mathscr{I}^+$ if K>0 and $\mathscr{I}^-$ if K<0. Hence in a foliation, K-surfaces of both signs cannot reach null infinity.

2.3. ψN-Hypersurfaces

The significance of observer-dependence in the entire process needs to be better understood, not only for linearly accelerated observers, but for Hawking radiation as well. It has been argued[27] that there is a physically 'preferred' frame corresponding to an observer falling freely from infinity, which was called the pseudo-Newtonian (ψN) frame. The application of the ψN-formalism to astrophysical phenomena and further understanding the implications of the Classical Relativity[43] lend support to this claim.

The ψN-hypersurfaces are orthogonal to the ψN-observers. In this section we give the foliation of the Schwarzschild spacetime by ψN-hypersurfaces. Let t^μ be the tangent vector of the ψN-observers and T^μ be the tangent vector of the ψN-hypersurfaces, which are orthogonal to the ψN-observers, such that

$$t^\mu t_\mu = 1, \quad T^\mu T_\mu = -1, \quad T^\mu t_\mu = 0, \tag{2.3.1}$$

where

$$t^\mu = (t^0, t^1, 0, 0), \quad T^\mu = (T^0, T^1, 0, 0). \tag{2.3.2}$$

For the Schwarzschild spacetime, we have

$$t^0 = (1 - \frac{2m}{r})^{-1}, \quad t^1 = -\sqrt{\frac{2m}{r}}\ . \tag{2.3.3}$$

Substitution of Eqs.(2.3.3) into Eqs.(2.3.1) give

$$T^0 = -\sqrt{\frac{2m}{r}}\,(1 - \frac{2m}{r})^{-1}, \quad T^1 = 1. \tag{2.3.4}$$

Hence the world lines of ψN-observers are obtained by solving Eqs.(2.3.3), to be[32]

$$t = t_c - \frac{2}{3}(r + 6m)\sqrt{\frac{r}{2m}} - 2m\ \ell n\left|\frac{\sqrt{\frac{r}{2m}} - 1}{\sqrt{\frac{r}{2m}} + 1}\right|, \qquad (2.3.5)$$

and the ψN-hypersurfaces, by solving Eqs.(2.3.4), to be

$$t = t_o - 4m\sqrt{\frac{r}{2m}} - 2m\ \ell n\left|\frac{\sqrt{\frac{r}{2m}} - 1}{\sqrt{\frac{r}{2m}} + 1}\right|, \qquad (2.3.6)$$

where t_c and t_o are the constants of integration.

The problem with this description of the ψN-hypersurface is that it breaks down at $r = 2m$ (in gravitational units). However, these hypersurfaces must pass through the event horizon even though their description by Eq.(2.3.6) breaks down there. What is required is that the ψN-hypersurfaces provide a complete foliation of the Schwarzschild spacetime. To avoid the above problem we use the KS coordinates (v,u) given by Eq.(1.1.2).

For the SH, given by Eq.(2.3.6) v, u are related parametrically by

$$\left.\begin{aligned} v &= [\cosh\{A(r)\} + \sqrt{\frac{r}{2m}}\ \sinh\{A(r)\}]\exp(\frac{r}{4m}), \\ u &= [\sinh\{A(r)\} + \sqrt{\frac{r}{2m}}\ \cosh\{A(r)\}]\exp(\frac{r}{4m}), \end{aligned}\right\} \qquad (2.3.7)$$

where

$$A(r) = \frac{t_o}{4m} - \sqrt{\frac{r}{2m}}\ . \qquad (2.3.8)$$

Notice that v, u given by Eqs.(2.3.7) satisfy the relation (1.1.4).

Next, To obtain the MEC of the ψN-hypersurfaces, the normal vector n^μ will be

$$n^{\mu} = (n^{0},\ n^{1},\ 0,\ 0). \tag{2.3.9}$$

Thus from Eqs.(2.1.3), (2.3.4), (2.3.7)-(2.3.9), we have

$$\left.\begin{aligned} n^{0} &= \dot{v} = \sqrt{\frac{r}{2m}}\ \frac{\sinh A}{4m}\ \exp(\frac{r}{4m}), \\ n^{1} &= \dot{u} = \sqrt{\frac{r}{2m}}\ \frac{\cosh A}{4m}\ \exp(\frac{r}{4m}), \end{aligned}\right\} \tag{2.3.10}$$

and

$$\left.\begin{aligned} r_{,0} &= -\ \frac{8m^{2}}{r}\ v\ \exp(-\frac{r}{2m}), \\ r_{,1} &= \frac{8m^{2}}{r}\ u\ \exp(-\frac{r}{2m}), \end{aligned}\right\} \tag{2.3.11}$$

where u and v are given by Eqs.(2.3.7). Also, from Eq.(2.1.3), the MEC is

$$-K = n^{0}{}_{,0}+n^{1}{}_{,1}+(\ln\sqrt{|g|})_{,0}n^{0}+(\ln\sqrt{|g|})_{,1}n^{1}. \tag{2.3.12}$$

Eqs.(2.3.8), (2.3.10) and (2.3.11) yields

$$\left.\begin{aligned} n^{0}{}_{,0} &= -\frac{v}{2r}\exp(-\frac{r}{4m})[(\sqrt{\frac{r}{2m}}+\sqrt{\frac{2m}{r}})\sinh A-\cosh A], \\ n^{1}{}_{,1} &= \frac{u}{2r}\ \exp(-\frac{r}{4m})[(\sqrt{\frac{r}{2m}}+\sqrt{\frac{2m}{r}})\cosh A-\sinh A]. \end{aligned}\right\} \tag{2.3.13}$$

Also, Eqs.(2.1.2), (2.1.7) and (2.3.11) gives

$$\left.\begin{aligned} (\ln\sqrt{|g|})_{,0} &= \frac{4mv}{r}\ (1-\frac{2m}{r})\ \exp(-\frac{r}{2m}), \\ (\ln\sqrt{|g|})_{,1} &= -\ \frac{4mu}{r}\ (1-\frac{2m}{r})\ \exp(-\frac{r}{2m}). \end{aligned}\right\} \tag{2.3.14}$$

Thus, by substituting Eqs.(2.3.13) and (2.3.14) into Eq.(2.3.12), we get

$$K = \frac{1}{4m} - \frac{2}{r}\ . \tag{2.3.15}$$

Again Eqs.(2.3.10) imply that

$$\frac{dv}{du} = \tanh A\ . \tag{2.3.16}$$

For the spatial 3-geometry, Eqs.(2.1.1) and (2.3.16) gives the metric tensor

$$d\sigma^{2}_{\psi N} = f^{2}\operatorname{sech}^{2}A\ du^{2} + r^{2}(d\theta^{2}+\sin^{2}\theta\ d\phi^{2}). \tag{2.3.17}$$

Also, the relation

$$\frac{du}{dr} = \frac{du}{ds}\frac{ds}{dr} = \frac{du}{ds}\frac{1}{dr/ds} = \frac{du}{ds}\frac{1}{T^1} ,$$

using (2.3.4) and (2.3.10), yields

$$\frac{du}{dr} = \frac{1}{4m}\sqrt{\frac{r}{2m}}\,exp(\frac{r}{4m})\,cosh\mathcal{A} . \qquad (2.3.18)$$

Now, Eqs.(2.1.2), (2.2.17) and (2.3.18) imply that

$$\left.\begin{aligned} G_{11,1} &= \frac{64m^3}{r}\sqrt{\frac{2m}{r}}exp(-\frac{3r}{4m})sech^3\mathcal{A} \\ &\quad \times [\sqrt{\frac{2m}{r}}tanh\mathcal{A}-(1+\frac{2m}{r})], \\ G_{22,1} &= 8mr\sqrt{\frac{2m}{r}}exp(-\frac{r}{4m})sech\mathcal{A}, \\ G_{33,1} &= G_{22,1}sin^2\theta,\ G_{33,2} = 2r^2sin\theta\,cos\theta, \end{aligned}\right\} \qquad (2.3.19)$$

where we have used the fact that

$$\{h(r)\}_{,1} = h_{,r}\frac{1}{du/dr} .$$

Substituting Eqs.(2.3.17) and (2.3.19) into Eq.(2.1.15) the non-zero Christoffel symbols become

$$\left.\begin{aligned} \Gamma^1_{11} &= \sqrt{\frac{2m}{r}}exp(-\frac{r}{4m})sech\mathcal{A}[\sqrt{\frac{2m}{r}}tanh\mathcal{A}-(1+\frac{2m}{r})], \\ \Gamma^1_{22} &= -\frac{r^2}{8m^2}\sqrt{\frac{2m}{r}}exp(\frac{r}{4m})\,cosh\mathcal{A} = cosec^2\theta\,\Gamma^1_{33}, \\ \Gamma^2_{12} &= \Gamma^3_{13} = \frac{4m}{r}\sqrt{\frac{2m}{r}}exp(-\frac{r}{4m})sech\mathcal{A}, \\ \Gamma^2_{33} &= -sin\theta\,cos\theta,\quad \Gamma^3_{23} = cot\theta, \end{aligned}\right\} \qquad (2.3.20)$$

and Eqs.(2.3.17), (2.3.18) give

$$\left.\begin{aligned} (ln\sqrt{|G|})_{,1} &= \sqrt{\frac{2m}{r}}exp(\frac{r}{4m})sech\mathcal{A} \\ &\quad \times [\sqrt{\frac{2m}{r}}tanh\mathcal{A}-(1-\frac{6m}{r})], \\ (ln\sqrt{|G|})_{,2} &= cot\theta. \end{aligned}\right\} \qquad (2.3.21)$$

Further, Eqs.(2.3.18), (2.3.20) and (2.3.21) yield

$$\left.\begin{aligned}
&\Gamma^{1}_{11} - \left(\ln\sqrt{|G|}\right)_{,1} = -2\,\Gamma^{2}_{12}\,,\\
&\Gamma^{2}_{12,1} = \frac{8m^{2}}{r^{2}}\,sech^{2}A\,\exp(-\frac{r}{2m})\\
&\qquad\times\left[\sqrt{\frac{2m}{r}}\tanh A - (1+\frac{6m}{r})\right] = \Gamma^{3}_{31,1},\\
&\Gamma^{1}_{22,1} = \frac{r}{4m}\left[\sqrt{\frac{2m}{r}}\tanh A - (1+\frac{6m}{r})\right].
\end{aligned}\right\} \qquad (2.3.22)$$

Substituting Eqs.(2.3.20)-(2.3.22) into Eqs.(2.1.22) and (2.1.27), all the Ricci and Riemanian curvature tensors become zero. Therefore, the curvature invariants, given by Eqs.(1.1.1) are all zero.

Notice that the MEC K given by Eq.(2.3.15) is well-behaved at infinity while it tends to infinity only at the singularity, r = 0, and the intrinsic curvature invariants for the ψN-hypersurfaces are zero. The foliating ψN-hypersurface hit the singularity[44]. This foliation arises from a reference frame that has been discussed in a different context[45].

For visualizing the asymptotic structure of spacetime, we convert the KS coordinates into the compactified KS coordinates (ψ, ξ), which are given by the relations (1.1.7) and (1.1.8). Now, from Eqs.(2.3.7), we have

$$\left.\begin{aligned}
v + u &= (1 + \sqrt{\frac{r}{2m}})\exp\{\frac{r}{4m} + A\},\\
v - u &= (1 - \sqrt{\frac{r}{2m}})\exp\{\frac{r}{4m} - A\}.
\end{aligned}\right\} \qquad (2.3.23)$$

Thus the compactified KS coordinates , by substituting Eqs.(2.3.23) into Eqs.(1.1.7), becomes

$$\left.\begin{aligned}\psi &= \tan^{-1}\left[\left(1+\sqrt{\frac{r}{2m}}\right)\exp\left(\frac{r}{4m}+A\right)\right] \\ &\quad + \tan^{-1}\left[\left(1-\sqrt{\frac{r}{2m}}\right)\exp\left(\frac{r}{4m}-A\right)\right], \\ \xi &= \tan^{-1}\left[\left(1+\sqrt{\frac{r}{2m}}\right)\exp\left(\frac{r}{4m}+A\right)\right] \\ &\quad - \tan^{-1}\left[\left(1-\sqrt{\frac{r}{2m}}\right)\exp\left(\frac{r}{4m}-A\right)\right].\end{aligned}\right\} \qquad (2.3.24)$$

Notice that these hypersurfaces start at $r = 0$ with $\frac{d\psi}{d\xi} = 0$ and end up at $r = \infty$ with $\frac{d\psi}{d\xi} = 1$.

The remarkable feature of these hypersurfaces is that they provide a complete foliation of the upper half of the Penrose diagram *without entering the other half!* In other words these hypersurfaces come from spatial infinity and hit the singularity without going through the throat of the Einstein-Rosen bridge. The foliation is depicted in Fig.2.4. Notice that as $t_o \longrightarrow -\infty$ the hypersurfaces tend to BAD, the union of the null surface $\{r = 2m,\ t = -\infty\}$ and past null infinity $\mathscr{I}^-$, while as $t_o \longrightarrow +\infty$ the hypersurfaces tend to $\mathscr{I}^+$. That spacelike hypersurfaces, in the limit, tend to null hypersurfaces is not unusual. For example in the constant mean extrinsic curvature foliation of the Schwarzschild geometry[22], as $K \longrightarrow -\infty$, the hypersurfaces tend to the union of the two lower edges of the Penrose diagram and the singularity, $r = 0$.

The above foliation shows that the upper left corner, D, of the Penrose diagram is simultaneous with the lower right corner, A, in this particular frame. Since the geometry does not depend on the choice of frames we would

argue that D should be labelled I^- and not I^+. This is also reasonable from another point of view. Inside the horizon t is a spacelike coordinate and r a timelike coordinate. Thus

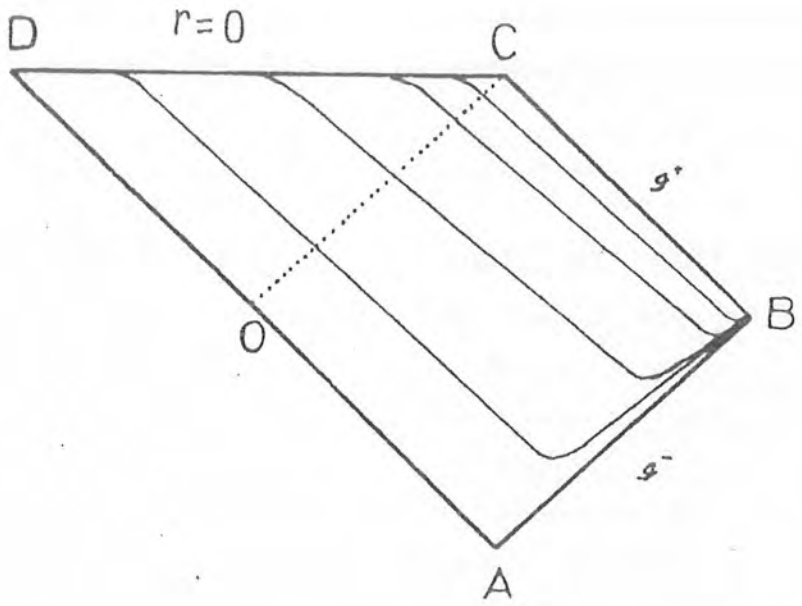

Figure 2.4. The SH for the Schwarzschild geometry are shown in the upper part of the Penrose diagram, for different values of t_o, which pass smoothly through the event horizon, OC = $\{r=2m,\ t_o=+\infty\}$ shown by a dotted line. The compactification gives the null surface BAD = $\{r=2m,\ t_o=-\infty\} \cup \mathscr{I}^-$ and BC = $\mathscr{I}^+$ as $t_o \longrightarrow -\infty$ and $+\infty$ respectively, shown as hard lines. A is past timelike infinity $I^- = \{\xi = \pi/2 = -\psi\}$, C is future timelike infinity $I^+ = \{\xi = \pi/2 = \psi\}$ and B is spacelike infinity $I^o = \{\xi = \pi,\ \psi = 0\}$.

$r = 0$ is a spacelike singularity whose points are labelled by different values of t. (In our foliation these are the t_o values for the points where the hypersurfaces hit the singularity.) Since C is at $t = +\infty$, D should be at $t = -\infty$. Hence it *should* be I^-. The edge joining D and E should, then, be $\mathscr{I}^-$ in the maximal extension. The "arrow of time" having been defined, it is clear that the other edge is $\mathscr{I}^+$ and F is I^+. Changing ξ to $-\xi$ in Eq.(2.3.24) flips the foliating hypersurfaces into the maximal extension. Now no part of the foliation enters the original part of the spacetime. The compactification of the union of these two sequences of foliating hypersurfaces gives the complete Penrose diagram (see Fig.2.5).

The re-labelling discussed above is important in that it changes the significance of the maximal extension of the spacetime. Now there are no future directed geodesics emerging *out* of a black hole, as the initial Cauchy surface is BAD, but only geodesics going *into* it (at OC). Time reversal does *not* take the geodesics out but instead provides a "mirror image" (the maximal extension) with the geodesics always still going into the black hole (now at OF). As such there are no white holes but only time reversed black holes.

Notice that we have complete Cauchy surfaces in the non-extended spacetime, for its future development, with the data on the hypersurface at the singularity not

propagating off the singularity. (BAD is a complete Cauchy surface for future and past development.) One of the main reasons for introducing the maximal extension of the Schwarzschild spacetime was to provide complete SHs. Since these can be provided without reference to the maximal extension, it is worth questioning whether any greater physical significance should be attached to the maximal extension.

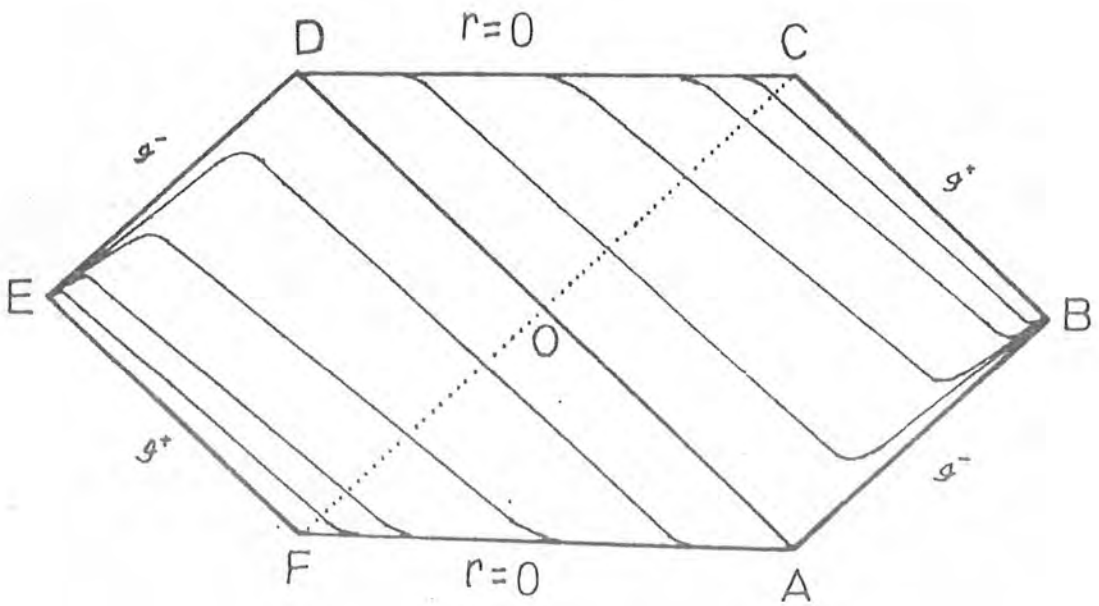

Figure 2.5. The union of the two sequences of spacelike hypersurfaces for the Schwarzschild foliates the entire Penrose diagram. The compactification now gives $\mathscr{I}^- \cup \mathscr{I}^+ \cup$ AD twice over. Notice that it is natural to regarded D as I^- and F as I^+.

In §.3.5 we discuss the quantisation of the scalar field on the $\psi\mathcal{N}$-hypersurfaces. The point of difference from Hawking is that he quantised the scalar fields on null hypersurfaces at $\mathscr{I}^+$, but we quantise them on $\psi\mathcal{N}$-hypersurfaces.

CHAPTER THREE

QUANTISATION OF SCALAR FIELDS ON SPACELIKE HYPERSURFACES

In this chapter, to find the VEV of the number operator, we will quantise the massive scalar fields on: i) CKST hypersurfaces; ii) CMEC hypersurfaces; and iii) ψN-hypersurfaces.

3.1. The Scalar Field Equation in KS Coordinates

Consider a massive scalar field $\Phi(x^o,x)$ defined at all points (x^o,x) of the Schwarzschild spacetime satisfying the KG equation (1.2.2). In this section we will solve Eq.(1.2.2) in KS coordinates. Usually the KG equation can be solved by the method of separation of variables. We know that the line element given by Eq.(2.1.1) is spherically symmetric, which guarantees that the spherical harmonics provide a complete basis for the angular part. Inserting Eq.(2.1.1) into Eq.(1.2.2), we have

$$\frac{1}{f^2}\frac{\partial}{\partial v}(r^2\frac{\partial\Phi}{\partial v})-\frac{1}{f^2}\frac{\partial}{\partial u}(r^2\frac{\partial\Phi}{\partial u})+M^2r^2\Phi$$
$$=\frac{1}{\sin\theta}\frac{\partial}{\partial\theta}(\sin\theta\frac{\partial\Phi}{\partial\theta})+\frac{1}{\sin^2\theta}\frac{\partial^2}{\partial\phi^2}. \qquad (3.1.1)$$

The right hand side of Eq.(3.1.1) gives the spherical harmonics $Y_{lm}(\theta,\phi)$ by putting the separation constant $\lambda^2 = l(l+1)$, l being the usual angular momentum quantum number, $l=0,1,2...$ and m an integer taking values $-l, -l+1, ...,l$.

Therefore, the L.H.S. of Eq.(3.1.1), by substituting the separation constant λ^2, takes the form

$$\frac{\partial^2 L_{lm}}{\partial v^2} - \frac{\partial^2 L_{lm}}{\partial u^2} + 2\frac{r_{,0}}{r}\frac{\partial L_{lm}}{\partial v} - 2\frac{r_{,1}}{r}\frac{\partial L_{lm}}{\partial u} + f^2(M^2+\frac{\lambda^2}{r^2})L_{lm}=0. \qquad (3.1.2)$$

Since r is a function of u and v, this equation is not separable.

To solve Eq.(3.1.2), we take the ansatz that $L_{lm}(v,u)$ can be written as

$$L_{lm}(v,u) = \sum_n R_{lmn\omega}(u)\ exp(-i\omega v), \qquad (3.1.3)$$

where

$$\omega = \sqrt{l^2+m^2+n^2+M^2}.$$

Then by substituting Eq.(3.1.3) into Eq.(3.1.2), we have

$$\frac{d^2R_{lmn\omega 1}(u)}{du^2} + 2\frac{r_{,1}}{r}\frac{dR_{lmn\omega 1}(u)}{du} - 2\omega\frac{r_{,0}}{r}R_{lmn\omega 2}(u)$$
$$+\{\omega^2 - f^2(M^2 + \frac{\lambda^2}{r^2})\}R_{lmn\omega 1}(u) = 0, \qquad (3.1.4)$$

and

$$\frac{d^2R_{lmn\omega 2}(u)}{du^2} + 2\frac{r_{,1}}{r}\frac{dR_{lmn\omega 2}(u)}{du} + 2\omega\frac{r_{,0}}{r}R_{lmn\omega 1}(u)$$
$$+\{\omega^2 - f^2(M^2 + \frac{\lambda^2}{r^2})\}R_{lmn\omega 2}(u) = 0, \qquad (3.1.5)$$

where

$$R_{lmn\omega}(u) = R_{lmn\omega 1}(u) + iR_{lmn\omega 2}(u). \qquad (3.1.6)$$

It does not appear that there is an analytic solution of the coupled differential equations (3.1.4) and (3.1.5).

We need to demonstrate that there exists a complete orthonormal basis for $L_{lm}(v,u)$ given by $R_{lmn\omega}(u)$ which solve Eqs.(3.1.4) and (3.1.5). In the absence of an analytic solution we solve these equations numerically, using the Runge-Kutta method for different choices of SHs. We solve these coupled differential equations term by term for each value of l, m, n and M.

We now check, for a given number of l, m, n that the solutions are orthonormal. The full orthonormal basis is then given by

$$\psi_{lmn\omega}(v,u,\theta,\phi) = A_{lmn}R_{lmn\omega}(u)Y_{lm}(\theta,\phi)exp(-i\omega v), \qquad (3.1.7)$$

where A_{lmn} are normalisation constants, ω is the energy of the nth mode (in Planck units i.e. $\hbar = 1 = c = G$) and $R_{lmn\omega}(u)$ satisfies the radial part of Eq.(1.2.2). In §.3.2, we give a complete procedure of quantisation of spacelike hypersurfaces.

3.2. Quantisation on Spacelike Hypersurfaces

In this section we will give the complete procedure of quantisation of scalar fields on SHs. For this purpose, suppose that $R_{lmn\omega}(u)$ satisfy the orthonormality condition

$$\int_{u_i}^{u_f} R_{lmn\omega}(u)R^{*}_{l',m',n',\omega'}(u)r^2(u)du=\delta_{ll'}\delta_{mm'}\delta_{nn'}\delta(\omega-\omega'), \qquad (3.2.1)$$

over the SH. To evaluate the normalisation constant, we put

Eq.(3.1.7) into Eq.(1.2.5), for the SH, then

$$
\begin{aligned}
&(\psi_{lmn\omega},\ \psi_{l'm'n'\omega'}) = \delta_{ll'}\delta_{mm'}\delta_{nn'}\delta(\omega-\omega') \\
&=\int -i\ [A_{lmn}R_{lmn\omega}(u)Y_{lm}(\theta,\phi)\exp(-i\omega v) \\
&\times A^{*}_{l'm'n'}R^{*}_{l'm'n'\omega'}(u)Y^{*}_{l'm'}(\theta,\phi)\exp(i\omega' v)(i\omega')g^{oo}\sqrt{|g|} \\
&-(-i\omega)A_{lmn}R_{lmn\omega}(u)Y_{lm}(\theta,\phi)\exp(-i\omega v) \\
&\times A^{*}_{l'm'n'}R^{*}_{l'm'n'\omega'}(u)Y^{*}_{l'm'}(\theta,\phi)\exp(i\omega' v) \\
&\times g^{oo}\sqrt{|g|}]\,du\,d\theta\,d\phi \\
&=(\omega+\omega')A_{lmn}A^{*}_{l'm'n'}\int R_{lmn\omega}R^{*}_{l'm'n'\omega'}Y_{lm}Y^{*}_{l'm'} \\
&\times \exp\{-i(\omega-\omega')v\}\ r^{2}\sin\theta\ du\,d\theta\,d\phi\ .
\end{aligned}
$$

Applying Eqs.(3.2.1) and the orthonormality conditions for $Y_{lm}(\theta,\phi)$, we get

$$
\begin{aligned}
\delta_{ll'}\delta_{mm'}\delta_{nn'}\delta(\omega-\omega') = (\omega+\omega')A_{lmn}A^{*}_{l'm'n'}&\sqrt{\frac{(l+m)!}{(l-m)!}\frac{2}{2l+1}} \\
&\times \delta_{ll'}\delta_{mm'}\delta_{nn'}\sqrt{\frac{(l'+m')!}{(l'-m')!}\frac{2}{2l'+1}} \\
&\times 2\pi\ \exp\{-i(\omega-\omega')v\}.
\end{aligned}
$$

Therefore,

$$
A_{lmn} = \frac{1}{\sqrt{4\pi\omega}}\sqrt{\frac{(l-m)!}{(l+m)!}\frac{2}{2l+1}}\ . \qquad (3.2.2)
$$

Here we use the fact that $A_{lmn} = A^{*}_{lmn}$. Thus corresponding to the SH, one solution set of Eq.(1.2.2) is given by Eq.(3.1.7), where A_{lmn} is given by Eq.(3.2.2). This solution set satisfies the orthonormality conditions

$$
\left.
\begin{aligned}
&(\psi_{lmn\omega},\ \psi_{l'm'n'\omega'}) = \delta_{ll'}\delta_{mm'}\delta_{nn'}\delta(\omega-\omega'), \\
&(\psi_{lmn\omega},\ \psi^{*}_{l'm'n'\omega'}) = 0. \qquad (\forall\ l,m,n)
\end{aligned}
\right\} \qquad (3.2.3)
$$

Now, we quantise the massive scalar fields on the SH.

For canonical quantisation, we take Φ as an operator and impose the equal time commutation relations (1.2.9) on Φ. The canonically conjugate momentum Π, given by Eq.(1.2.10), becomes

$$\Pi(v,u,\theta,\phi) = r^2 \sin\theta \frac{\partial\Phi}{\partial v}. \tag{3.2.4}$$

Since the field modes $\psi_{lmn\omega}$ and their complex conjugates $\psi^*_{lmn\omega}$ form a complete orthonormal basis with scalar product (1.2.5), Φ can be expanded as

$$\Phi(v,u,\theta,\phi) = \sum_{lmn} (a_{lmn\omega}\psi_{lmn\omega} + a^\dagger_{lmn\omega}\psi^*_{lmn\omega}). \tag{3.2.5}$$

To find $a_{lmn\omega}$ and $a^\dagger_{lmn\omega}$, consider the integral over the SH

$$\begin{aligned}&\int\psi^*_{lmn\omega}\Phi\, g^{oo}\sqrt{|g|}\, du d\theta d\phi \\ &= \sum_{l'm'n'}\int\psi^*_{lmn\omega}(a_{l'm'n'\omega'}\psi_{l'm'n'\omega'} + a^\dagger_{l'm'n'\omega'}\psi^*_{l'm'n'\omega'}) \\ &\qquad \times r^2\sin\theta\, du d\theta d\phi\ .\end{aligned} \tag{3.2.6}$$

Using Eqs.(3.2.1), (3.2.2) and the orthonormality conditions for $Y_{lm}(\theta,\phi)$ into Eq.(3.2.6), we get

$$\begin{aligned}&\int\psi^*_{lmn\omega}\Phi\, g^{oo}\sqrt{|g|}\, du d\theta d\phi \\ &= \frac{1}{2\omega}\{a_{lmn\omega} + exp(2i\omega v)\, a^\dagger_{(-l)(-m)(-n)(-\omega)}\}.\end{aligned} \tag{3.2.7}$$

Similarly,

$$\begin{aligned}&\int\psi^*_{lmn\omega}(\frac{\partial\Phi}{\partial v})g^{oo}\sqrt{|g|}\, du d\theta d\phi \\ &= \frac{-i}{2}\{a_{lmn\omega} - exp(2i\omega v)a^\dagger_{(-l)(-m)(-n)(-\omega)}\}.\end{aligned} \tag{3.2.8}$$

Combining Eqs.(3.2.7) and (3.2.8), we have

$$a_{lmn\omega} = i\int_{\Sigma} \psi^{*}_{lmn\omega} \overleftrightarrow{f} \Phi \; d\Sigma \;, \tag{3.2.9}$$

$$a^{\dagger}_{lmn\omega} = -i\int_{\Sigma} \psi_{lmn\omega} \overleftrightarrow{f} \Phi \; d\Sigma \;, \tag{3.2.10}$$

where Σ is a SH. Further, Eqs.(3.2.9) and (3.2.10) yield

$$[a_{lmn\omega}, a^{\dagger}_{l'm'n'\omega'}] = \int_{\Sigma}\int_{\Sigma'} [\psi_{lmn\omega} \overleftrightarrow{f} \Phi, \; \psi^{*}_{l'm'n'\omega'} \overleftrightarrow{f} \Phi'] d\Sigma d\Sigma'$$

or

$$[a_{lmn\omega} \; a^{\dagger}_{l'm'n'\omega'}] \iint [\psi^{*}_{lmn\omega}(\frac{\partial\Phi}{\partial v}) - i\omega \; \psi^{*}_{lmn\omega}\Phi \;,$$

$$\psi^{*}_{l'm'n'\omega'}(\frac{\partial\Phi'}{\partial v}) + i\omega' \psi^{*}_{l'm'n'\omega'}\Phi']$$

$$\times g^{oo}\sqrt{|g|}\; du d\theta d\phi du' d\theta' d\phi' \;.$$

Using Eq.(3.2.4), we have

$$[a_{lmn\omega}, a^{\dagger}_{l'm'n'\omega'}] = \iint \{[\psi^{*}_{lmn\omega}\Pi, \psi_{l'm'n'\omega'}\Pi'] + i\omega' [\psi^{*}_{lmn\omega}\Pi \;, \psi_{l'm'n'\omega'}\Phi'] g^{oo}\sqrt{|g|} - i\omega [\psi^{*}_{lmn\omega}\Phi \;, \psi_{l'm'n'\omega'}\Pi'] g^{oo}\sqrt{|g|} + \omega\omega' [\psi^{*}_{lmn\omega}\Phi \;, \psi_{l'm'n'\omega'}\Phi'] g^{oo}|g|g^{oo}\}$$

$$\times du d\theta d\phi du' d\theta' d\phi' \;.$$

Applying Eqs.(1.2.9), we get

$$[a_{lmn\omega}, a^{\dagger}_{l'm'n'\omega'}] = -i\int_{\Sigma} \psi_{lmn\omega} \overleftrightarrow{f} \psi^{*}_{l'm'n'\omega'} d\Sigma$$

$$= (\psi_{lmn\omega}, \; \psi_{l'm'n'\omega'}). \tag{3.2.11}$$

Thus Eqs.(3.2.3) and (3.2.11) give

$$[a_{lmn\omega}, a^{\dagger}_{l'm'n'\omega'}] = \delta_{ll'}\delta_{mm'}\delta_{nn'}\;\delta(\omega-\omega'). \tag{3.2.12}$$

Similarly,

$$[a_{lmn\omega}, \; a_{l'm'n'\omega'}] = 0 = [a^{\dagger}_{lmn\omega}, \; a^{\dagger}_{l'm'n'\omega'}]. \tag{3.2.13}$$

The vacuum state $|0\rangle$ is annihilated by all $a_{lmn\omega}$ operators and $|1\rangle$ for a given mode is created by $a^{\dagger}_{lmn\omega}$ i.e.

$$\left.\begin{aligned} a_{lmn\omega}|0\rangle &= 0, \qquad (\forall\ l,m,n) \\ a^{\dagger}_{lmn\omega}|0\rangle &= |1_{lmn\omega}\rangle, \end{aligned}\right\} \tag{3.2.14}$$

and the number operator N is, therefore,

$$N = \sum_{lmn} N_{lmn\omega} = \sum_{lmn} a^{\dagger}_{lmn\omega} a_{lmn\omega}. \tag{3.2.15}$$

Hence by using Eqs.(3.2.14) and (3.2.15),

$$\langle 0|N_{lmn\omega}|0\rangle = 0$$

implies that

$$\langle 0|N|0\rangle = 0. \tag{3.2.16}$$

Now consider another solution set of Eq.(1.2.2)

$$\bar{\psi}_{lmn\omega}(v,u,\theta,\phi) = \bar{A}_{lmn}\bar{R}_{lmn\omega}(u)\bar{Y}_{lm}(\theta,\phi)\exp(-i\bar{\omega}v), \tag{3.2.17}$$

where

$$\bar{A}_{lmn} = \sqrt{\omega\ /\ \bar{\omega}}\ . \tag{3.2.18}$$

Then the solution (3.2.17) satisfies the orthonormality conditions

$$\left.\begin{aligned} (\bar{\psi}_{lmn\omega},\ \bar{\psi}_{l'm'n'\omega'}) &= \delta_{ll'}\delta_{mm'}\delta_{nn'}\delta(\bar{\omega}-\bar{\omega}'), \\ (\bar{\psi}_{lmn\omega},\ \bar{\psi}^{*}_{l'm'n'\omega'}) &= 0. \end{aligned}\right\} \tag{3.2.19}$$

Since $\bar{\psi}_{lmn\omega}$ and $\bar{\psi}^{*}_{lmn\omega}$ form a complete orthonormal basis, therefore,

$$\Phi(v,u,\theta,\phi) = \sum_{lmn}(\bar{a}_{lmn\omega}\bar{\psi}_{lmn\omega} + \bar{a}^{\dagger}_{lmn\omega}\bar{\psi}^{*}_{lmn\omega}), \tag{3.2.20}$$

where $\bar{a}_{lmn\omega}$ and $\bar{a}^{\dagger}_{lmn\omega}$ are the annihilation and creation operators respectively. Using Eqs.(3.2.6)-(3.2.8), (3.2.17) and (3.2.18), we have

$$\bar{a}_{lmn\omega}=i\int_{\Sigma}\bar{\psi}^{*}_{lmn\omega}\overleftrightarrow{f}\Phi\ d\Sigma\ , \tag{3.2.21}$$

$$\bar{a}^{\dagger}_{lmn\omega}=-i\int_{\Sigma}\bar{\psi}_{lmn\omega}\overleftrightarrow{f}\Phi\ d\Sigma\ . \tag{3.2.22}$$

Also, the operators $\bar{a}_{lmn\omega}$ and $\bar{a}^{\dagger}_{lmn\omega}$ satisfy the equal time commutation relations (1.2.9) as

$$\left.\begin{aligned}&[\bar{a}_{lmn\omega},\ \bar{a}^{\dagger}_{l'm'n'\omega'}]=\delta_{ll'}\delta_{mm'}\delta_{nn'}\delta(\bar{\omega}-\bar{\omega}'),\\&[\bar{a}_{lmn\omega},\ \bar{a}_{l'm'n'\omega'}]=0=[\bar{a}^{\dagger}_{lmn\omega},\ \bar{a}^{\dagger}_{l'm'n'\omega'}].\end{aligned}\right\} \tag{3.2.23}$$

The new vacuum state $|\bar{0}\rangle$ is such that

$$\left.\begin{aligned}&\bar{a}_{lmn\omega}|\bar{0}\rangle=0,\qquad(\forall\ l,m,n)\\&\bar{a}^{\dagger}_{lmn\omega}|\bar{0}\rangle=|\bar{1}_{lmn\omega}\rangle.\end{aligned}\right\} \tag{3.2.24}$$

Since both solution sets $\psi_{lmn\omega}$ and $\bar{\psi}_{lmn\omega}$ are complete, therefore, the new modes $\bar{\psi}_{lmn\omega}$ can be expressed[4] in terms of the old modes $\psi_{lmn\omega}$ by

$$\bar{\psi}_{lmn\omega}=\sum_{l'm'n'}(\alpha_{lmn\omega l'm'n'\omega'}\psi_{l'm'n'\omega'}+\beta_{lmn\omega l'm'n'\omega'}\psi^{*}_{l'm'n'\omega'}). \tag{3.2.25}$$

Similarly,

$$\psi_{l'm'n'\omega'}=\sum_{lmn}(\alpha^{*}_{lmn\omega l'm'n'\omega'}\bar{\psi}_{lmn\omega}-\beta_{lmn\omega l'm'n'\omega'}\bar{\psi}^{*}_{lmn\omega}). \tag{3.2.26}$$

The relations (3.2.25) and (3.2.26) are known as the *Bogoluibov transformations* and the coefficients $\alpha_{lmn\omega l'm'n'\omega'}$ and $\beta_{lmn\omega l'm'n'\omega'}$ are known as the *Bogoluibov coefficients*. Now, Eqs.(3.2.25) and (3.2.26) yield

$$(\bar{\psi}_{lmn\omega},\psi_{l''m''n''\omega''})=\sum_{l'm'n'}\{\alpha_{lmn\omega l'm'n'\omega'}(\psi_{l'm'n'\omega'},\psi_{l''m''n''\omega''})+\beta_{lmn\omega l'm'n'\omega'}(\psi^{*}_{l'm'n'\omega'},\psi_{l''m''n''\omega''})\}.$$

Using Eqs.(3.2.3), we get

$$(\bar{\psi}_{lmn\omega}, \psi_{l''m''n''\omega''}) = \sum_{l'm'n'} \alpha_{lmn\omega l'm'n'\omega'} \delta_{l'l''} \delta_{m'm''} \delta_{n'n''} \times \delta(\bar{\omega}'-\omega'') = \alpha_{lmn\omega l''m''n''\omega''}$$

or

$$\alpha_{lmn\omega l'm'n'\omega'} = (\bar{\psi}_{lmn\omega}, \psi_{l'm'n'\omega'}). \tag{3.2.27}$$

Similarly,

$$\beta_{lmn\omega l'm'n'\omega'} = -(\bar{\psi}_{lmn\omega}, \psi^{*}_{l'm'n'\omega'}). \tag{3.2.28}$$

Thus, from Eqs.(1.2.5), (3.1.7) and (3.2.17), we have

$$\alpha_{lmn\omega l'm'n'\omega'} = (\bar{\omega}+\omega')\bar{A}_{lmn} A^{*}_{l'm'n'} \left[\int \bar{R}_{lmn\omega} R^{*}_{l'm'n'\omega'} r^2 du \times \int_0^{2\pi} \int_0^{\pi} \bar{Y}_{lm} Y^{*}_{l'm'} \sin\theta \, d\theta d\phi \right] exp\{-i(\bar{\omega}-\omega')v\}. \tag{3.2.29}$$

Applying Eqs.(3.2.1), (3.2.2) and (3.2.18) into Eq.(3.2.19), we get

$$\alpha_{lmn\omega l'm'n'\omega'} = \frac{(\bar{\omega}+\omega')}{2\sqrt{\bar{\omega}\,\omega'}} \delta_{ll'} \delta_{mm'} \delta_{nn'} \delta(\bar{\omega}-\omega') \times exp\{-i(\bar{\omega}-\omega')v\}. \tag{3.2.30}$$

Similarly,

$$\beta_{lmn\omega l'm'n'\omega'} = -\frac{(\bar{\omega}-\omega')}{2\sqrt{\bar{\omega}\,\omega'}} \delta_{ll'} \delta_{mm'} \delta_{nn'} \delta(\omega-\omega') \times exp\{-i(\bar{\omega}+\omega')v\}. \tag{3.2.31}$$

Further, the operators $a_{lmn\omega}$ and $a^{\dagger}_{lmn\omega}$ can be written[4] in terms of $\bar{a}_{lmn\omega}$ and $\bar{a}^{\dagger}_{lmn\omega}$ as

$$\left.\begin{aligned} a_{lmn\omega} &= \sum_{l'm'n'} (\alpha_{lmn\omega l'm'n'\omega'} \bar{a}_{l'm'n'\omega'} \\ &\quad + \beta^{*}_{lmn\omega l'm'n'\omega'} \bar{a}^{\dagger}_{l'm'n'\omega'}), \\ a^{\dagger}_{lmn\omega} &= \sum_{l'm'n'} (\alpha^{*}_{lmn\omega l'm'n'\omega'} \bar{a}_{l'm'n'\omega'} \\ &\quad + \beta_{lmn\omega l'm'n'\omega'} \bar{a}^{\dagger}_{l'm'n'\omega'}). \end{aligned}\right\} \qquad (3.2.32)$$

For the VEV of the number operator N, we have

$$\langle\bar{0}|N_{lmn\omega}|\bar{0}\rangle = \langle\bar{0}|a^{\dagger}_{lmn\omega}a_{lmn\omega}|\bar{0}\rangle. \qquad (3.2.33)$$

Inserting Eqs.(3.2.32) into Eq.(3.2.33), we get

$$\begin{aligned} \langle\bar{0}|N_{lmn\omega}|\bar{0}\rangle = \sum_{l'm'n'} \Big\{ & |\alpha_{lmn\omega l'm'n'\omega'}|^2 \langle\bar{0}|\bar{a}^{\dagger}_{l'm'n'\omega'}\bar{a}_{l'm'n'\omega'}|\bar{0}\rangle \\ & + \alpha^{*}_{lmn\omega l'm'n'\omega'}\beta^{*}_{lmn\omega l'm'n'\omega'} \langle\bar{0}|\bar{a}^{\dagger}_{l'm'n'\omega'}\bar{a}^{\dagger}_{l'm'n'\omega'}|\bar{0}\rangle \\ & - \alpha_{lmn\omega l'm'n'\omega'}\beta_{lmn\omega l'm'n'\omega'} \langle\bar{0}|\bar{a}_{l'm'n'\omega'}\bar{a}_{l'm'n'\omega'}|\bar{0}\rangle \\ & + |\beta_{lmn\omega l'm'n'\omega'}|^2 \langle\bar{0}|\bar{a}^{\dagger}_{l'm'n'\omega'}\bar{a}_{l'm'n'\omega'}|\bar{0}\rangle \Big\}. \end{aligned} \qquad (3.2.34)$$

Thus Eqs.(3.2.24), (3.2.30), (3.2.31) and (3.2.34) yield

$$\langle\bar{0}|N_{lmn\omega}|\bar{0}\rangle = \sum_{l'm'n'} |\beta_{lmn\omega l'm'n'\omega'}|^2 = 0. \ (\forall\ l,m,n) \qquad (3.2.35)$$

Thus the canonical quantisation procedure on the set of SH give a zero VEV of the number operator. In the next three sections we apply the quantisation procedure on the three types of SHs.

3.3. Quantisation on Spacelike Hypersurfaces of CKST

For the quantisation of scalar field on the SH of CKST, first we solve Eqs.(3.1.4) and (3.1.5) over $v = v_o$ (constant) hypersurfaces. Now, for $v = v_o$, Eq.(1.1.4) yields

$$u^2 = v_o^2 + (\frac{r}{2m} - 1)\ exp(\frac{r}{2m}). \qquad (3.3.1)$$

Substituting Eqs.(2.1.8) and (2.1.16) into Eqs.(3.1.4) and (3.1.5), the coupled differential equations take the form

$$\frac{d^2R_{lmn\omega 1}(u)}{du^2} + \frac{f^2u}{2mr}\frac{dR_{lmn\omega 1}(u)}{du} + \omega\frac{f^2v_o}{2mr}R_{lmn\omega 2}(u) + \{\omega^2 - f^2(M^2 + \frac{\lambda^2}{r^2})\}R_{lmn\omega 1}(u) = 0, \qquad (3.3.2)$$

and

$$\frac{d^2R_{lmn\omega 2}(u)}{du^2} + \frac{f^2u}{2mr}\frac{dR_{lmn\omega 2}(u)}{du} - \omega\frac{f^2v_o}{2mr}R_{lmn\omega 1}(u) + \{\omega^2 - f^2(M^2 + \frac{\lambda^2}{r^2})\}R_{lmn\omega 2}(u) = 0, \qquad (3.3.3)$$

where u is given by Eq.(3.3.1). It is found that $R_{lmn\omega}(u)$ is practically independent of the choice of v_o. We integrate both the differential equations, simultaneously, over the SH $v = v_o$. Numerically, (see Appendix A), it is found that the solutions must satisfy the orthonormality condition (3.2.1) with $v = v_o$. Different numerical solutions for $R_{lmn\omega}(u)$ are depicted in Fig.3.1 for different values of l, m, n and M at $v_o = -0.9995,\ 0,\ 0.9995$. In all cases these solutions converge to zero as u tends to infinity. This fact enables us to normalise the wave function over the SH v_o. Note that in Fig.3.1, there are many graphs in which the solution $R_{lmn\omega 1}(u)$ and $R_{lmn\omega 2}(u)$ do not touch the u-axis. If we draw the graph of full values, then we can not see the initial behavior of $R_{lmn\omega 1}(u)$ and $R_{lmn\omega 2}(u)$. We do not bother about this situation, because we have verified that for each value of l, m, n and M, the solutions $R_{lmn\omega 1}(u)$ and $R_{lmn\omega 2}(u)$ both

go to zero for large u. Thus the one solution set of the wave equation (1.2.2) over the SH of CKST is given by Eq.(3.1.7) at $v = v_o$. This solution set satisfies the

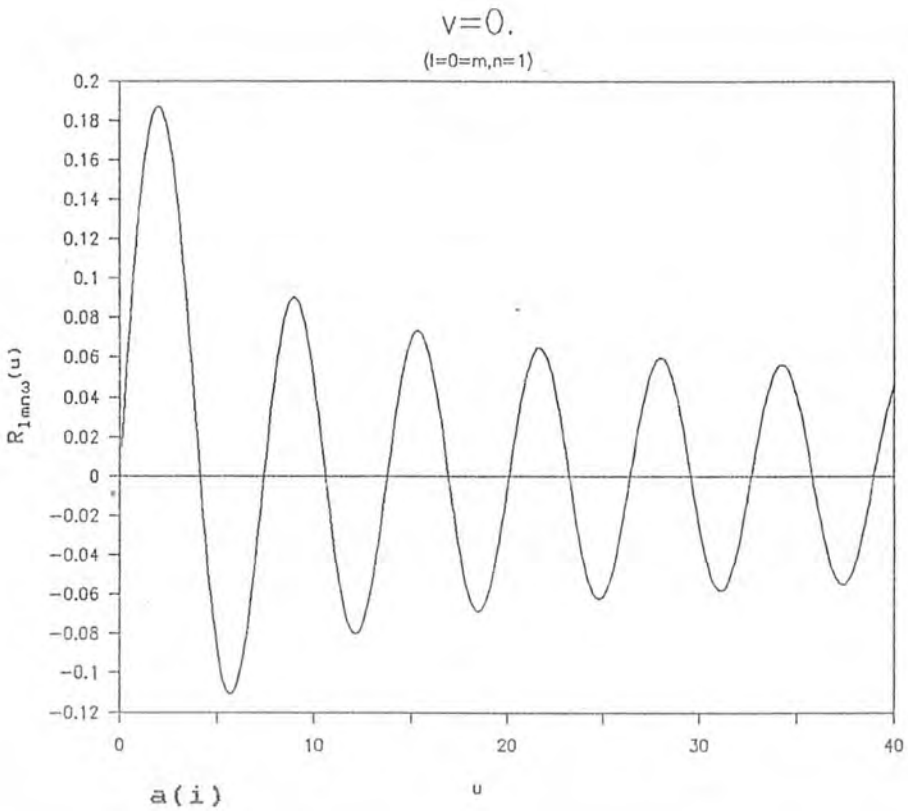

Figure 3.1. The normalised solutions of Eqs.(3.2.2) and (3.2.3) for massive fields for a) $l = 0$, $m = 0$, $n = 1$ b) $l = 0$, $m = 0$, $n = 2$ c) $l = 1$, $m = 1$, $n = 2$ d) $l = 2$, $m = +1$, $n = 3$ at i) $v_o = 0$, ii) $v_o = 0.9995$, iii) $v_o = -0.9995$ are shown, where for $v = 0$, $R_{lmn\omega_1}(u) = R_{lmn\omega_2}(u)$.

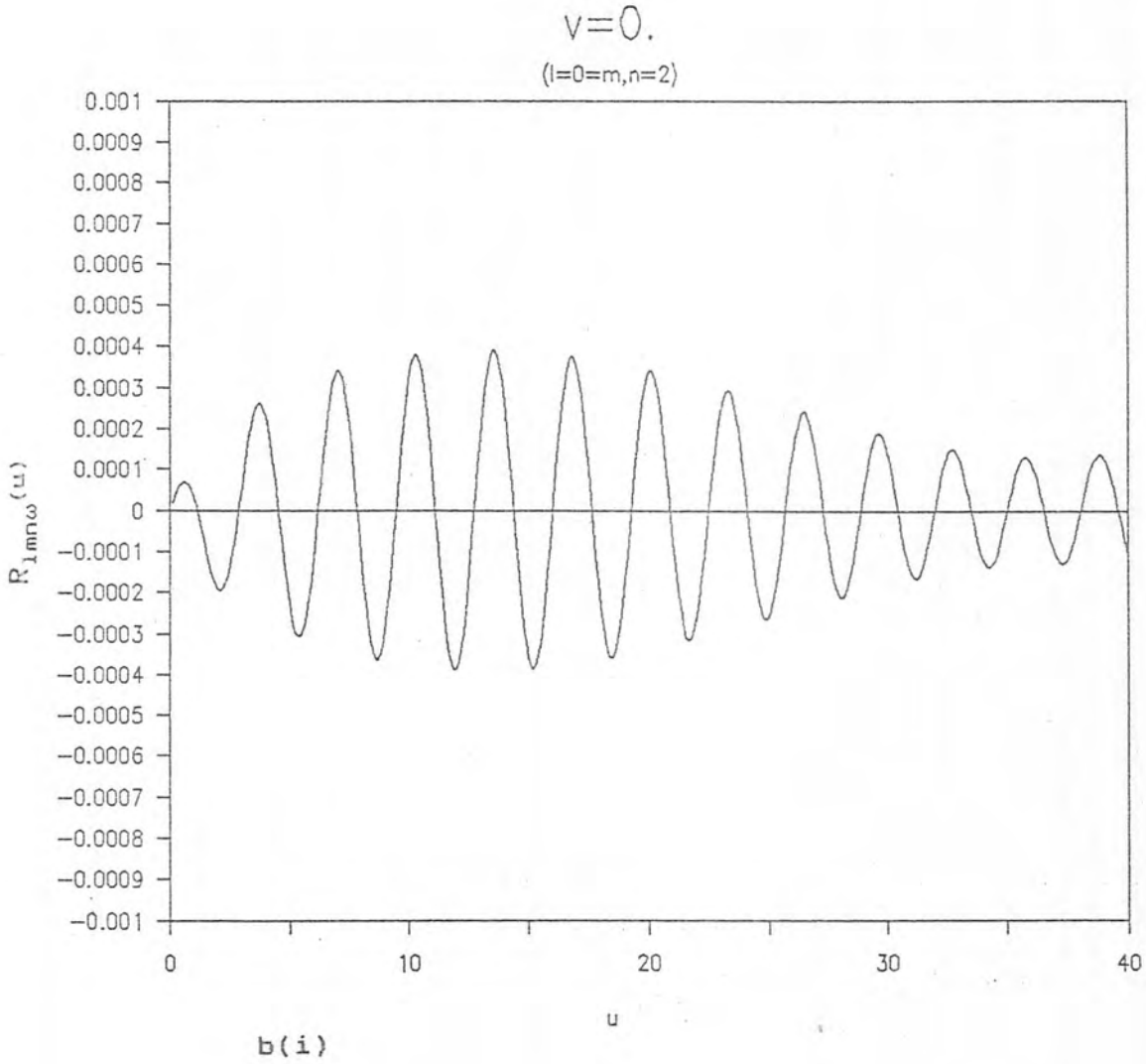
v=0.
(l=0=m,n=2)
0.001
0.0009
0.0008
0.0007
0.0006
0.0005
0.0004
0.0003
0.0002
0.0001
0
−0.0001
−0.0002
−0.0003
−0.0004
−0.0005
−0.0006
−0.0007
−0.0008
−0.0009
−0.001
$R_{lmn\omega}(u)$
0
10
20
30
40
u

b(i)

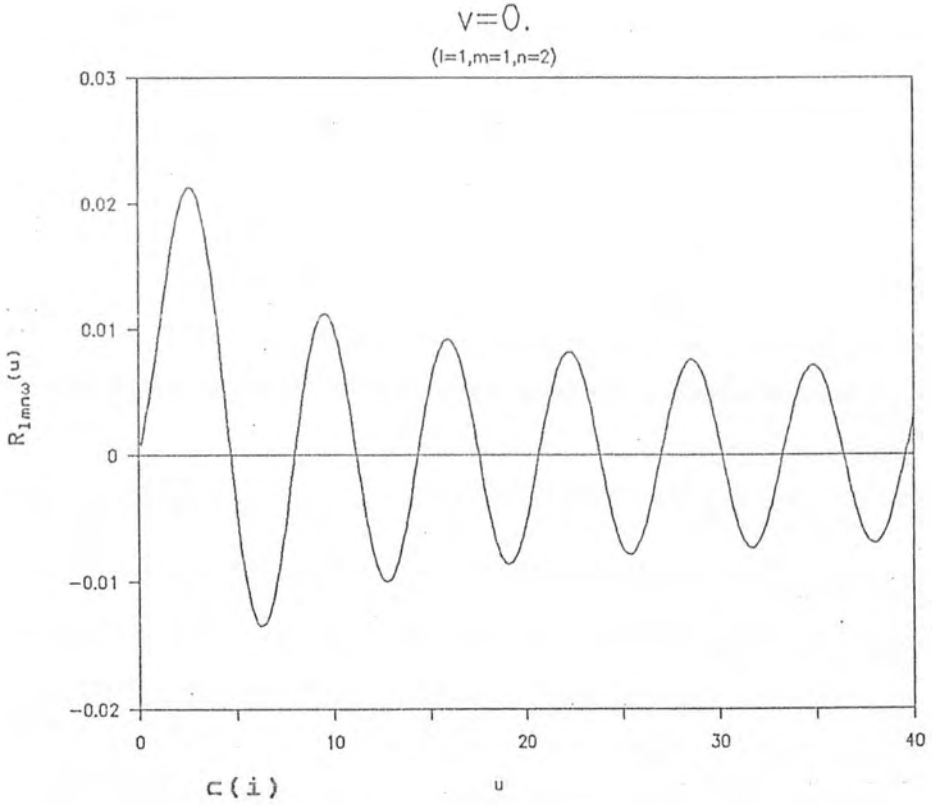
ν=0.
(l=1,m=1,n=2)
0.03
0.02
0.01
0
−0.01
−0.02
$R_{1mn\omega}(u)$
0
10
20
30
40
u
c(i)

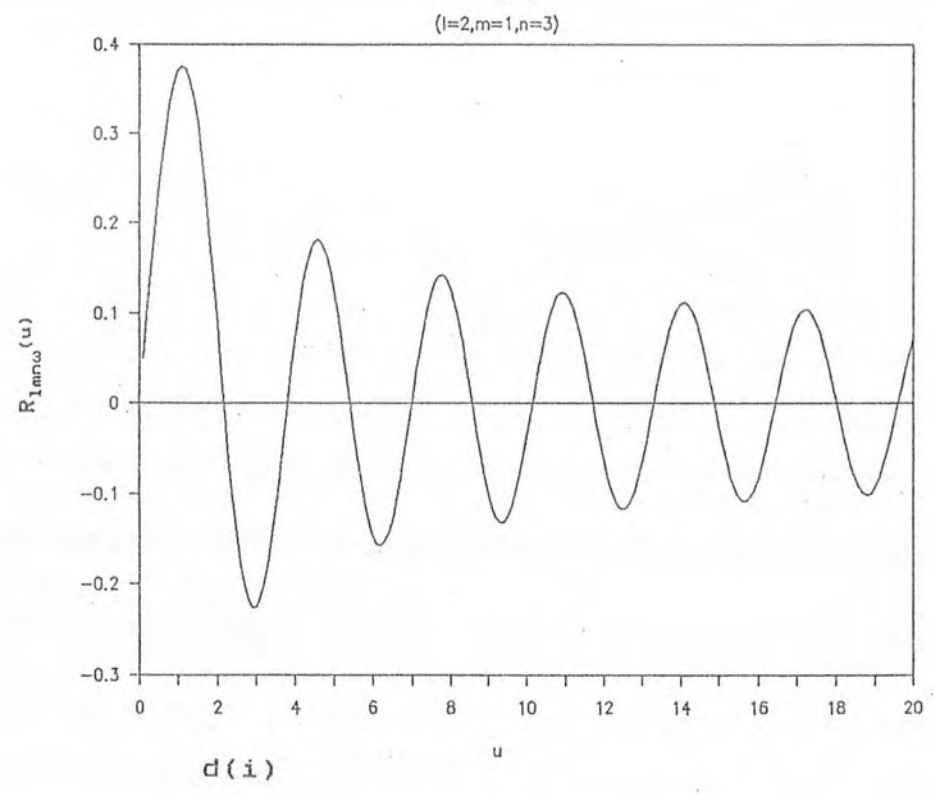
ν=0.
(l=2,m=1,n=3)
0.4
0.3
0.2
0.1
0
−0.1
−0.2
−0.3
$R_{1mn\omega}(u)$
0
2
4
6
8
10
12
14
16
18
20
u
d(i)

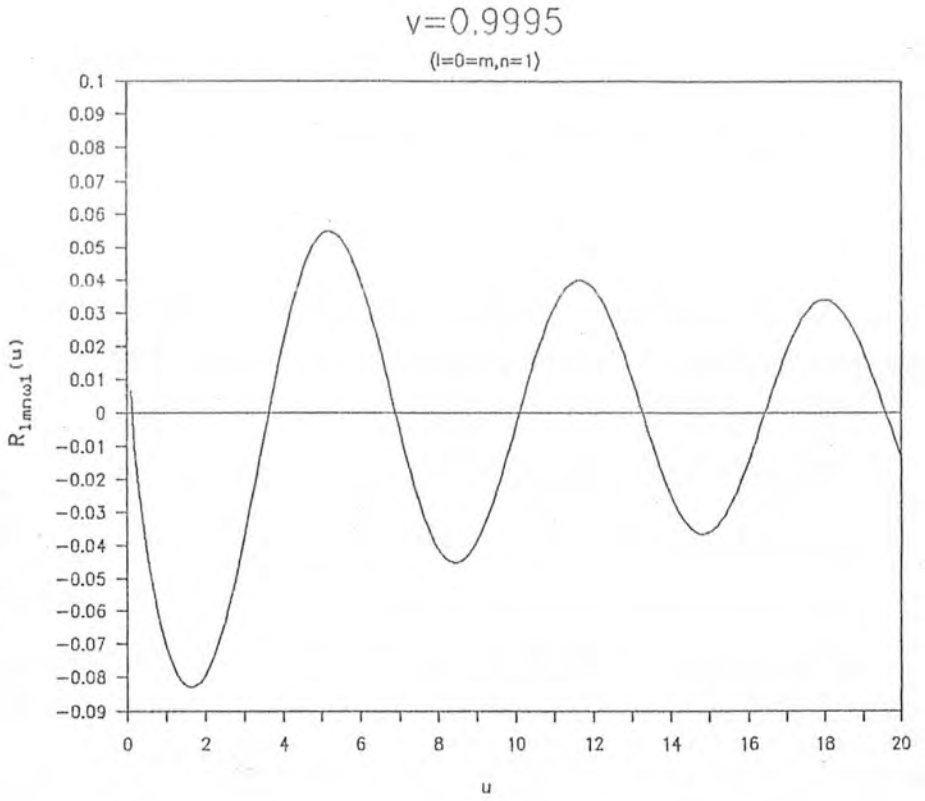

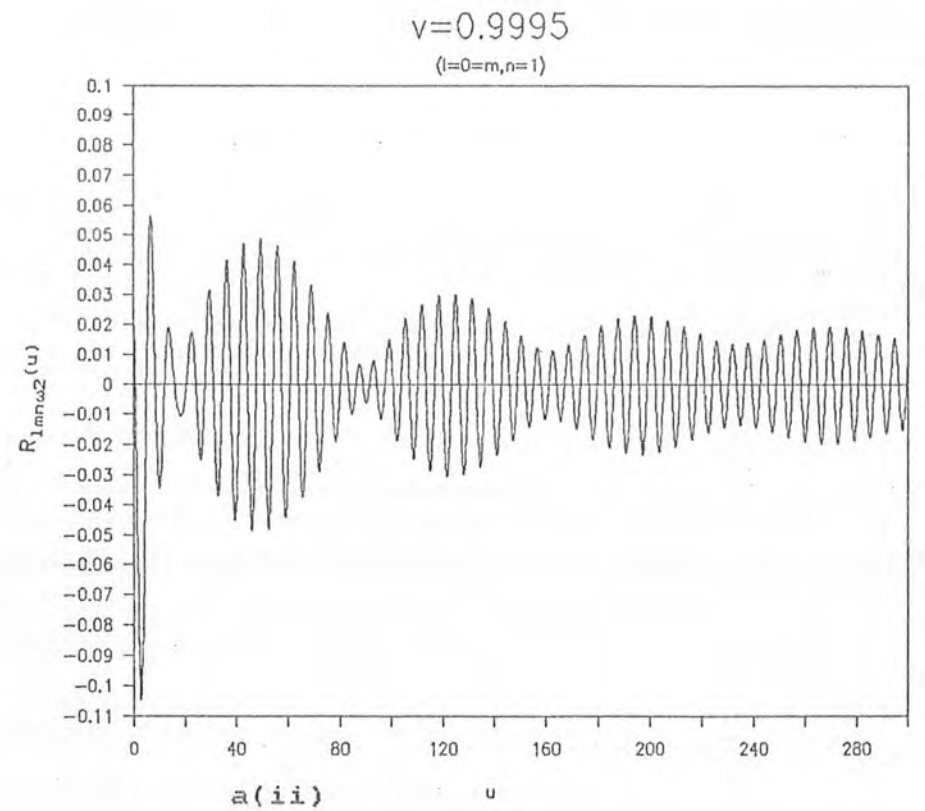

a(ii)

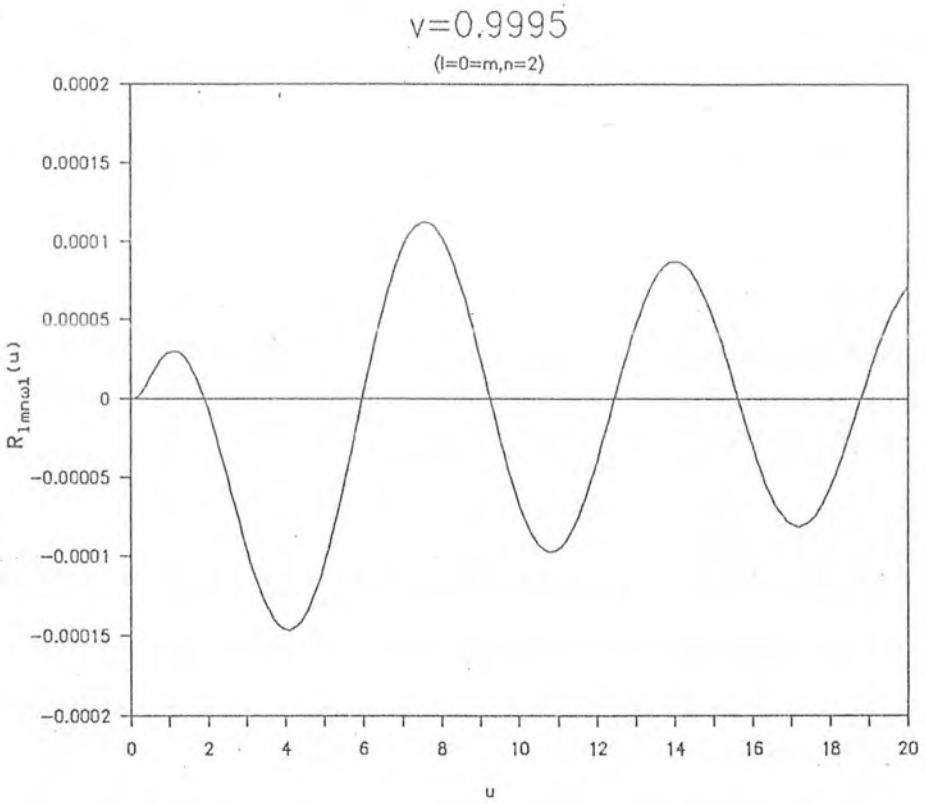
v=0.9995
(l=0=m,n=2)
0.0002
0.00015
0.0001
0.00005
0
−0.00005
−0.0001
−0.00015
−0.0002
$R_{1mn\omega1}(u)$
0
2
4
6
8
10
12
14
16
18
20
u

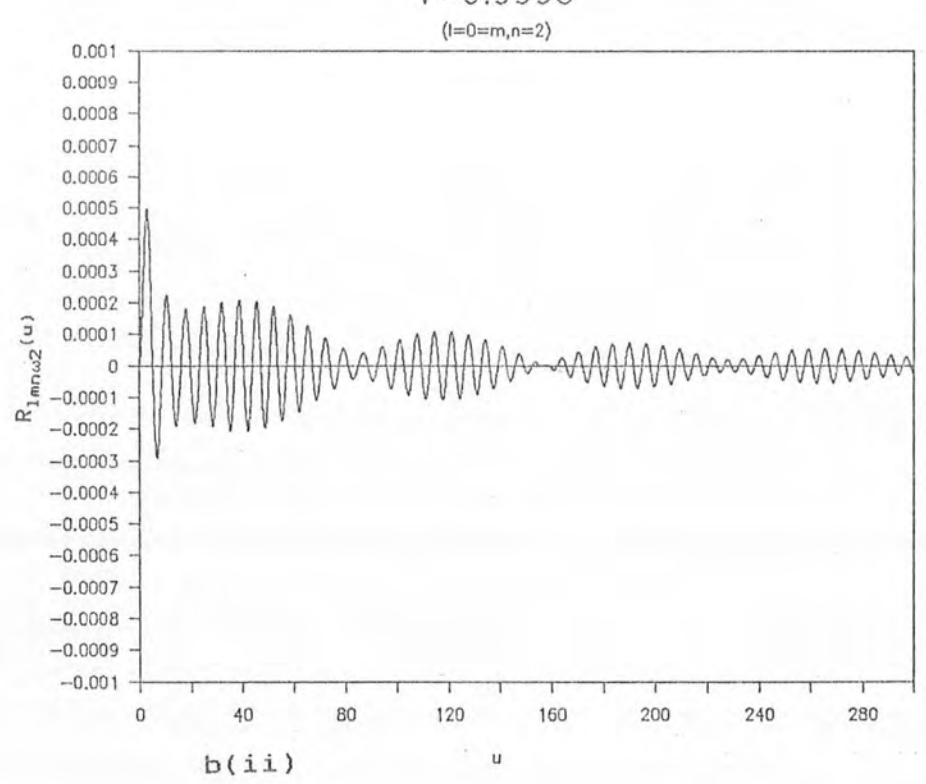
v=0.9995
(l=0=m,n=2)
0.001
0.0009
0.0008
0.0007
0.0006
0.0005
0.0004
0.0003
0.0002
0.0001
0
−0.0001
−0.0002
−0.0003
−0.0004
−0.0005
−0.0006
−0.0007
−0.0008
−0.0009
−0.001
$R_{1mn\omega2}(u)$
0
40
80
120
160
200
240
280
u

b(ii)

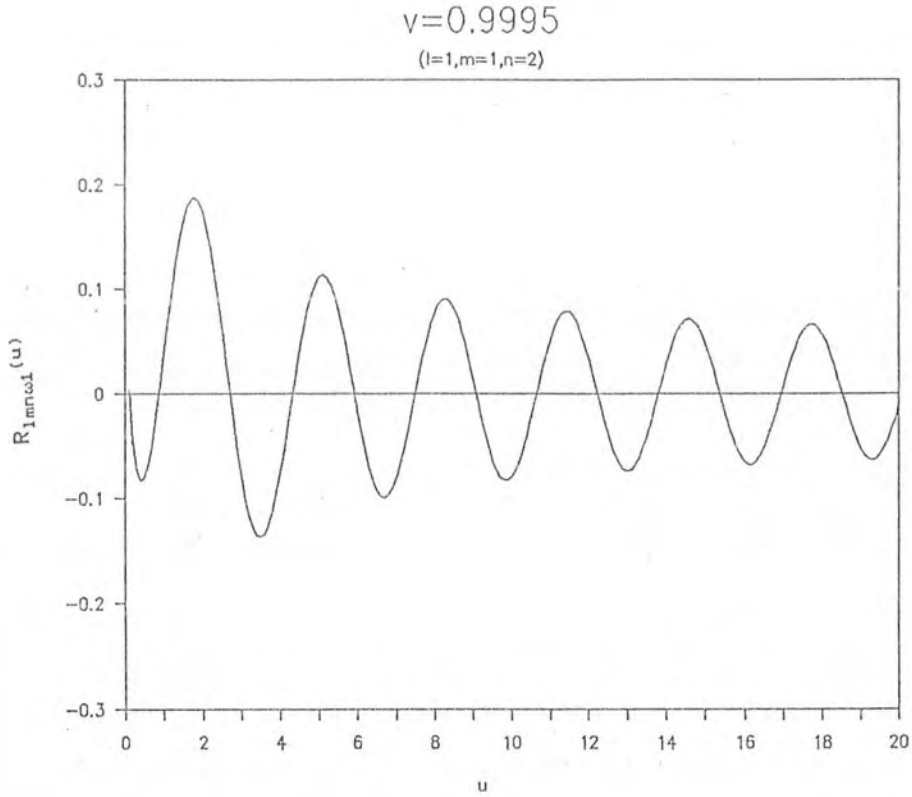

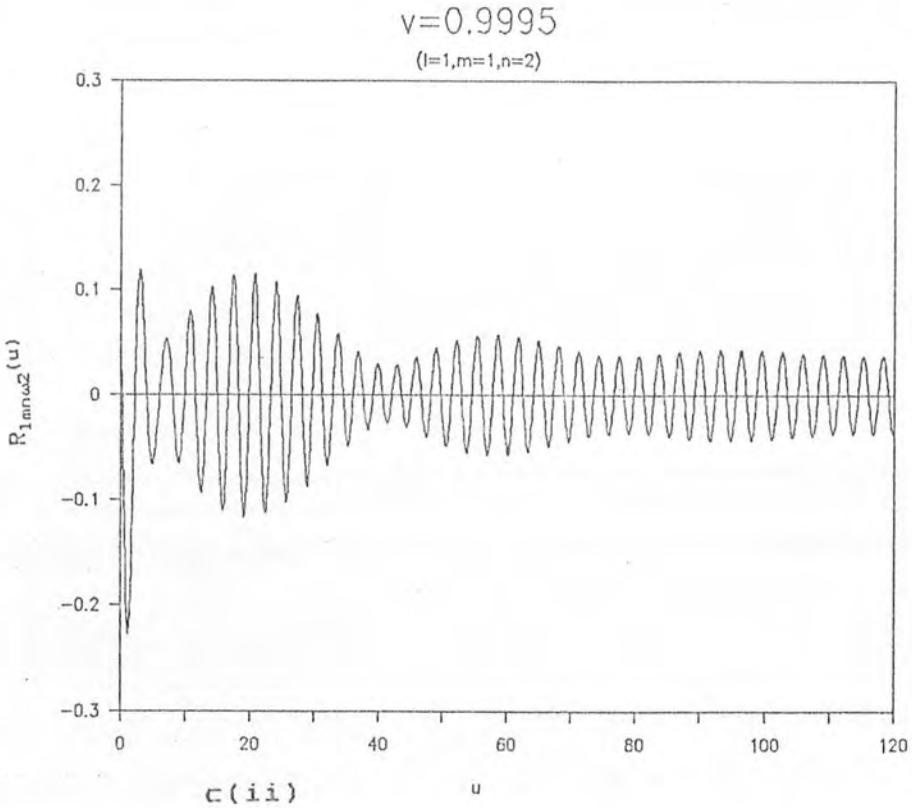

c(ii)

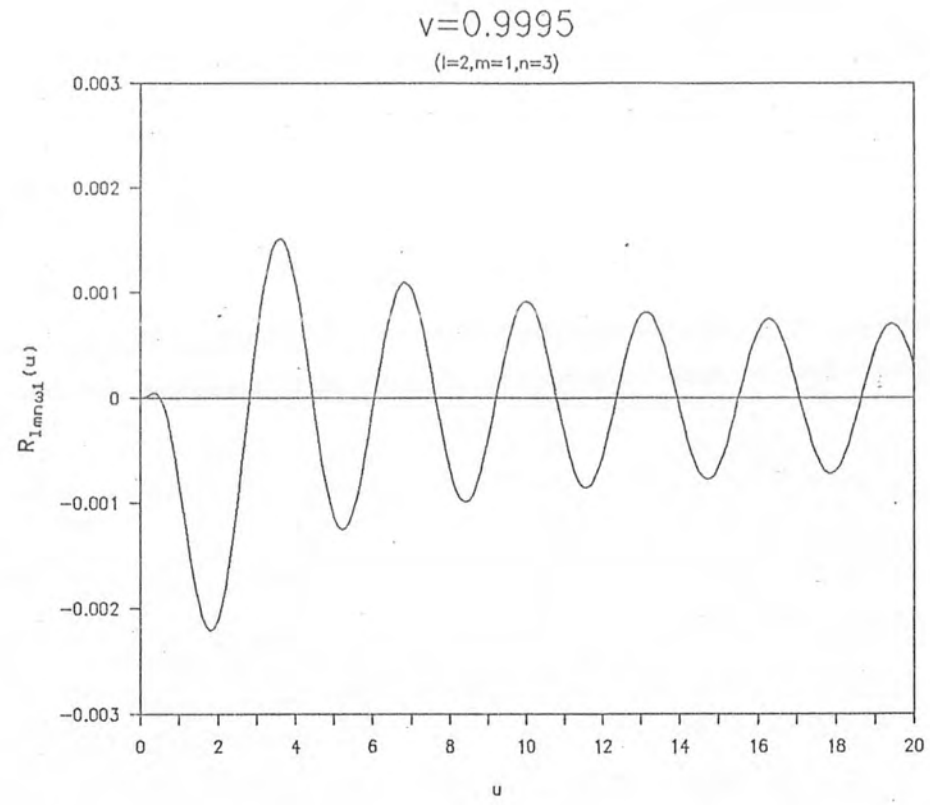
v=0.9995
(l=2,m=1,n=3)
0.003
0.002
0.001
0
−0.001
−0.002
−0.003
$R_{1mn\omega1}(u)$
0
2
4
6
8
10
12
14
16
18
20
u

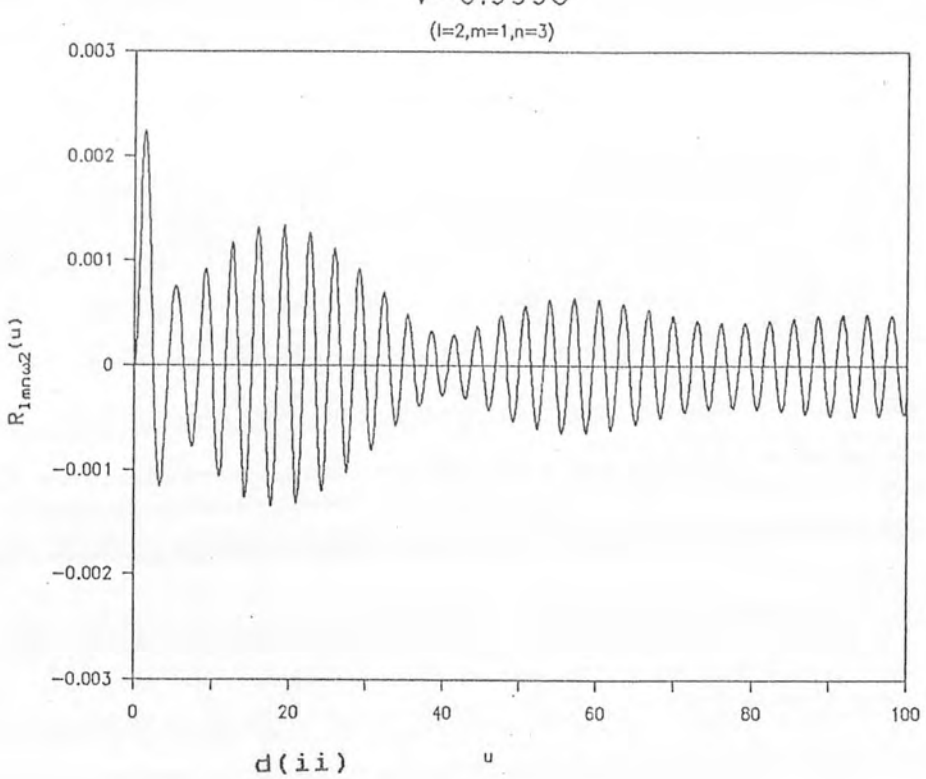
v=0.9995
(l=2,m=1,n=3)
0.003
0.002
0.001
0
−0.001
−0.002
−0.003
$R_{1mn\omega2}(u)$
0
20
40
60
80
100
u

d(ii)

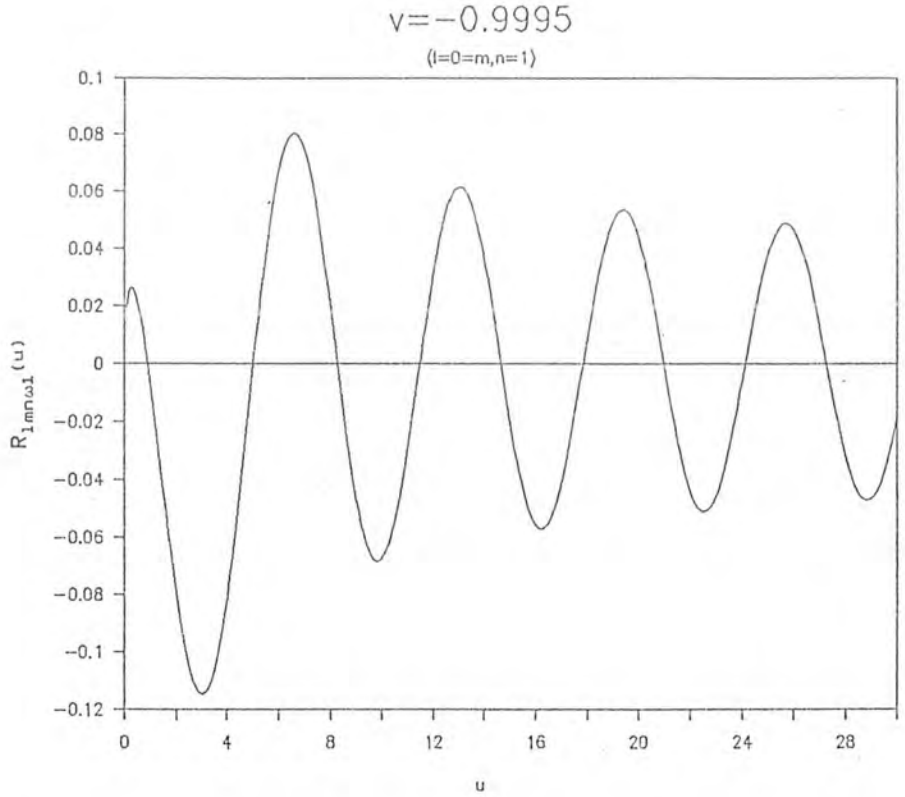

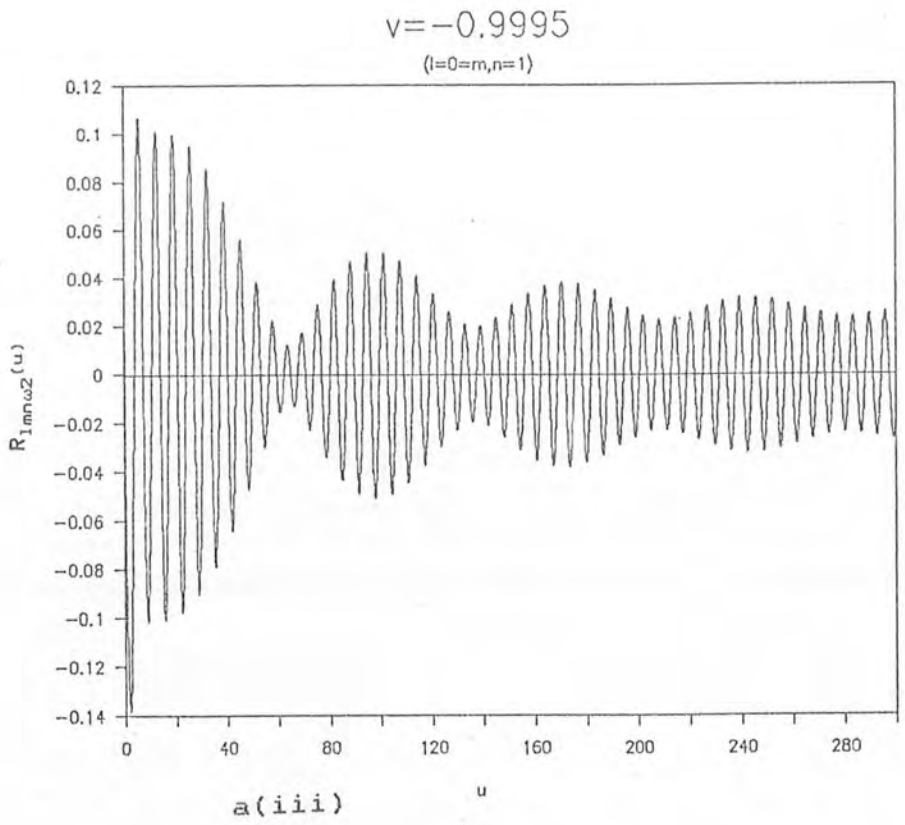

a(iii)

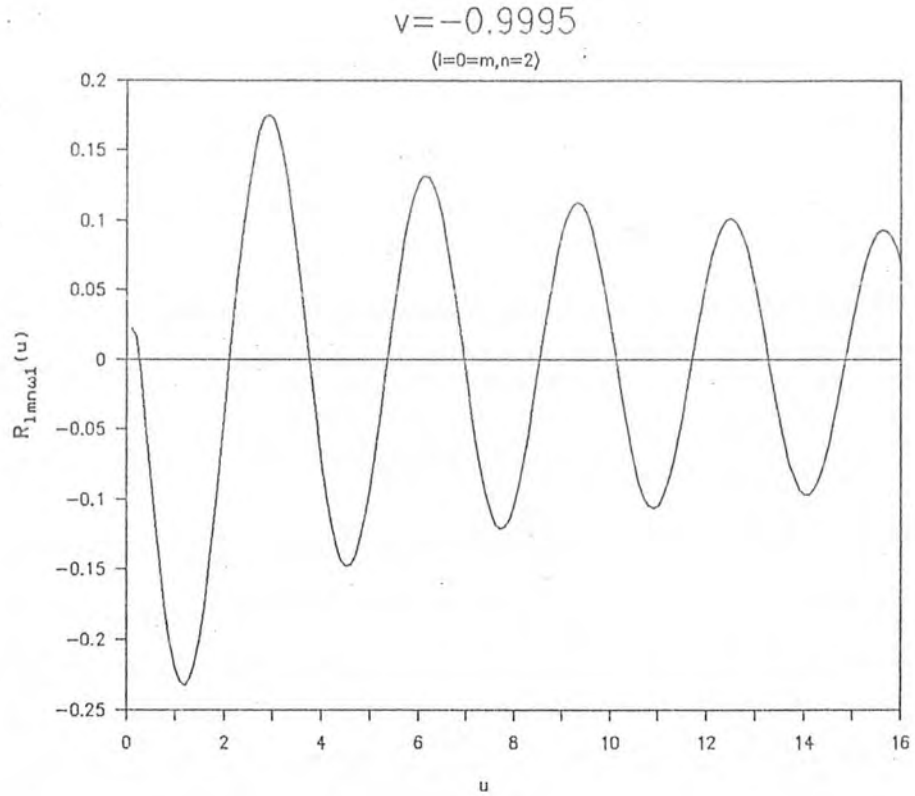

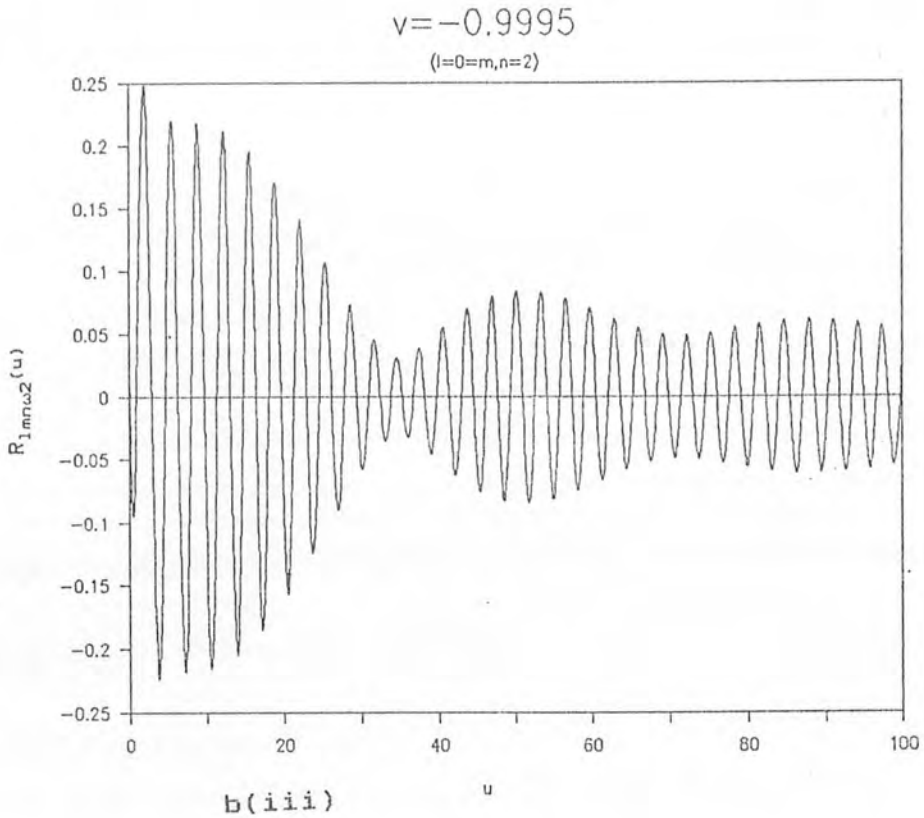

b(iii)

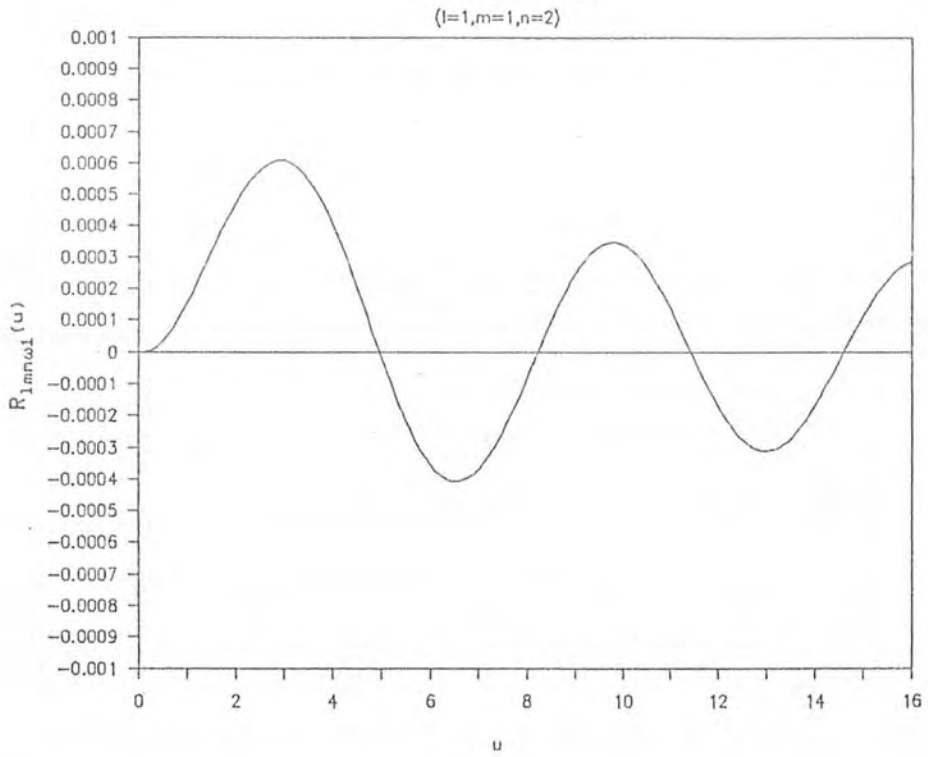

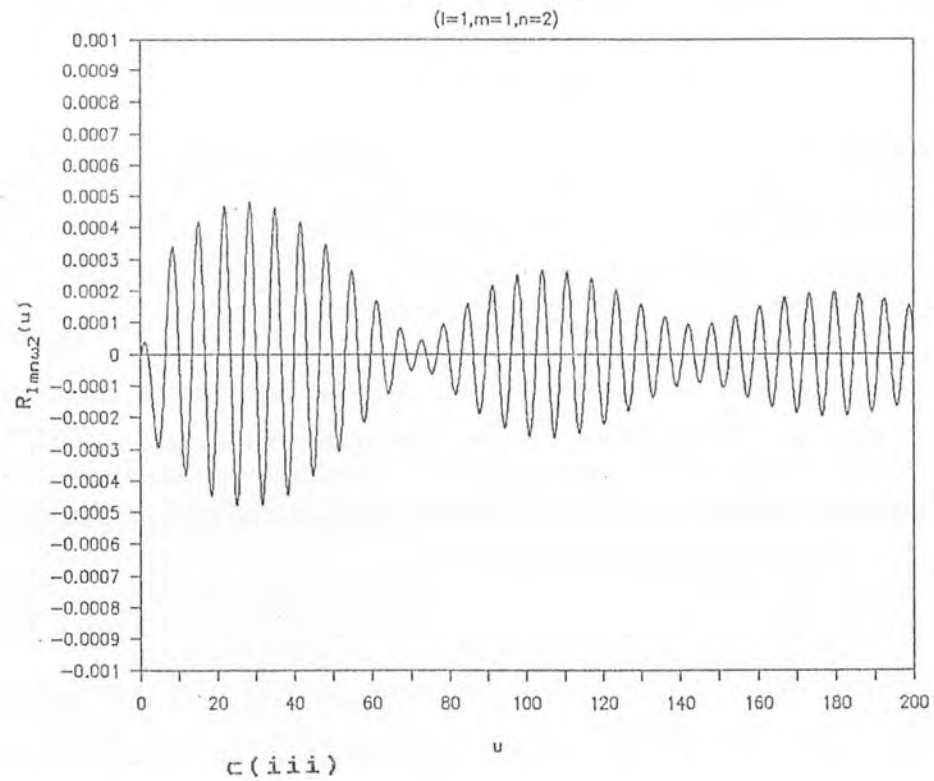

c(iii)

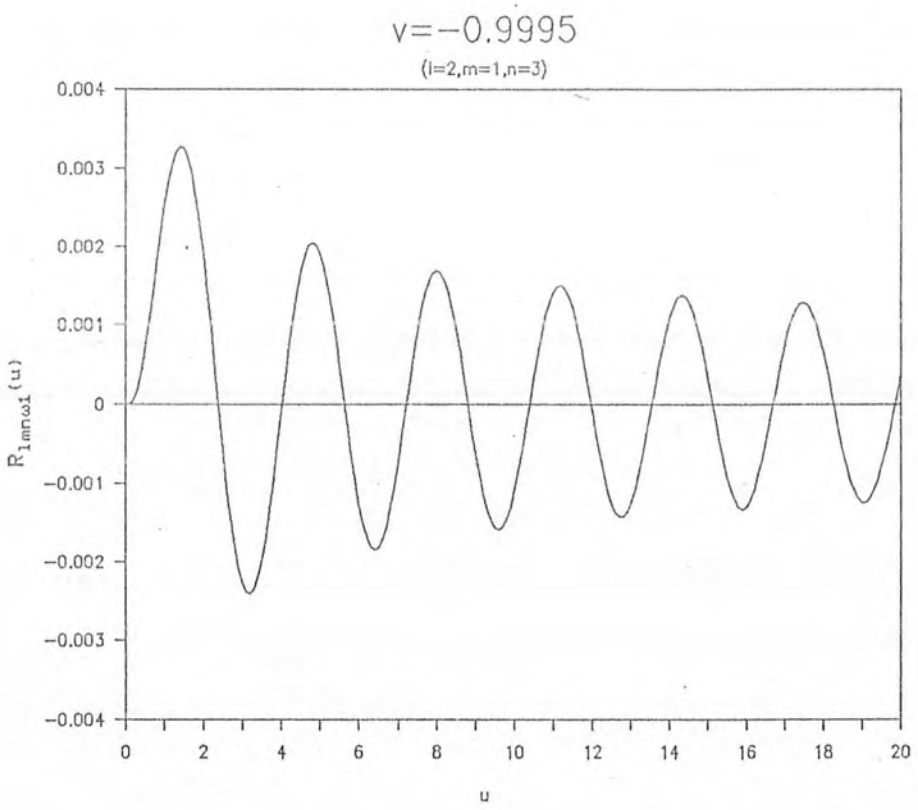

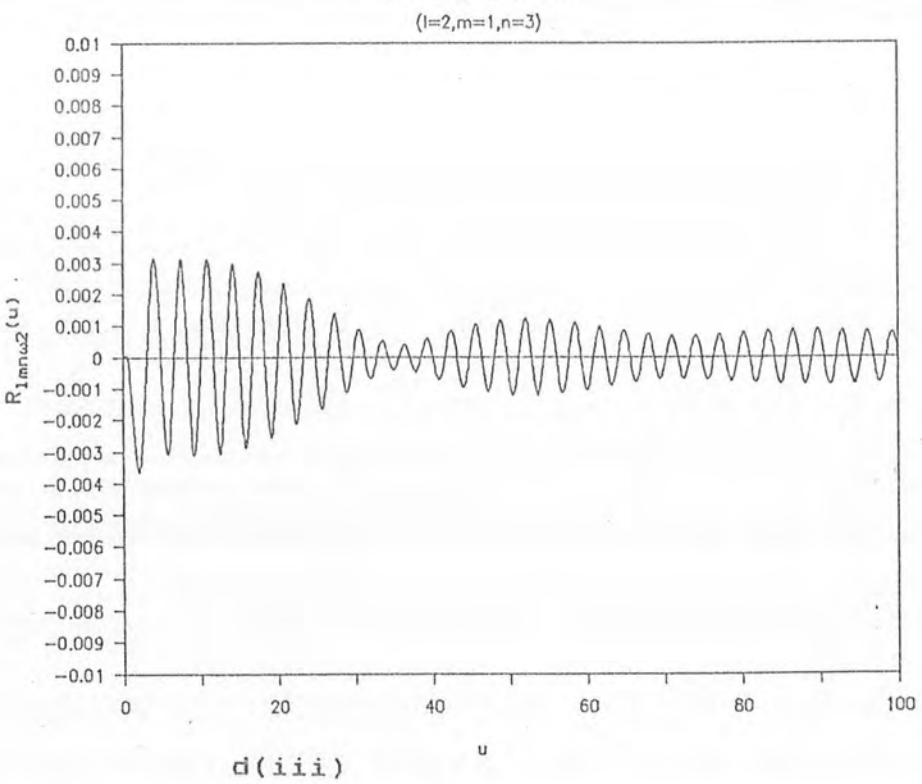

d(iii)

orthonormality conditions (3.2.3).

Following the canonical quantisation procedure given in § 3.2 on the set of SH in the region $-1<v_o<+1$, we found that the VEV of the number operator is zero. The VEV of the number operator could, in principle, be non-zero for the SH of CKST outside the region $-1 < v_o < 1$ on account of the ambiguity of the hypersurfaces. Thus we can not be sure that scalar fields on SHs of CKST give no VEV of the number operator in the asymptotic limit $v_o \longrightarrow \infty$, which is required for comparison with Hawking's calculations. A more complete discussion will be given in chapter four.

3.4. Quantisation on Spacelike Hypersurfaces of CMEC

In this section we quantise the massive scalar fields on the SH of CMEC (K-Surfaces). For this purpose, we consider the York time[24]

$$\tau_Y = \frac{4}{3} K, \qquad (3.4.1)$$

where K represent the CMEC. We would like to use coordinate which move along these hypersurfaces for space, say ρ_Y, and orthogonal to τ_Y. It turns out that for any choice of τ_Y, we can, indeed, specify ρ_Y,

$$\rho_Y = \int \frac{r^4 dr}{AE} , \qquad (3.4.2)$$

where E and A are given by Eqs.(2.2.19) and the constant of integration is fixed by requiring that $\rho_Y = 0$ at the place on the hypersurface in which the KS u is zero. However, we

do not have a coordinate basis in that the equations for $d\tau_Y$ and $d\rho_Y$ are not integrable. It appears that no coordinate system can be provided for our purpose. The equations for $d\tau_Y$ and $d\rho_Y$ are

$$d\tau_Y = dt - \frac{E}{(1-2m/r)A}\,dr, \qquad d\rho_Y = -dt + \frac{A}{(1-2m/r)E}\,dr. \tag{3.4.3}$$

The Schwarzschild line element (1.4.1), in view of Eqs.(3.4.3), takes the form

$$ds^2 = \frac{A^2}{r^4}\,d\tau_Y^2 - \frac{E^2}{r^4}\,d\rho_Y^2 - r^2(d\theta^2 + \sin^2\theta\, d\phi^2). \tag{3.4.4}$$

Since we have no coordinate system, we will use the anholonomic coordinates[31,46], for which we define the commutation coefficient $C^{\mu}{}_{\nu\rho}$ by

$$C^{\mu}{}_{\nu\rho} = \frac{1}{2}(\Gamma^{\mu}{}_{\nu\rho} - \Gamma^{\mu}{}_{\rho\nu}), \tag{3.4.5}$$

or

$$[e_\nu, e_\rho] = 2\, C^{\mu}{}_{\nu\rho}\, e_\mu, \tag{3.4.6}$$

where e_μ is the basis for the non-coordinate system. For the coordinate basis, the commutation coefficients will be zero. The non-zero commutation coefficients are

$$C^{0}{}_{10} = -\frac{Er^3}{8A^2} = -C^{0}{}_{01}, \tag{3.4.7a}$$

$$C^{1}{}_{10} = -\frac{r^3}{8E} = -C^{1}{}_{01}. \tag{3.4.7b}$$

Now, we substitute

$$\Phi(\tau_Y,\rho_Y,\theta,\phi) = \sum_{lm} L_{lm}(\tau_Y,\rho_Y)\, Y_{lm}(\theta,\phi), \tag{3.4.8}$$

into the KG equation (1.2.2), then $L_{lm}(\tau_Y,\rho_Y)$ satisfy the

partial differential equation

$$B_1 \frac{\partial^2 L_{lm}}{\partial \tau_Y^2} + \frac{\partial B_1}{\partial \tau_Y} \frac{\partial L_{lm}}{\partial \tau_Y} + B_2 \frac{\partial^2 L_{lm}}{\partial \rho_Y^2} + \frac{\partial B_2}{\partial \rho_Y} \frac{\partial L_{lm}}{\partial \rho_Y} + (M^2 r^2 + \lambda^2) B_3 L_{lm} = 0. \tag{3.4.9}$$

where

$$B_1 = B_3 \, g^{00} \, r^2,$$

$$B_2 = B_3 \, g^{11} \, r^2, \tag{3.4.10}$$

$$B_3 = (-g_{00} g_{11})^{+1/2}.$$

Further, we consider an ansatz

$$L_{lm}(\tau_Y, \rho_Y) = \sum_n B_4 \, exp(-i\omega\tau_Y) \, X_{lmn\omega}(\rho_Y), \tag{3.4.11}$$

where

$$B_4 = \left| \frac{A}{E \, r^2} \right|^{1/2}, \tag{3.4.12}$$

then $X_{lmn\omega}(\rho_Y)$ must satisfy the coupled differential equations

$$\frac{d^2 X_{lmn\omega 1}(\rho_Y)}{d\rho_Y^2} - D_1 \frac{d X_{lmn\omega 1}(\rho_Y)}{d\rho_Y} - D_2 X_{lmn\omega 2}(\rho_Y) + D_3 X_{lmn\omega 1}(\rho_Y) = 0, \tag{3.4.13a}$$

$$\frac{d^2 X_{lmn\omega 2}(\rho_Y)}{d\rho_Y^2} - D_1 \frac{d X_{lmn\omega 2}(\rho_Y)}{d\rho_Y} + D_2 X_{lmn\omega 1}(\rho_Y) + D_3 X_{lmn\omega 2}(\rho_Y) = 0, \tag{3.4.13b}$$

where, by using Eqs.(3.4.3)-(3.4.7), we get

$$D_1 = -2r \left| \frac{E}{A} \right|^{1/2} \frac{\partial B_4}{\partial \rho_Y} + \frac{E}{A r^2} \frac{\partial B_2}{\partial \rho_Y}, \tag{3.4.14a}$$

$$D_2 = \frac{\omega E}{rA}\{2\left|\frac{E}{A}\right|^{3/2}\frac{\partial B_4}{\partial \tau_Y} + \frac{1}{r}\frac{\partial B_1}{\partial \tau_Y}\}\ , \qquad (3.4.14b)$$

$$D_3 = \omega^2\frac{E^2}{A^2} - \frac{E^2}{r^6}(M^2r^2+\lambda^2) + \frac{1}{r}\left|\frac{E}{A}\right|^{1/2}$$
$$\times\ [\frac{\partial^2 B_4}{\partial \rho_Y^2} - \frac{E}{A}\frac{\partial B_2}{\partial \rho_Y}\frac{\partial B_4}{\partial \rho_Y}$$
$$- \frac{E^2}{A^2}\frac{\partial^2 B_4}{\partial \tau_Y^2} - \frac{E}{A}\frac{\partial B_1}{\partial \tau_Y}\frac{\partial B_4}{\partial \tau_Y}], \qquad (3.4.14c)$$

$$\left.\begin{aligned}
\frac{\partial B_1}{\partial \tau_Y} &= -m\frac{E^2}{A^2} - \frac{3Er^3(r-2m)}{4A^2}\tau_Y + \frac{2E^4}{r^9A^2} + \frac{r^5(4E^2-5A^2)}{16A^3}\ ,\\
\frac{\partial B_2}{\partial \rho_Y} &= -m - \frac{3r^3(r-2m)}{4E}\tau_Y + \frac{2E^2-3A^2}{r^3} - \frac{r^5}{16A}\ ,\\
\frac{\partial B_4}{\partial \tau_Y} &= \frac{1}{2r}\frac{A_{,0}}{|AE|^{1/2}} - \frac{1}{2r}\frac{|A|^{1/2}E_{,0}}{|E|^{3/2}} - \frac{A^{3/2}|E|^{1/2}}{r^5}\ ,\\
\frac{\partial B_4}{\partial \rho_Y} &= \frac{1}{2r}\frac{A_{,1}}{|AE|^{1/2}} - \frac{1}{2r}\frac{|A|^{1/2}E_{,1}}{|E|^{3/2}} - \frac{A^{3/2}|E|^{1/2}}{r^5}\ ,
\end{aligned}\right\} \qquad (3.4.15a)$$

$$\left.\begin{aligned}
\frac{\partial^2 B_4}{\partial \tau_Y^2} &= \frac{EA_{,00} - AE_{,00}}{2r|A|^{1/2}|E|^{3/2}} - \frac{|A|^{1/2}}{|E|^{1/2}}\frac{EA_{,0} - AE_{,0}}{2r^6}\\
&\quad - \frac{E^2A^2_{,0} - 3A^2E^2_{,0}}{4r|A|^{3/2}|E|^{5/2}} - \frac{A_{,0}E_{,0}}{2r|A|^{1/2}|E|^{3/2}}\ ,\\
\frac{\partial^2 B_4}{\partial \rho_Y^2} &= \frac{EA_{,11} - AE_{,11}}{2r|A|^{1/2}|E|^{3/2}} - \frac{|A|^{1/2}}{|E|^{1/2}}\frac{EA_{,1} - AE_{,1}}{2r^6}\\
&\quad - \frac{E^2A^2_{,1} - 3A^2E^2_{,1}}{4r|A|^{3/2}|E|^{5/2}} - \frac{A_{,1}E_{,1}}{2r|A|^{1/2}|E|^{3/2}}\ ,
\end{aligned}\right\} \qquad (3.4.15b)$$

$$\left.\begin{aligned}
E_{,0} &= -\frac{r^3}{4} - \frac{3AE}{4r^2}\tau_Y\ ,\\
E_{,1} &= -\frac{3AE}{4r^2}\tau_Y\ ,
\end{aligned}\right\} \qquad (3.4.15c)$$

$$A_{,o} = \frac{E\,E_{,o} + r^2(2r-3m)r_{,o}}{A}\,, \quad r_{,o} = \frac{AE}{r^4}\,,$$
$$A_{,1} = \frac{E\,E_{,1} + r^2(2r-3m)r_{,1}}{A}\,, \quad r_{,1} = r_{,o}\,, \qquad \text{(3.4.15d)}$$

$$E_{,oo} = -\frac{3AE}{2r^2} - \frac{3}{4}\left(\frac{E\,A_{,o} + A\,E_{,o}}{r^2} - 2\,\frac{A^2E^2}{r^7}\right)\tau_Y\,,$$
$$E_{,11} = -\frac{3}{4}\left(\frac{E\,A_{,1} + A\,E_{,1}}{r^2} - 2\,\frac{A^2E^2}{r^7}\right)\tau_Y\,, \qquad \text{(3.4.15e)}$$

$$A_{,oo} = \frac{E\,E_{,oo} + E_{,o}^2 + 6r(r-2m)r_{,o} + r^2(2r-3m)r_{,oo} - A_{,o}^2}{A}\,,$$
$$A_{,11} = \frac{E\,E_{,11} + E_{,1}^2 + 6r(r-2m)r_{,1} + r^2(2r-3m)r_{,11} - A_{,1}^2}{A}\,,$$
$$r_{,oo} = \frac{E\,A_{,o} + A\,E_{,o}}{r^4} - \frac{4A^2E^2}{r^9}\,,$$
$$r_{,11} = \frac{E\,A_{,1} + A\,E_{,1}}{r^4} - \frac{4A^2E^2}{r^9}\,, \qquad \text{(3.4.15f)}$$

$$X_{lmn\omega}(\rho_Y) = X_{lmn\omega 1}(\rho_Y) + i\,X_{lmn\omega 2}(\rho_Y)\,. \qquad \text{(3.4.15g)}$$

As before, since these differential equations can not be easily solved analytically, they have been solved numerically (see Appendix B). To obtain $X_{lmn\omega}(\rho_Y)$ from Eqs.(3.4.15g) and (3.4.13), we solve Eqs.(3.4.13) numerically over the complete SH of CMEC, for each value of l, m, n, and H. For each case, it is found that the solutions of Eqs.(3.4.13) converge to zero as ρ_Y tends to infinity. Some typical solutions are shown in Fig.3.2 corresponding to different values of l, m, n and K.

Numerically, these solutions satisfy the orthonormality condition (3.2.1) over the K-surfaces. Since the K-surfaces are asymptotically hyperboloids and completely foliate the

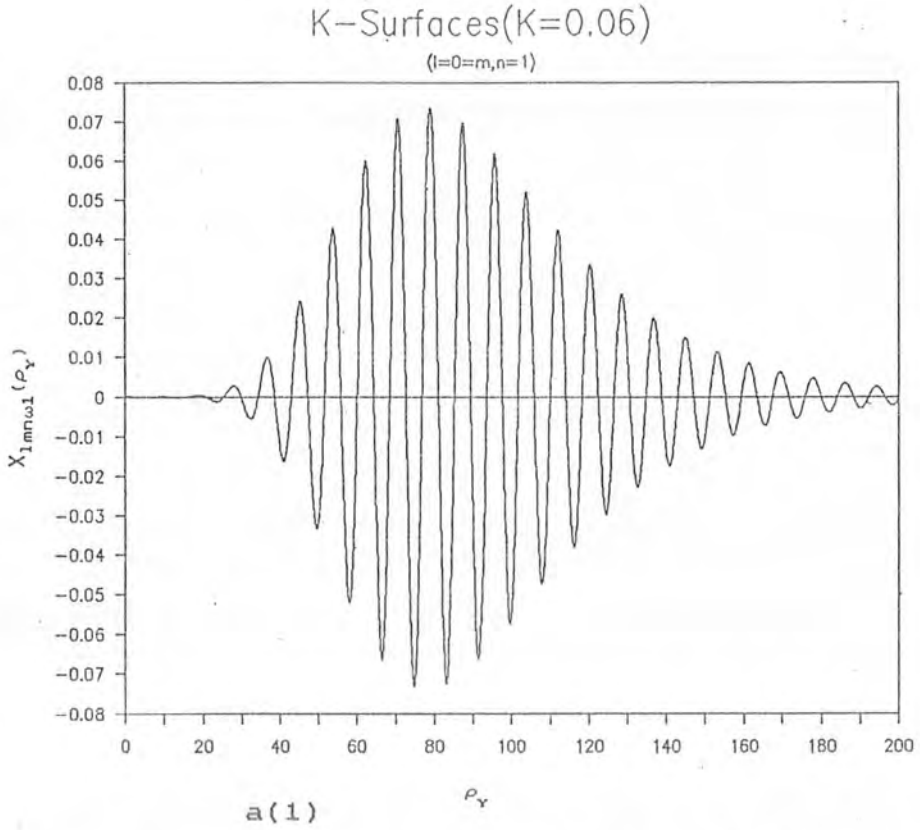

Figure 3.2. The normalised solutions of Eqs.(3.4.13) for a) n = 1, l = 0, m = 0; b) n = 2, l = 0, m = 0; c) n = 2, l = 1, m = 0; d) n = 2, l = 1, m = 1; e)n = 3, l = 0, m = 0; f) n = 3, l = 1, m = 0; g) n = 3, l = 1, m = 1; h) n = 3, l = 2, m = 0; i) n = 3, l = 2, m = 1; j) n = 3, l = 2, m = 2; corresponding to 1) K = 0.06, H = 0.5; 2) K = 0.9, H = 0.5 are shown.

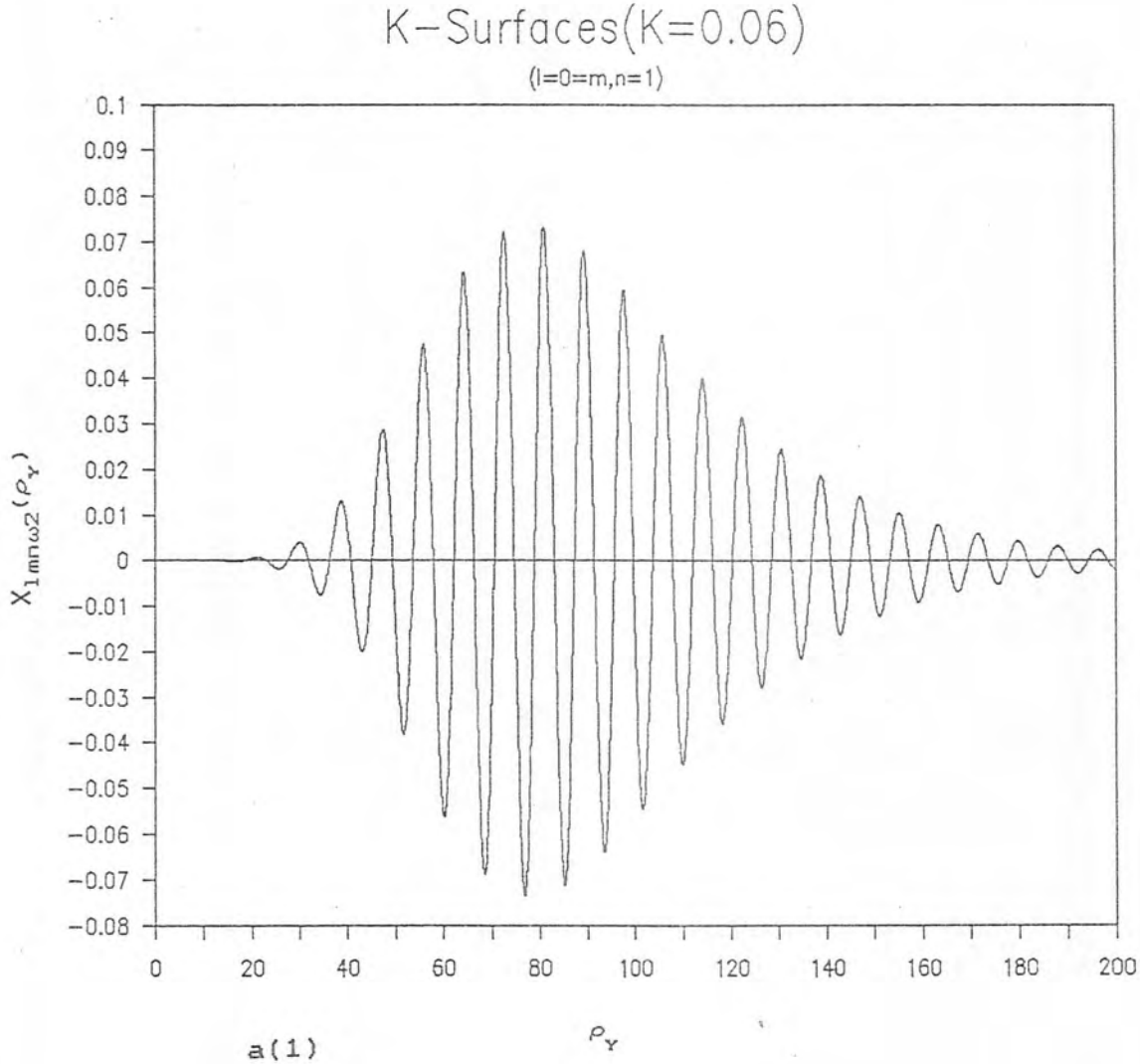
K-Surfaces(K=0.06)
(l=0=m,n=1)
0.1
0.09
0.08
0.07
0.06
0.05
0.04
0.03
0.02
0.01
0
-0.01
-0.02
-0.03
-0.04
-0.05
-0.06
-0.07
-0.08
0
20
40
60
80
100
120
140
160
180
200
$X_{1mn\omega 2}(\rho_Y)$
ρ_Y
a(1)

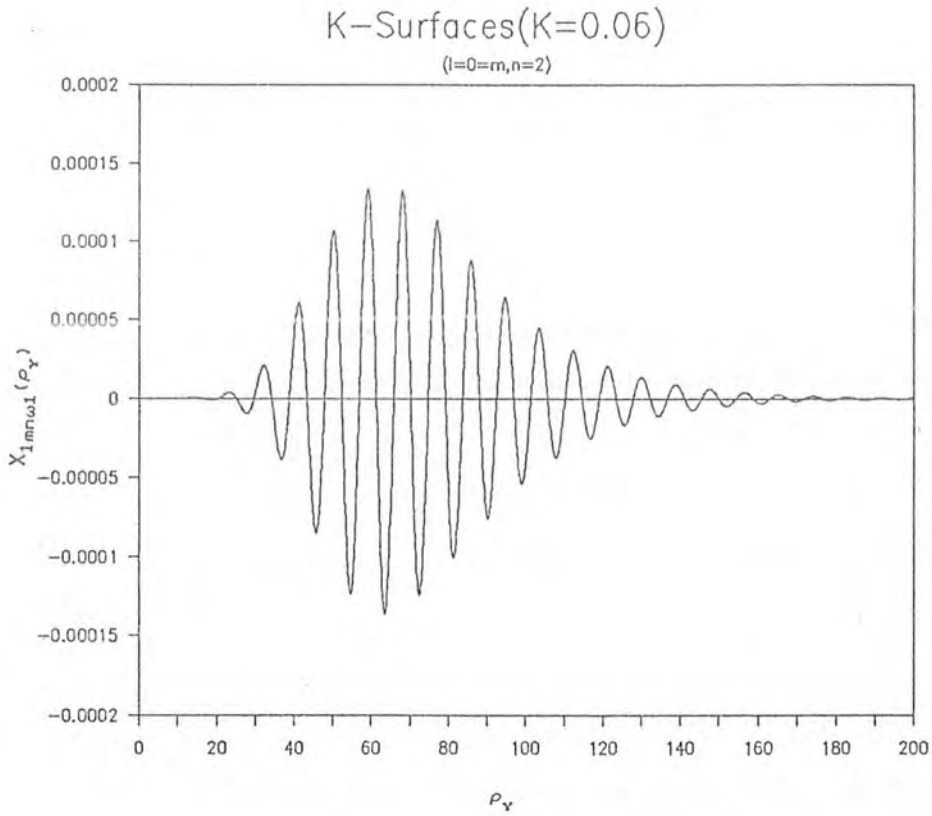
K-Surfaces(K=0.06)
(l=0=m,n=2)
0.0002
0.00015
0.0001
0.00005
0
-0.00005
-0.0001
-0.00015
-0.0002
0
20
40
60
80
100
120
140
160
180
200
$X_{1mn\omega1}(p_Y)$
p_Y

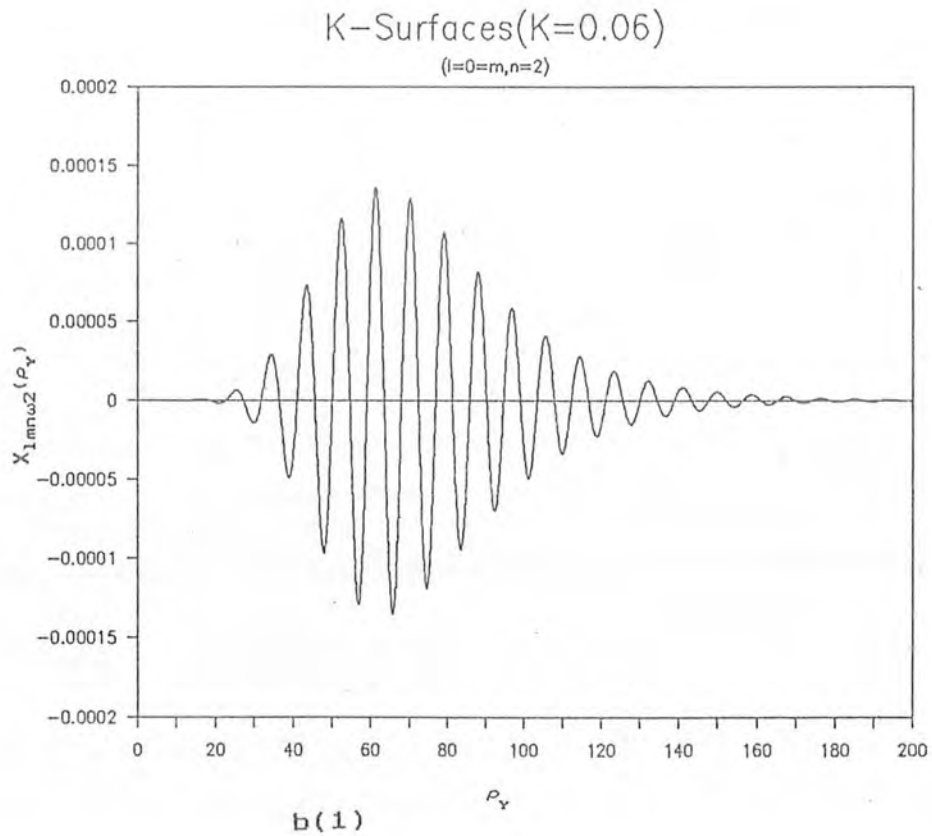
K-Surfaces(K=0.06)
(l=0=m,n=2)
0.0002
0.00015
0.0001
0.00005
0
-0.00005
-0.0001
-0.00015
-0.0002
0
20
40
60
80
100
120
140
160
180
200
$X_{1mn\omega2}(p_Y)$
p_Y

b(1)

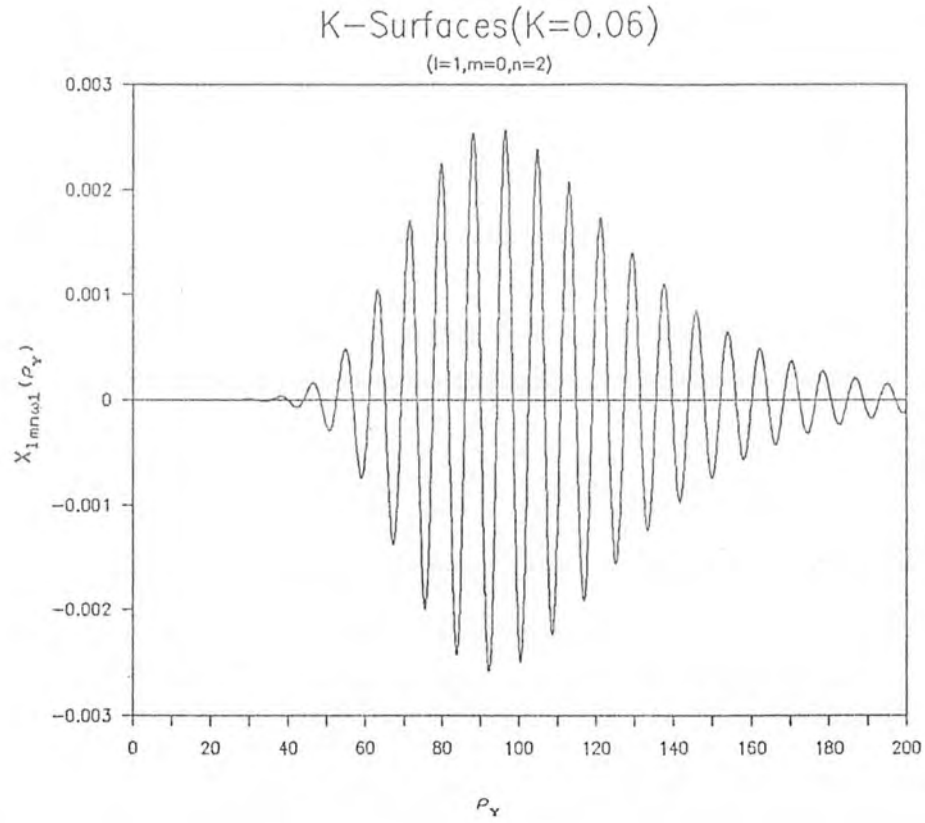
K-Surfaces(K=0.06)
(l=1,m=0,n=2)
0.003
0.002
0.001
0
-0.001
-0.002
-0.003
0
20
40
60
80
100
120
140
160
180
200
$X_{1m n\omega 1}(\rho_Y)$
ρ_Y

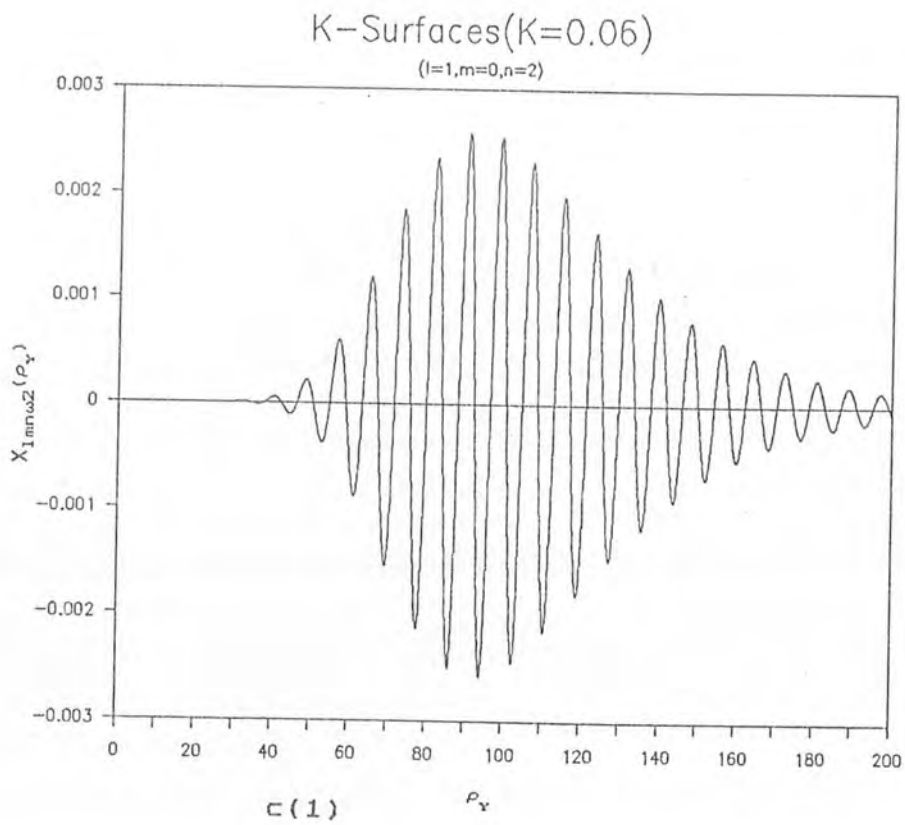
K-Surfaces(K=0.06)
(l=1,m=0,n=2)
0.003
0.002
0.001
0
-0.001
-0.002
-0.003
0
20
40
60
80
100
120
140
160
180
200
$X_{1m n\omega 2}(\rho_Y)$
ρ_Y
c(1)

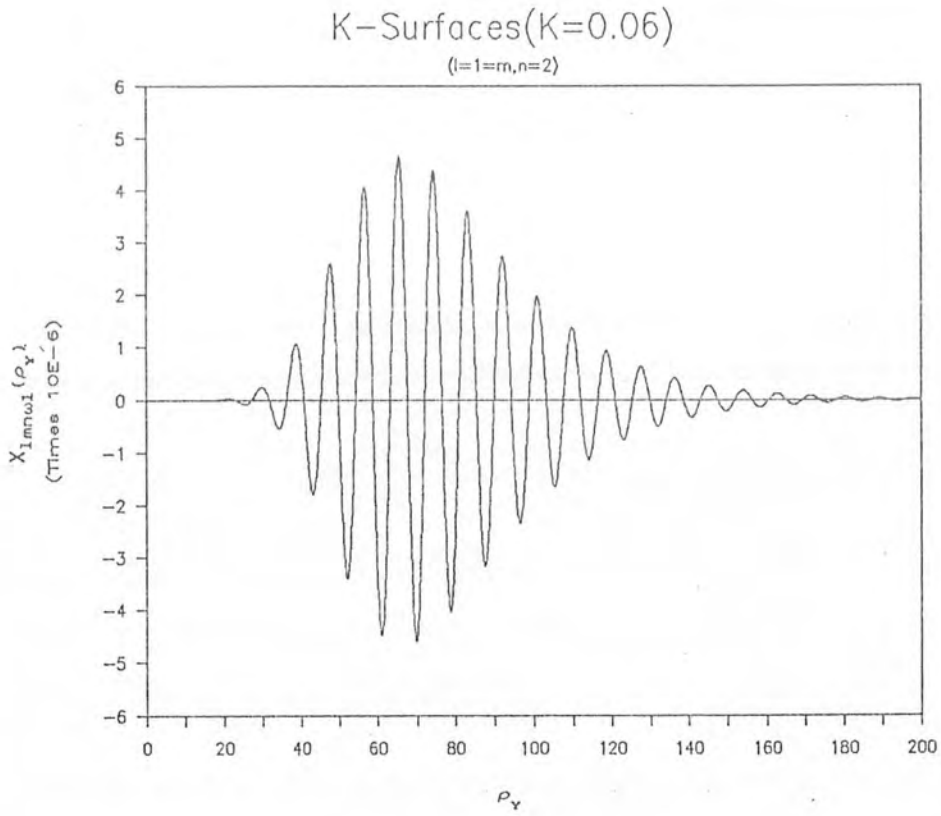
K-Surfaces(K=0.06)
(l=1=m,n=2)
$X_{1mn\omega1}(\rho_Y)$
(Times 10E-6)
ρ_Y

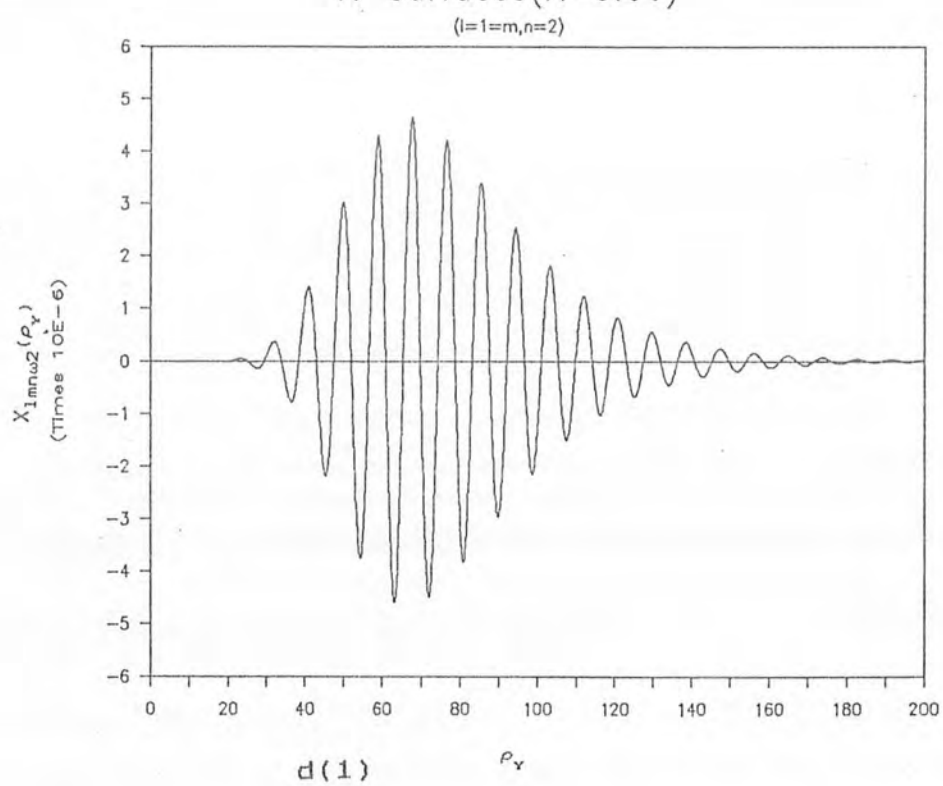
K-Surfaces(K=0.06)
(l=1=m,n=2)
$X_{1mn\omega2}(\rho_Y)$
(Times 10E-6)
ρ_Y
d(1)

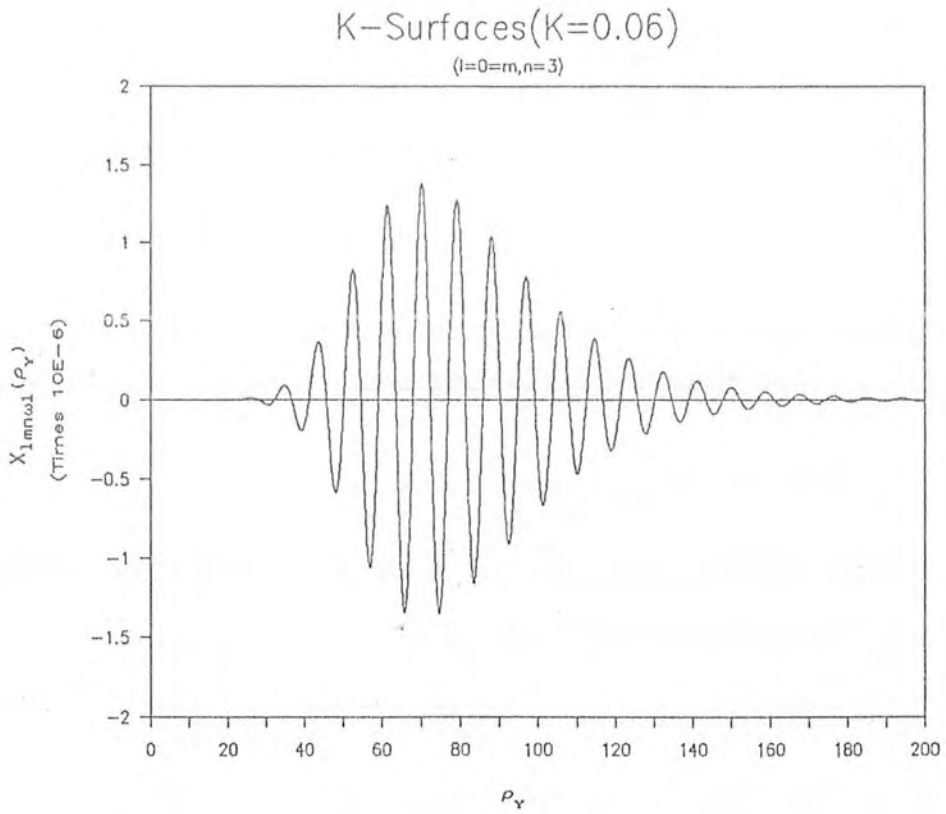
K-Surfaces(K=0.06)
(l=0=m,n=3)
$X_{1mn\omega1}(\rho_Y)$
(Times 10E-6)
2
1.5
1
0.5
0
-0.5
-1
-1.5
-2
0
20
40
60
80
100
120
140
160
180
200
ρ_Y

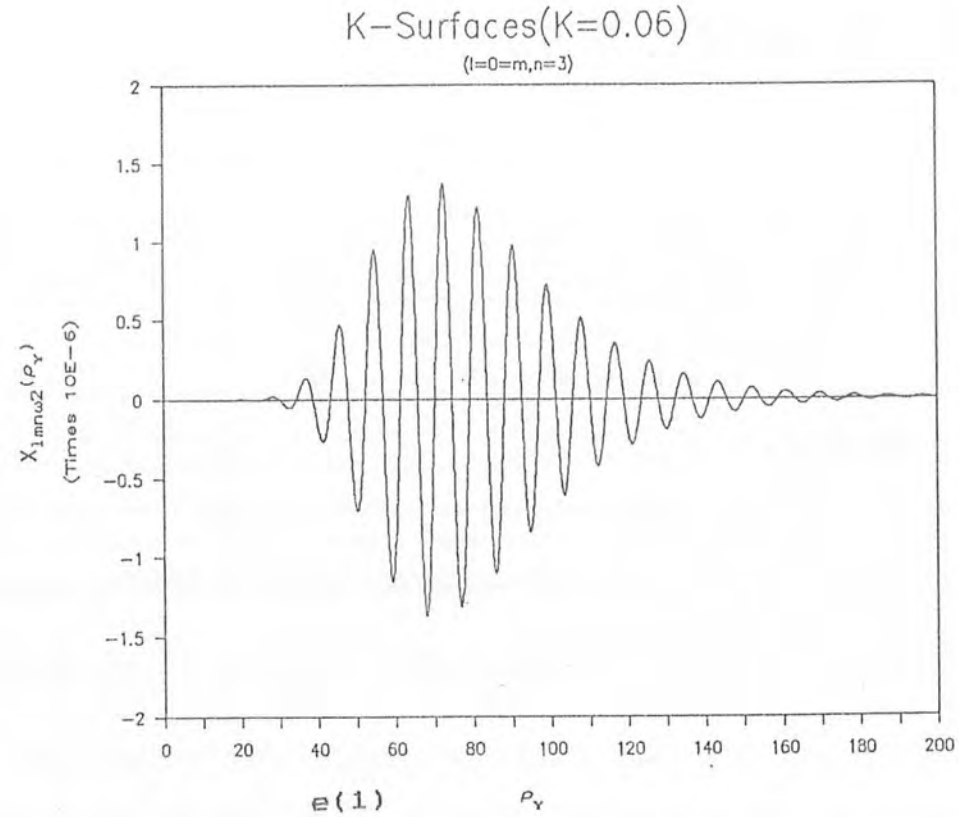
K-Surfaces(K=0.06)
(l=0=m,n=3)
$X_{1mn\omega2}(\rho_Y)$
(Times 10E-6)
2
1.5
1
0.5
0
-0.5
-1
-1.5
-2
0
20
40
60
80
100
120
140
160
180
200
e(1)
ρ_Y

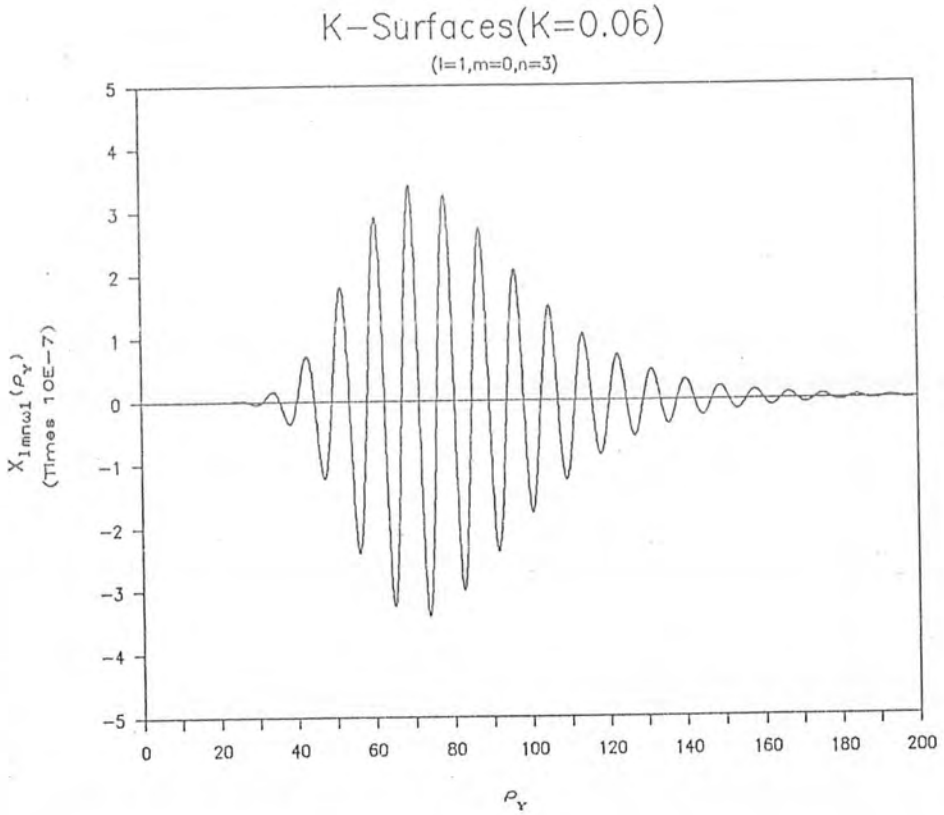
K-Surfaces(K=0.06)
(l=1,m=0,n=3)
$X_{1mn\omega1}(\rho_Y)$
(Times 10E-7)
5
4
3
2
1
0
-1
-2
-3
-4
-5
0
20
40
60
80
100
120
140
160
180
200
ρ_Y

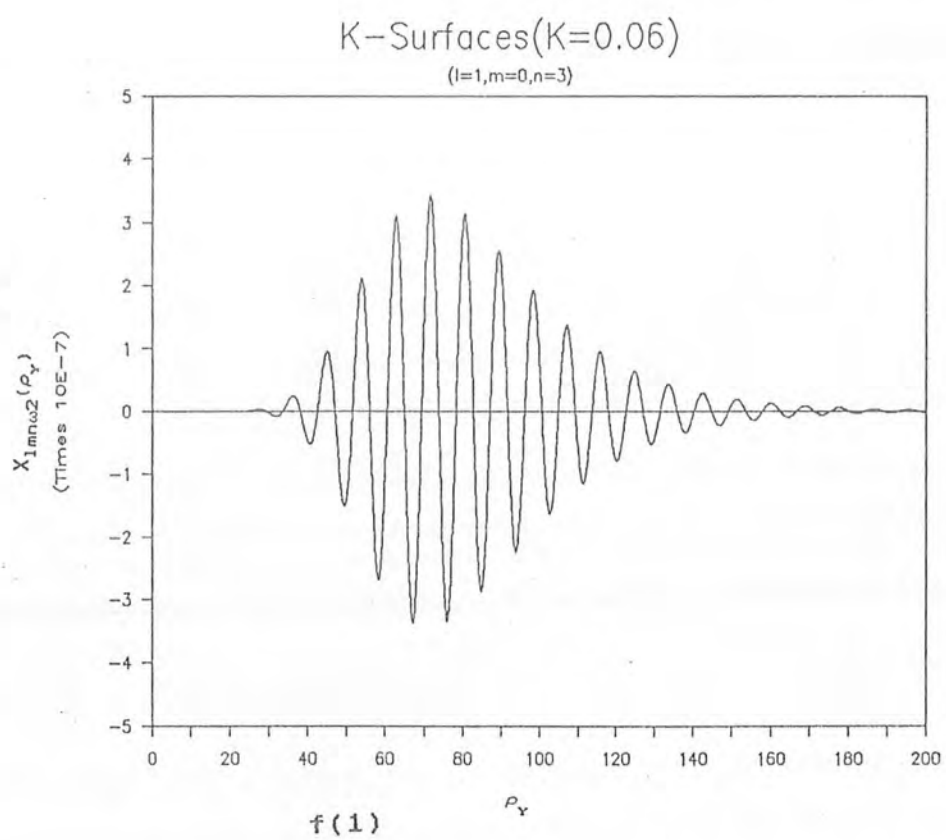
K-Surfaces(K=0.06)
(l=1,m=0,n=3)
$X_{1mn\omega2}(\rho_Y)$
(Times 10E-7)
5
4
3
2
1
0
-1
-2
-3
-4
-5
0
20
40
60
80
100
120
140
160
180
200
ρ_Y

f(1)

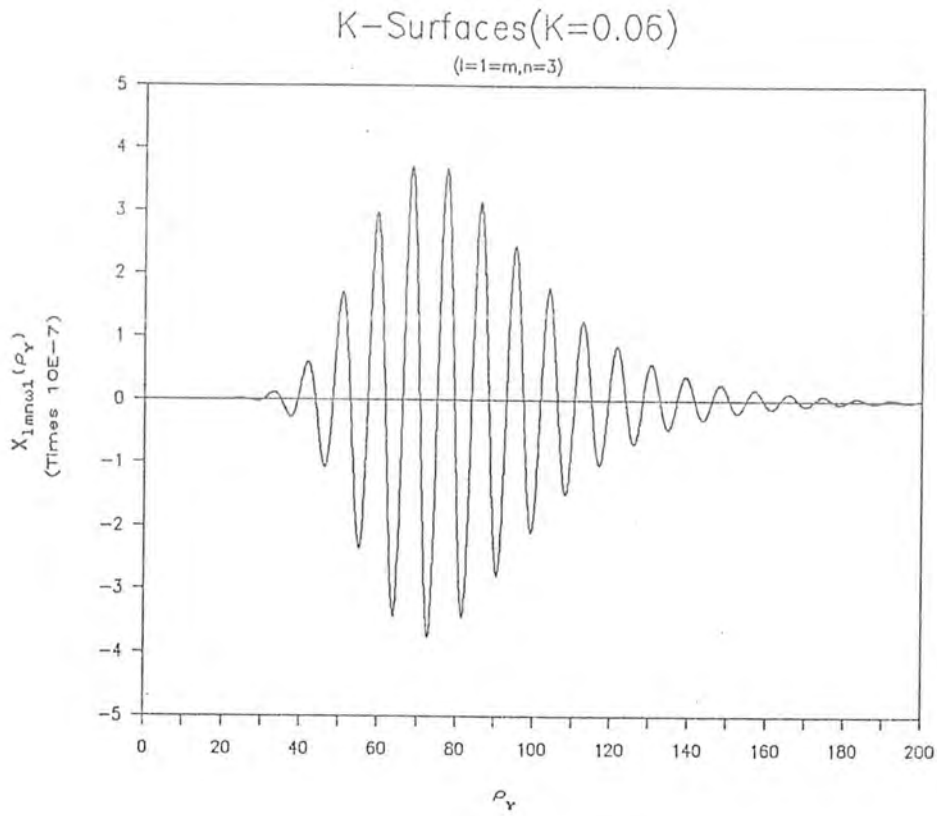
K-Surfaces(K=0.06)
(l=1=m,n=3)
$X_{1mn\omega1}(\rho_Y)$
(Times 10E-7)
ρ_Y

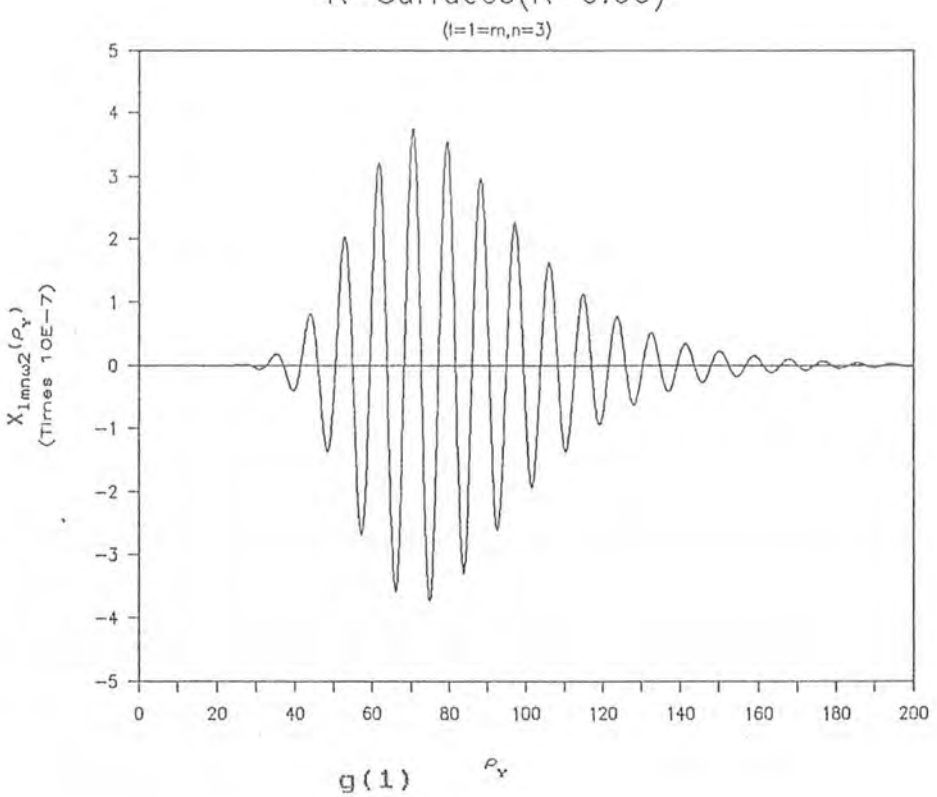
K-Surfaces(K=0.06)
(l=1=m,n=3)
$X_{1mn\omega2}(\rho_Y)$
(Times 10E-7)
ρ_Y

g(1)

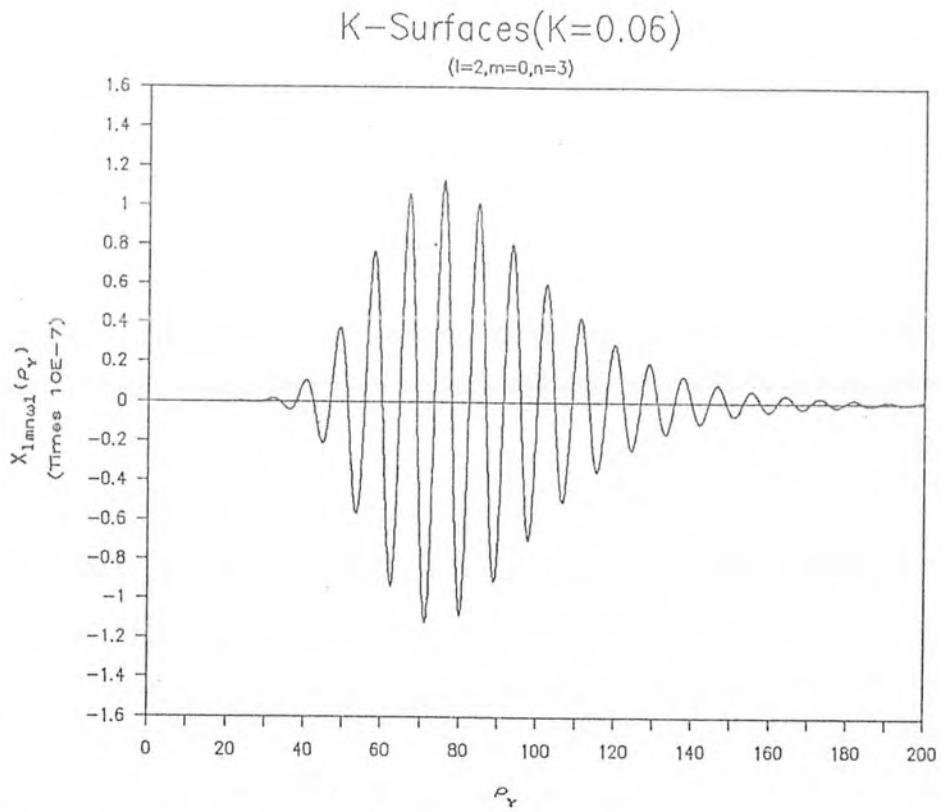
K-Surfaces(K=0.06)
(l=2,m=0,n=3)
$X_{1mn\omega1}(\rho_Y)$
(Times 10E-7)
1.6
1.4
1.2
1
0.8
0.6
0.4
0.2
0
-0.2
-0.4
-0.6
-0.8
-1
-1.2
-1.4
-1.6
0
20
40
60
80
100
120
140
160
180
200
ρ_Y

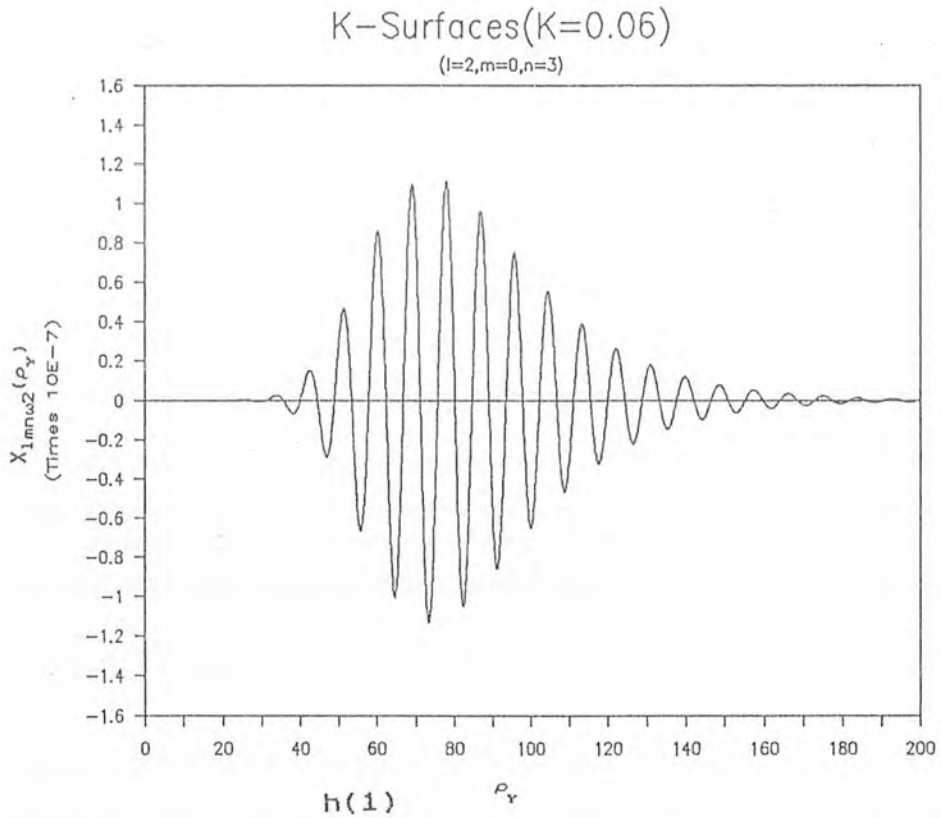
K-Surfaces(K=0.06)
(l=2,m=0,n=3)
$X_{1mn\omega2}(\rho_Y)$
(Times 10E-7)
1.6
1.4
1.2
1
0.8
0.6
0.4
0.2
0
-0.2
-0.4
-0.6
-0.8
-1
-1.2
-1.4
-1.6
0
20
40
60
80
100
120
140
160
180
200
ρ_Y
h(1)

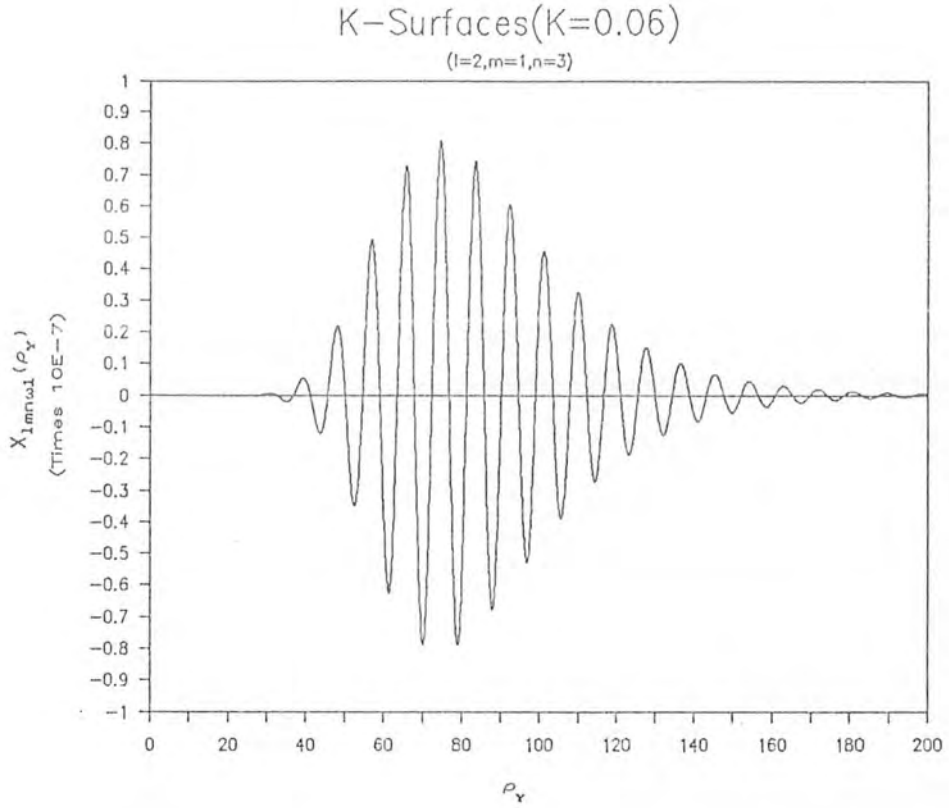
K-Surfaces(K=0.06)
(l=2,m=1,n=3)
$X_{lmn\omega 1}(\rho_Y)$
(Times 10E-7)
ρ_Y

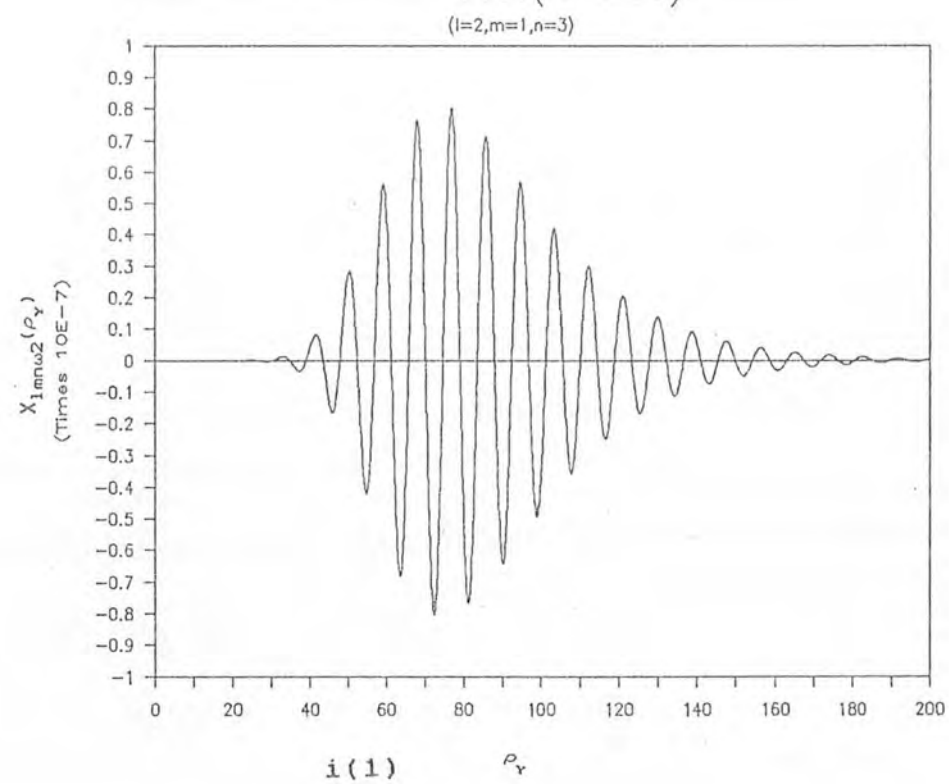
K-Surfaces(K=0.06)
(l=2,m=1,n=3)
$X_{lmn\omega 2}(\rho_Y)$
(Times 10E-7)
ρ_Y

i(1)

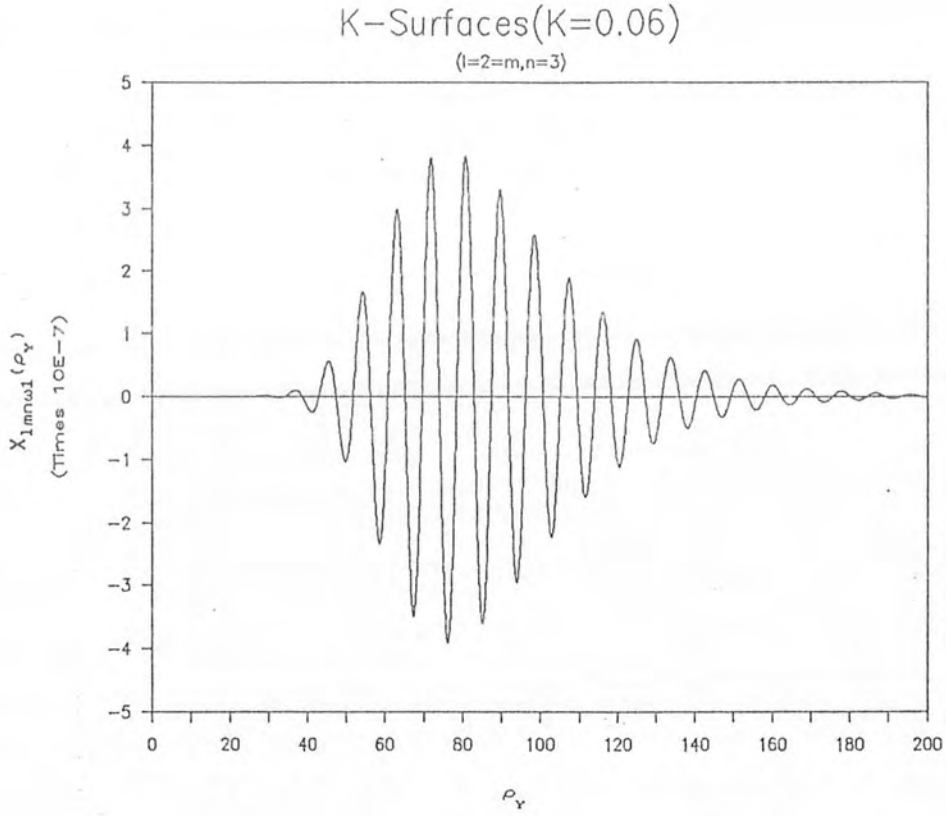
K-Surfaces(K=0.06)
(l=2=m,n=3)
$X_{1mn\omega1}(\rho_Y)$
(Times 10E-7)
5
4
3
2
1
0
-1
-2
-3
-4
-5
0
20
40
60
80
100
120
140
160
180
200
ρ_Y

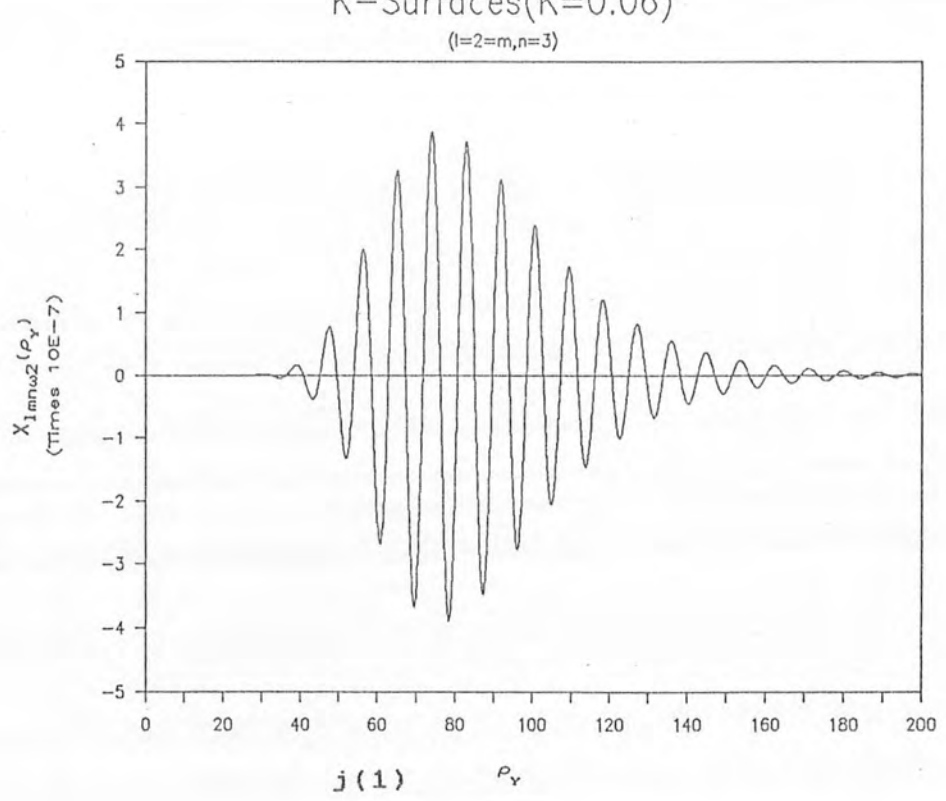
K-Surfaces(K=0.06)
(l=2=m,n=3)
$X_{1mn\omega2}(\rho_Y)$
(Times 10E-7)
5
4
3
2
1
0
-1
-2
-3
-4
-5
0
20
40
60
80
100
120
140
160
180
200
j(1)
ρ_Y

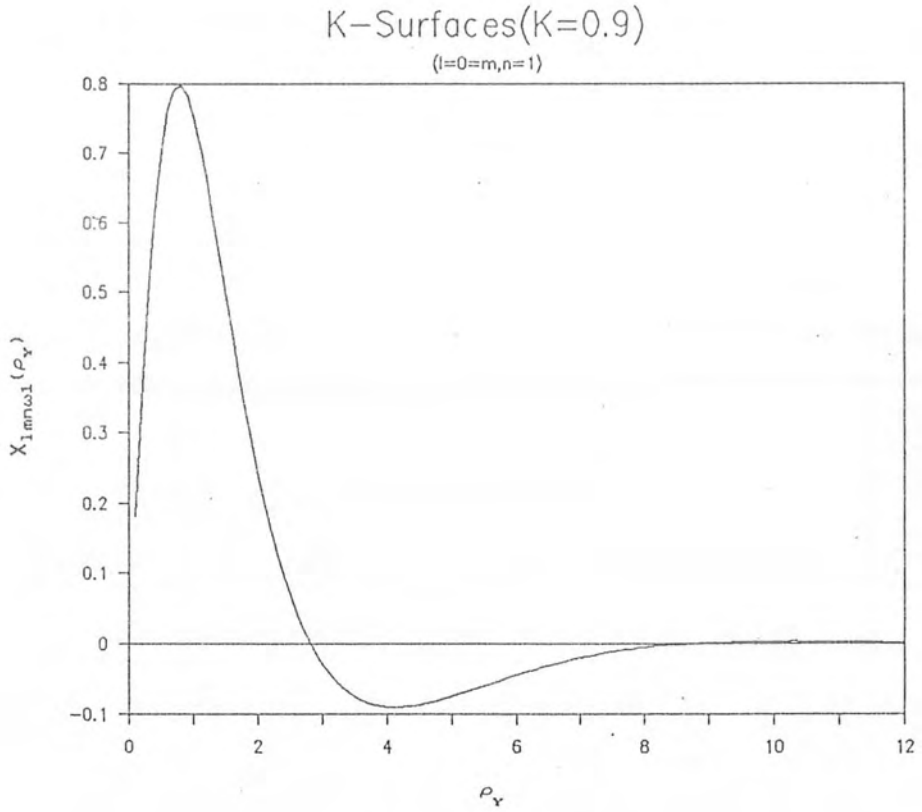
K-Surfaces(K=0.9)
(l=0=m,n=1)
$X_{1mn\omega1}(\rho_Y)$
ρ_Y

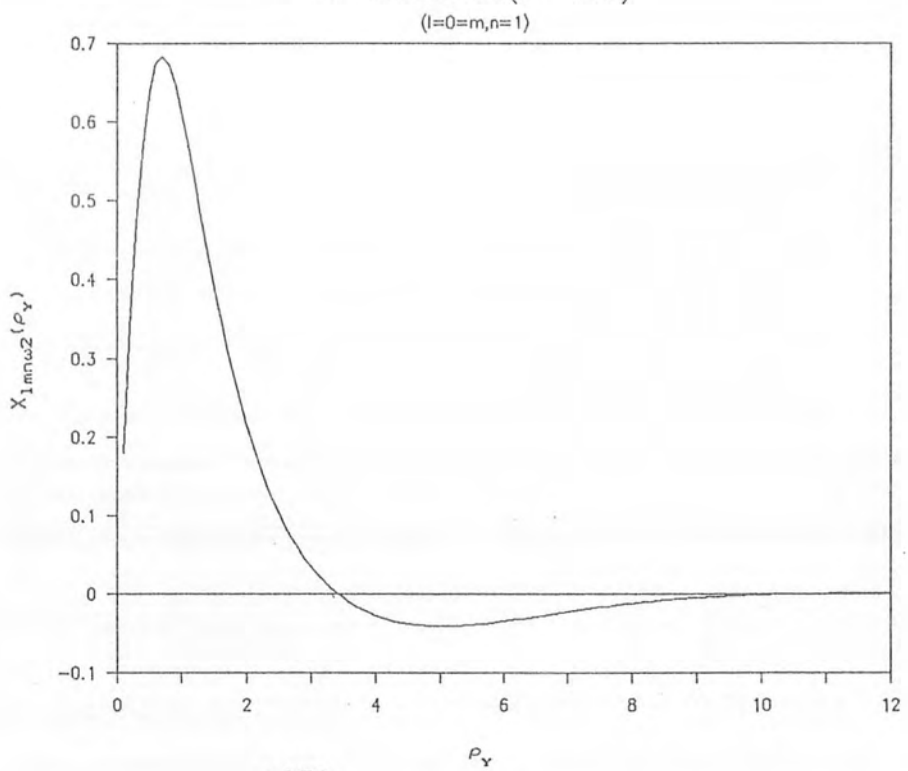
K-Surfaces(K=0.9)
(l=0=m,n=1)
$X_{1mn\omega2}(\rho_Y)$
ρ_Y

a(2)

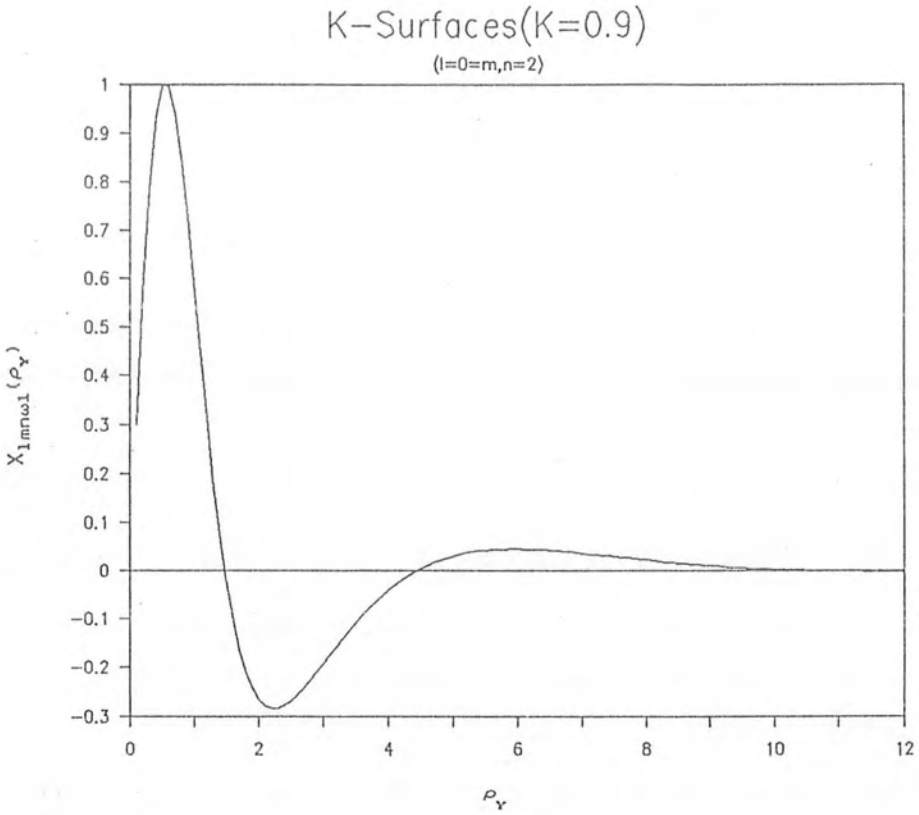
K-Surfaces(K=0.9)
(l=0=m,n=2)
$X_{1mn\omega 1}(\rho_Y)$
ρ_Y

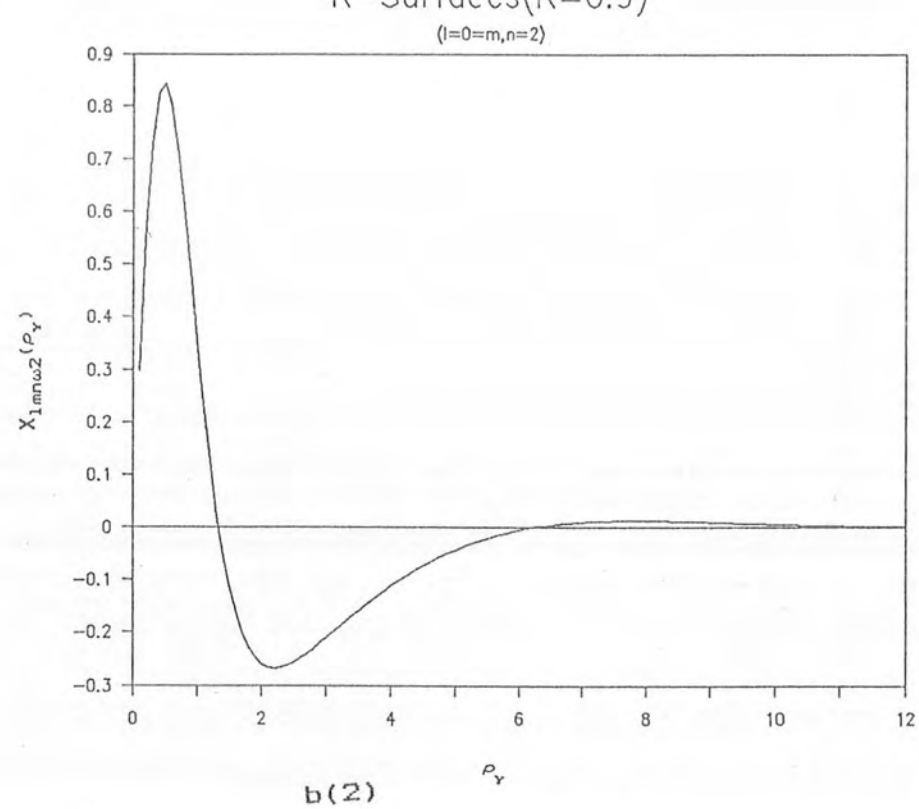
K-Surfaces(K=0.9)
(l=0=m,n=2)
$X_{1mn\omega 2}(\rho_Y)$
ρ_Y

b(2)

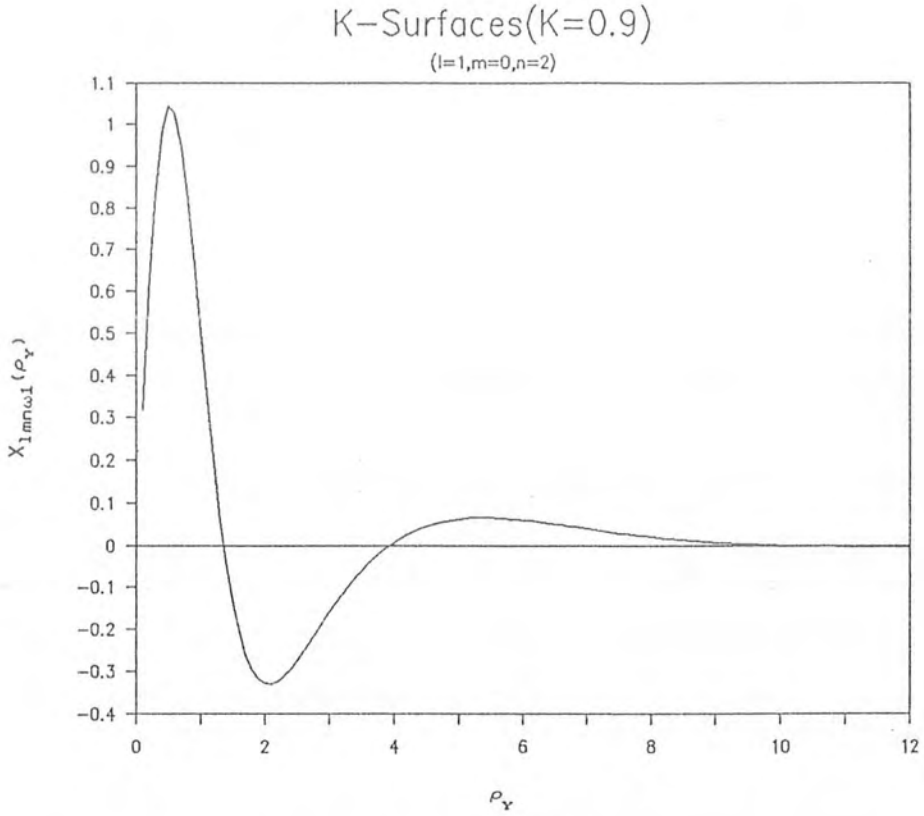
K−Surfaces(K=0.9)
(l=1,m=0,n=2)
$X_{1mn\omega 1}(\rho_Y)$
ρ_Y

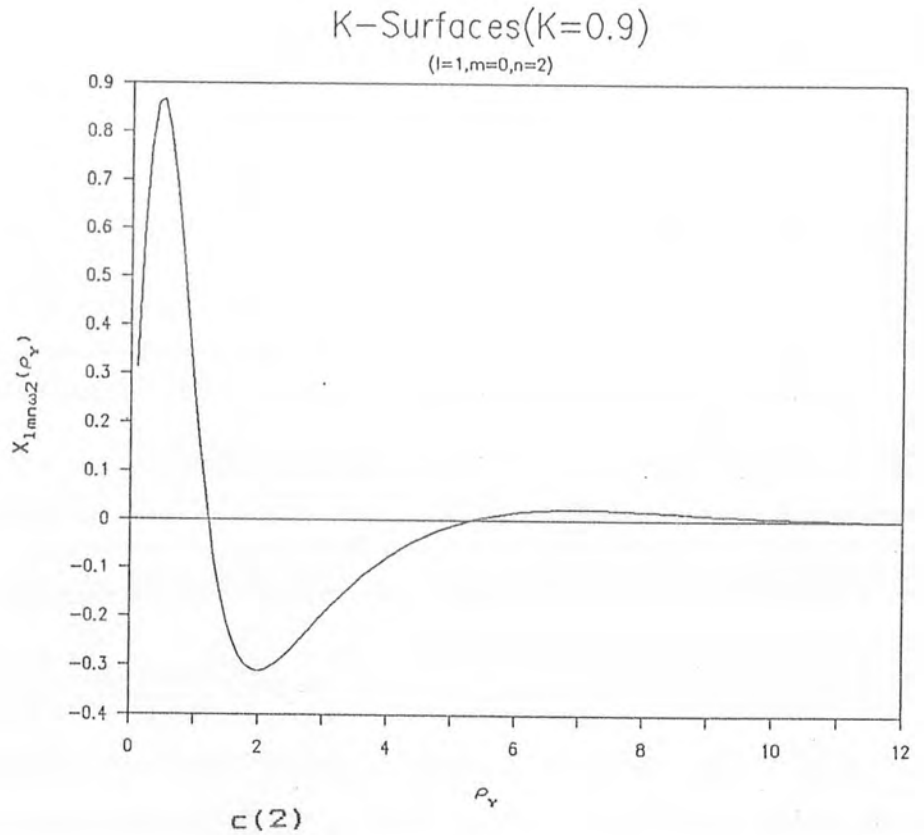
K−Surfaces(K=0.9)
(l=1,m=0,n=2)
$X_{1mn\omega 2}(\rho_Y)$
ρ_Y

c(2)

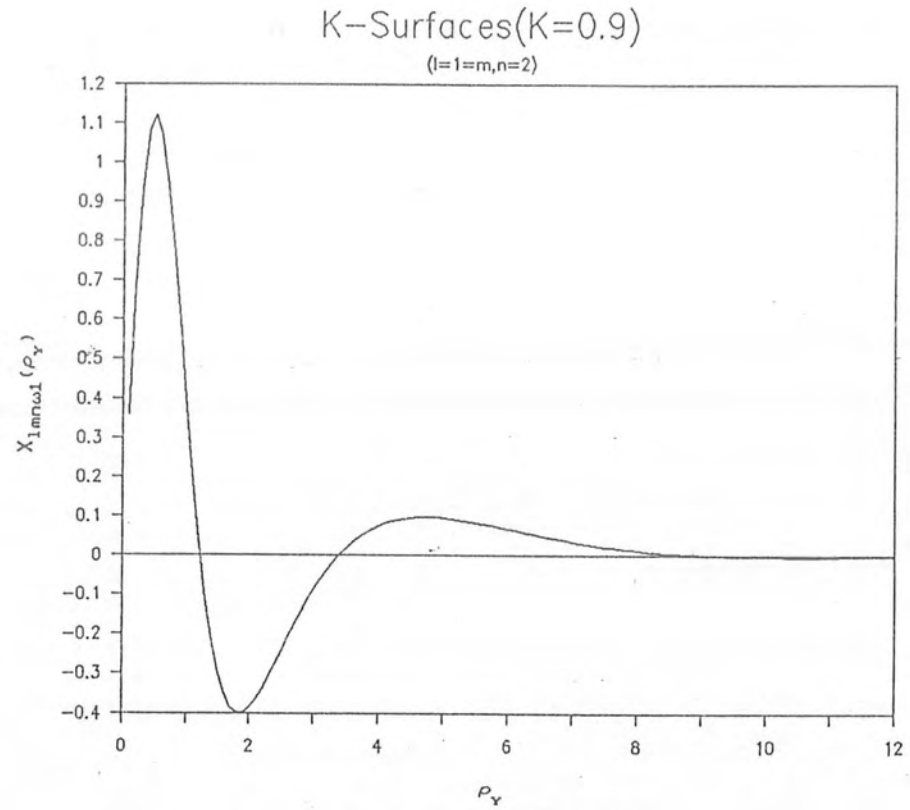
K-Surfaces(K=0.9)
(l=1=m,n=2)
$X_{1mn\omega1}(\rho_Y)$
ρ_Y

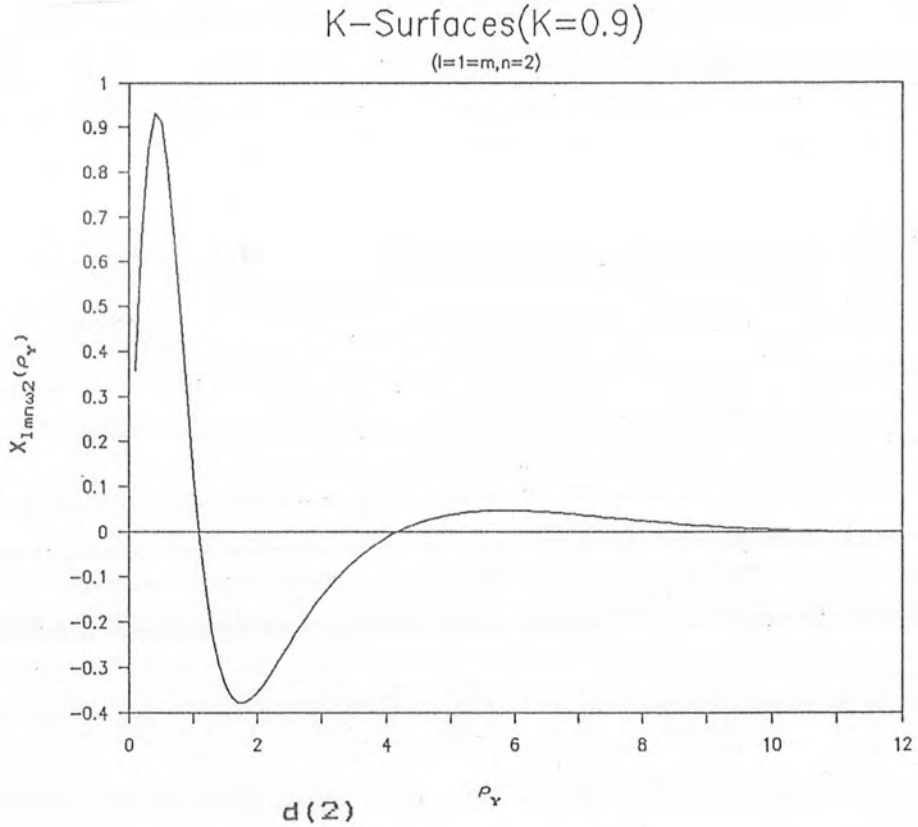
K-Surfaces(K=0.9)
(l=1=m,n=2)
$X_{1mn\omega2}(\rho_Y)$
ρ_Y

d(2)

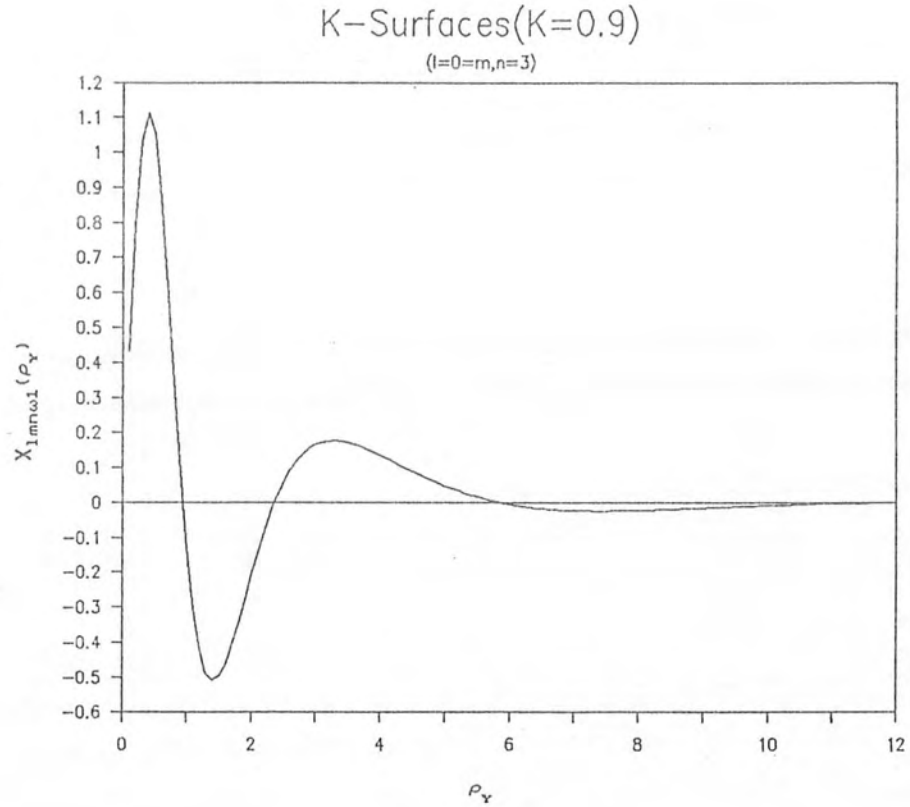
K-Surfaces(K=0.9)
(l=0=m,n=3)
$X_{1mn\omega1}(\rho_Y)$
ρ_Y

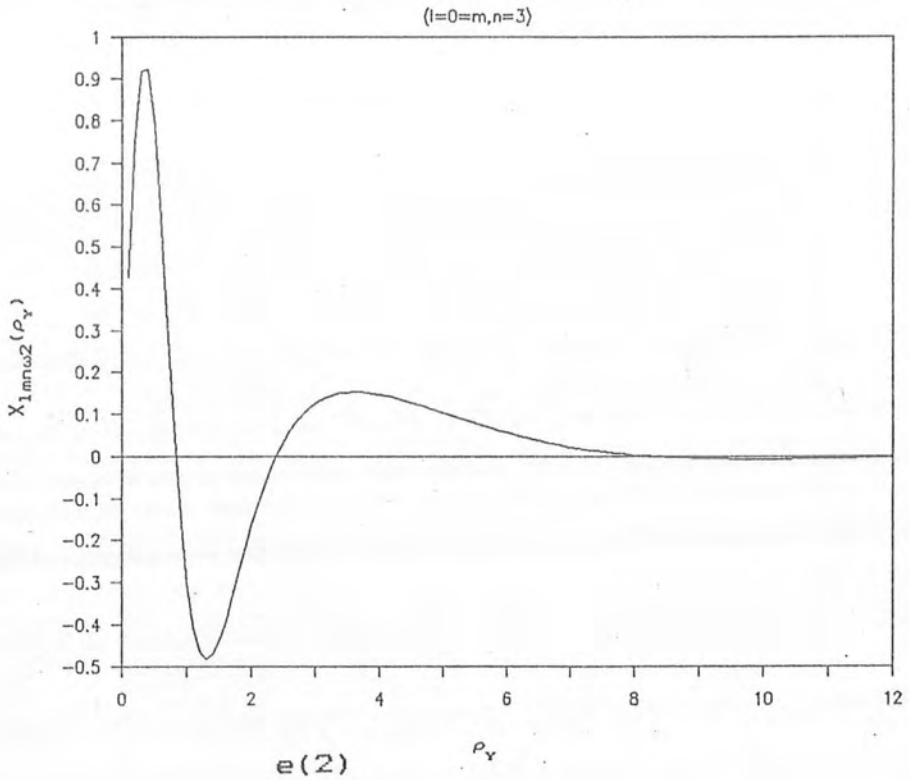
K-Surfaces(K=0.9)
(l=0=m,n=3)
$X_{1mn\omega2}(\rho_Y)$
ρ_Y

e(2)

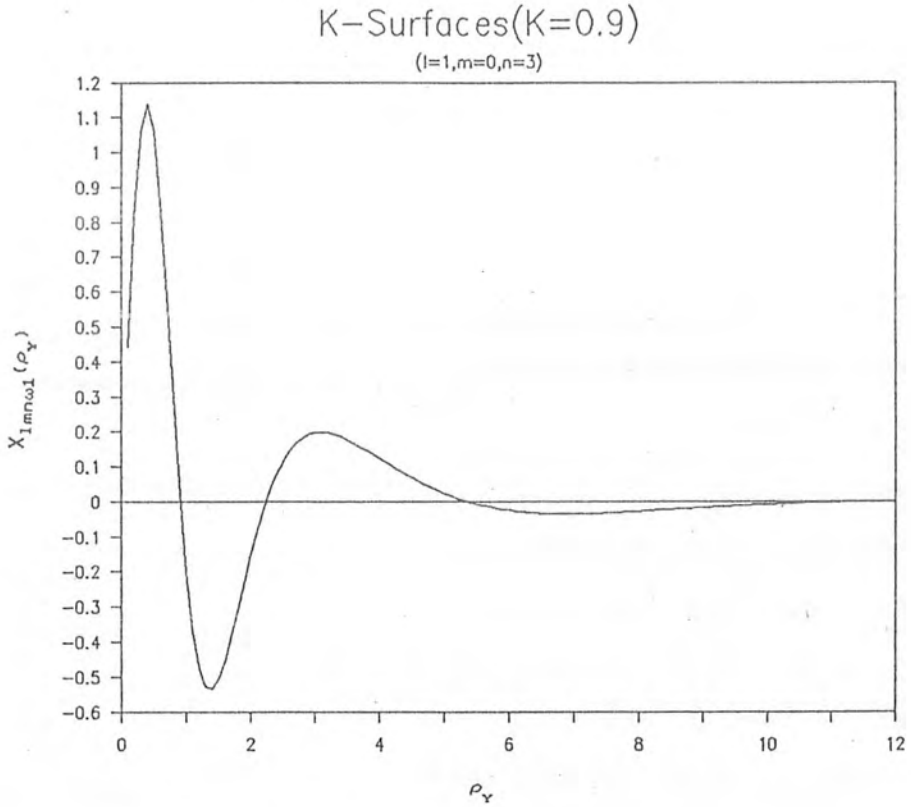
K-Surfaces(K=0.9)
(l=1,m=0,n=3)
$X_{1mn\omega 1}(\rho_Y)$
ρ_Y

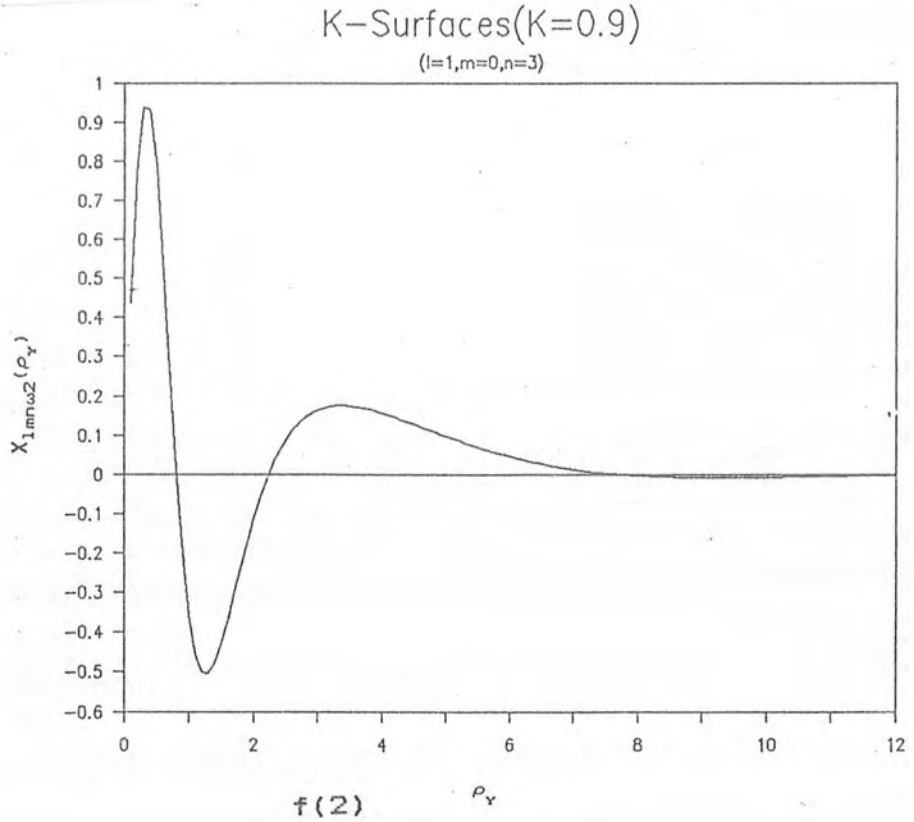
K-Surfaces(K=0.9)
(l=1,m=0,n=3)
$X_{1mn\omega 2}(\rho_Y)$
ρ_Y

f(2)

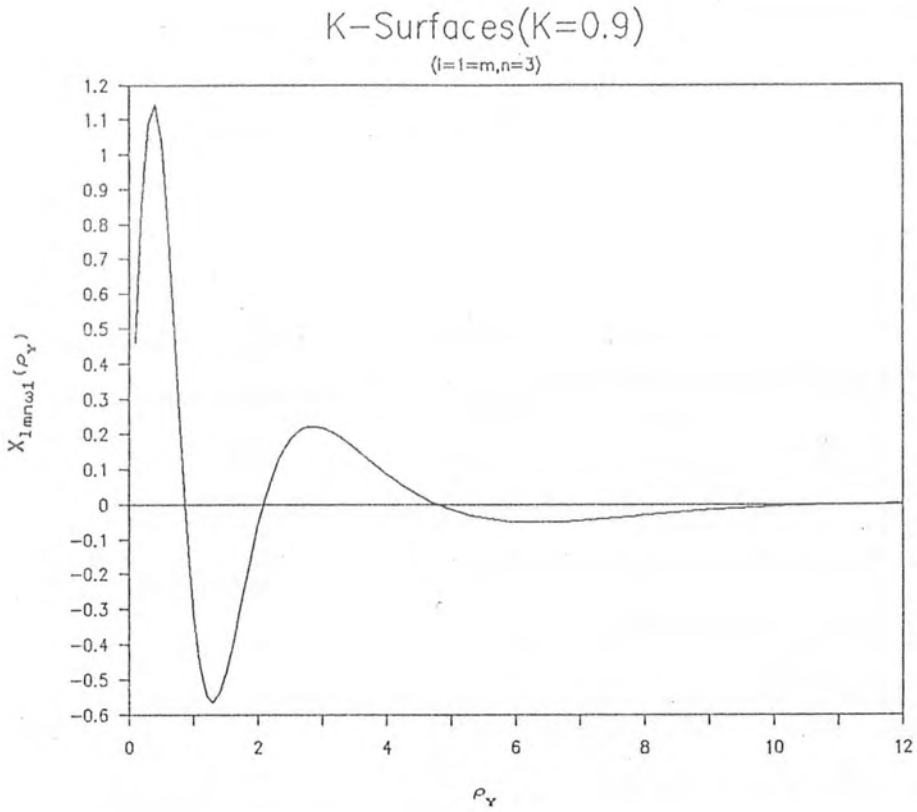
K-Surfaces(K=0.9)
(l=1=m,n=3)
$X_{1mn\omega1}(\rho_r)$
ρ_r

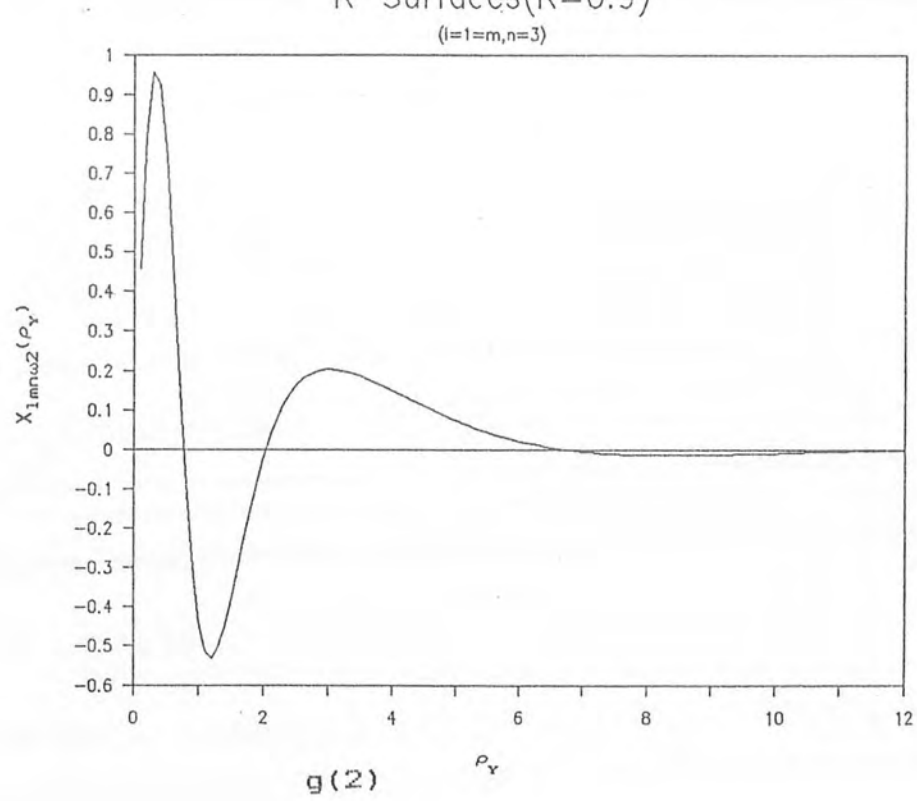
K-Surfaces(K=0.9)
(l=1=m,n=3)
$X_{1mn\omega2}(\rho_r)$
ρ_r

g(2)

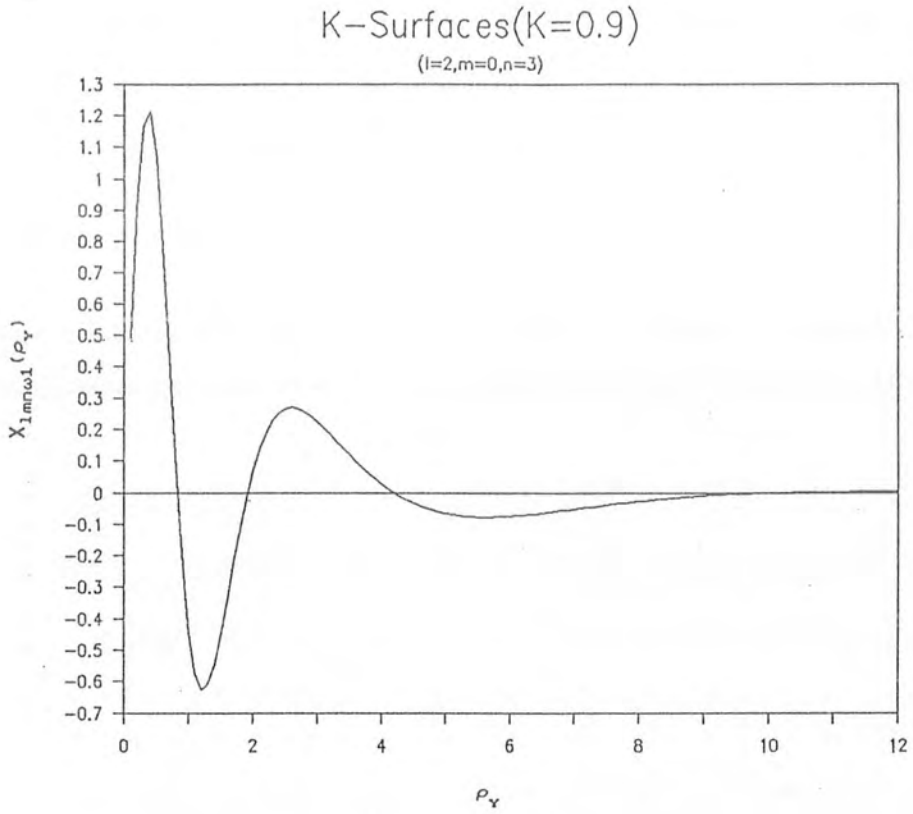
K-Surfaces(K=0.9)
(l=2,m=0,n=3)
$X_{1mn\omega1}(\rho_Y)$
ρ_Y

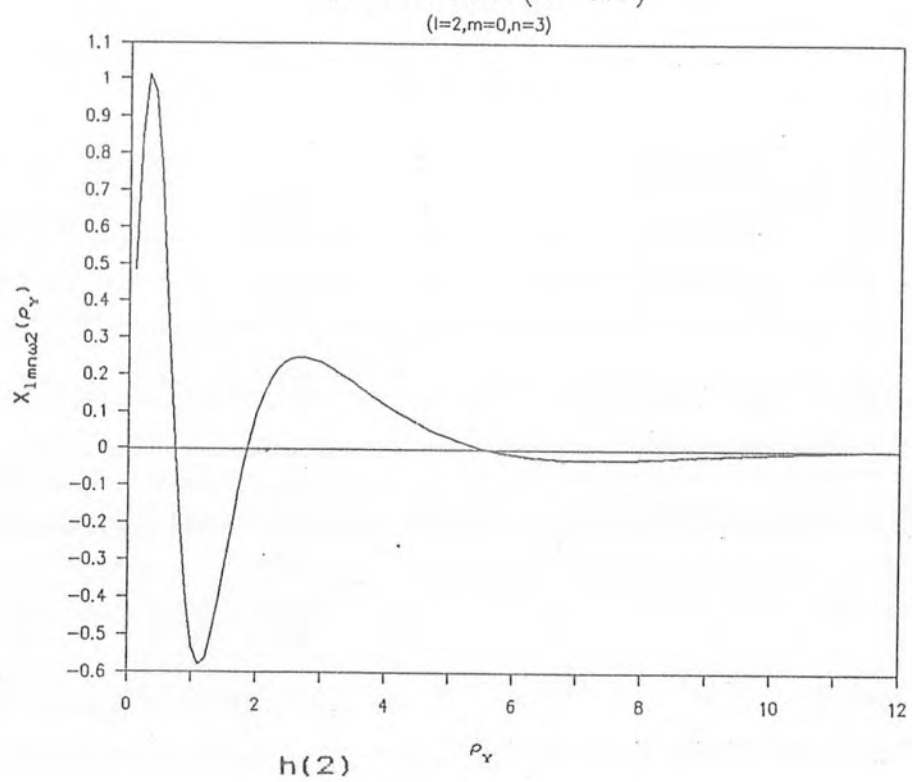
K-Surfaces(K=0.9)
(l=2,m=0,n=3)
$X_{1mn\omega2}(\rho_Y)$
ρ_Y

h(2)

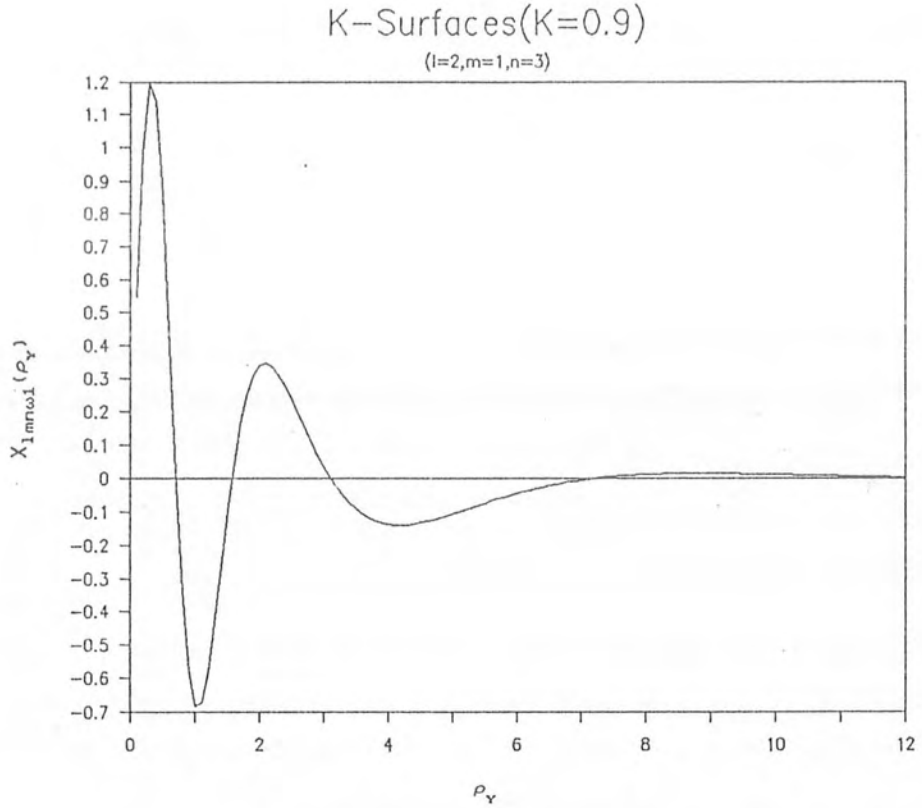
K-Surfaces(K=0.9)
(l=2,m=1,n=3)
$X_{1mn\omega 1}(\rho_Y)$
ρ_Y

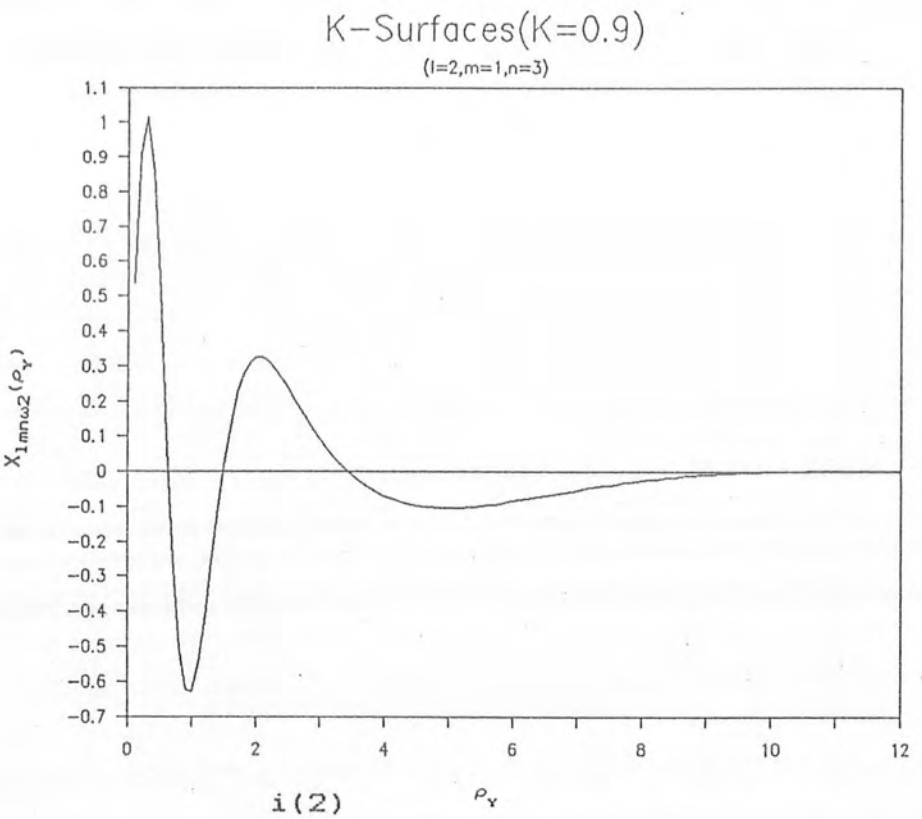
K-Surfaces(K=0.9)
(l=2,m=1,n=3)
$X_{1mn\omega 2}(\rho_Y)$
ρ_Y

i(2)

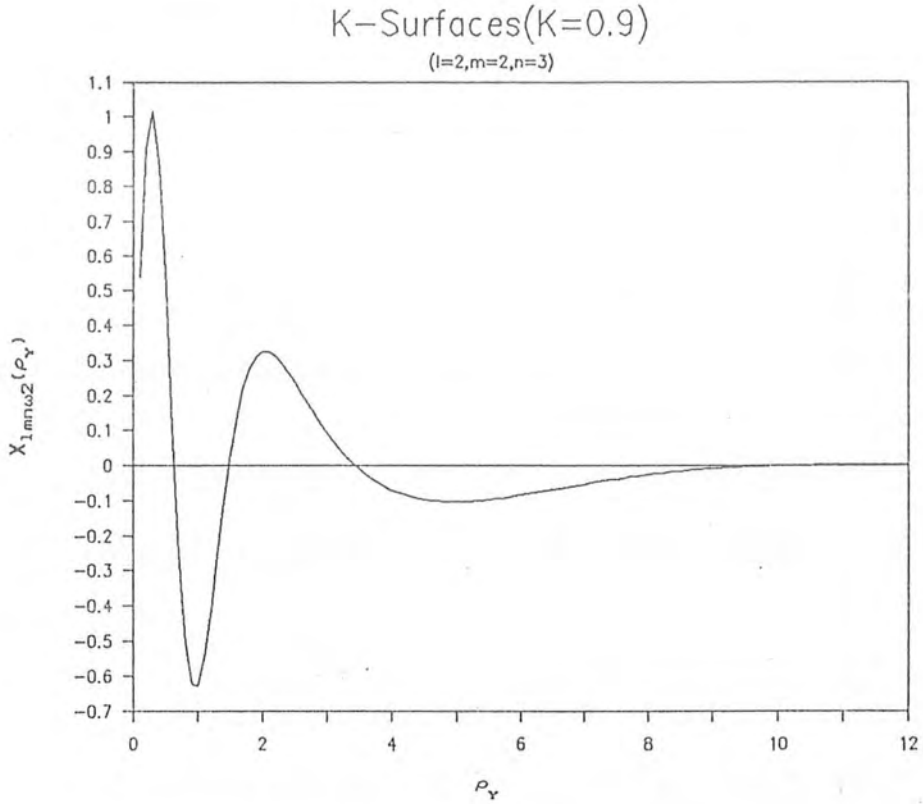
K−Surfaces(K=0.9)
(l=2,m=2,n=3)
$\chi_{1mn\omega 2}(\rho_Y)$
ρ_Y

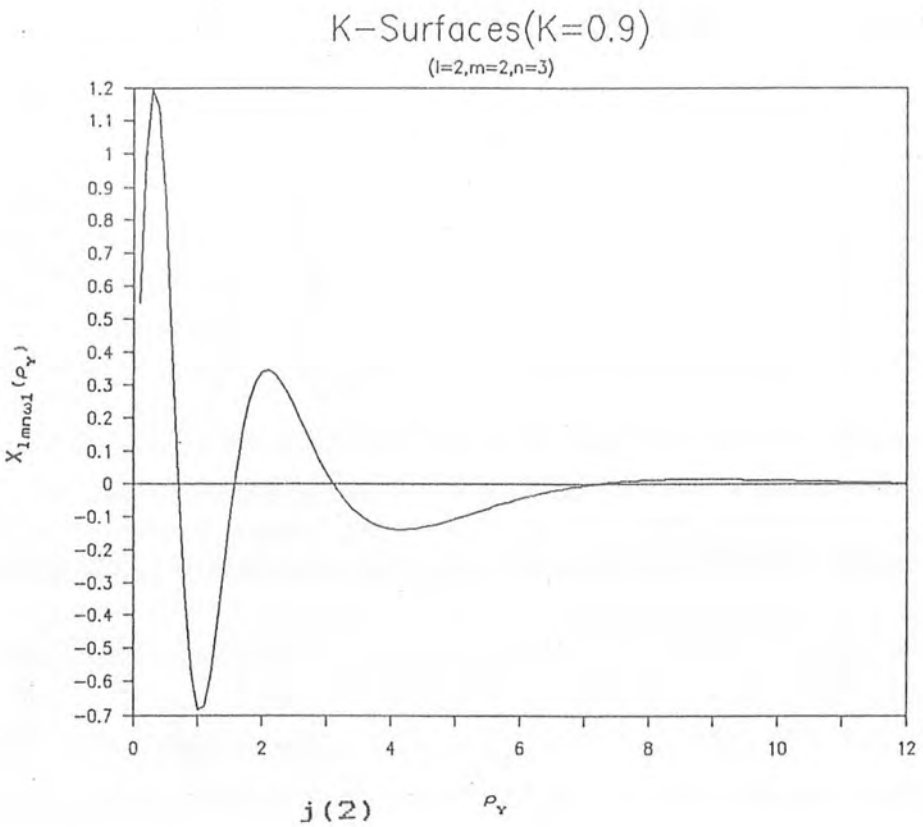
K−Surfaces(K=0.9)
(l=2,m=2,n=3)
$\chi_{1mn\omega 1}(\rho_Y)$
ρ_Y
j(2)

spacetime, therefore, the solution of the wave equation (1.2.2) corresponding to the K-surfaces is given by Eq.(3.1.7) by replacing v by τ_Y and $R_{lmn\omega}(u)$ by $B_4 X_{lmn\omega}(\rho_Y)$, where B_4 is given by Eq.(3.4.12). Under the conditions (3.2.1) and of $Y_{lm}(\theta,\phi)$, the solution of Eq.(1.2.2) must satisfy the orthonormality conditions (3.2.3) by replacing $R_{lmn\omega}(u)$ by $X_{lmn\omega}(\rho_Y)$ and r^2du by $d\rho_Y$.

For the quantisation of massive scalar fields on the K-surfaces we treat, as before, the field Φ as an operator with the equal time commutation relations (1.2.9), where the canonically conjugate momentum, given by Eq.(1.2.10), for the K-surfaces becomes

$$\Pi(\tau_Y,\rho_Y,\theta,\phi) = \frac{|E|}{A} r^2 \sin\theta \frac{\partial\Phi}{\partial\tau_Y}. \qquad (3.4.16)$$

Further, following the quantisation procedure, given in § 3.2 we find a zero value of the VEV of the number operator over the K-surfaces. Hence the procedure of canonical quantisation of massive scalar fields on the K-surfaces shows that the VEV of the number operator remains zero.

In §.3.3, we discussed the quantisation of the massive scalar fields on the SH of CKST only inside the region $-1 < v_o < 1$. In this section we quantised massive scalar fields on K-surfaces, where there is no ambiguity, and infact they provide a complete foliation of the spacetime. As such we are able to take the asymptotic limit

and compare with Hawking's results. Thus whereas the K-surfaces are more complicated for quantisation on, they are better than the SHs of CKST for drawing conclusions regarding the canonical quantisation of scalar fields.

3.5. Quantisation on ψN-Hypersurfaces

In §.2.3, we saw that the ψN-hypersurfaces completely foliate the Schwarzschild spacetime (though they did not avoid the singularity at $r = 0$). In this section we quantise the massive scalar fields on ψN-hypersurfaces. For this purpose we use the Lemaitre[47] coordinates. These coordinates are given by

$$\left.\begin{aligned} d\tau &= dt + \frac{\sqrt{2m/r}}{1-2m/r}\, dr, \\ d\rho &= d\tau + \sqrt{r/2m}\, dr = dt + \frac{\sqrt{r/2m}}{1-2m/r}\, dr, \end{aligned}\right\} \qquad (3.5.1)$$

where

$$r = \{\frac{3}{2}\,(\rho - \tau)\,(2m)^{1/2}\}^{2/3}. \qquad (3.5.2)$$

Notice that here we use τ instead of t_o which was used in §.2.3. In these coordinates, the Schwarzschild metric (1.4.1) becomes

$$ds^2 = d\tau^2 - \frac{2m}{r}\, d\rho - r^2\, d\theta^2 - r^2 \sin^2\theta\, d\phi^2. \qquad (3.5.3)$$

Eq.(3.5.3) shows that there is no coordinate singularity.

Now we use Eq.(3.5.3) in the KG equation (1.2.2) and substitute

$$\Phi(\tau,\rho,\theta,\phi) = \sum_{lm} L_{lm}(\tau,\rho)\; Y_{lm}(\theta,\phi) \qquad (3.5.4)$$

into Eq.(1.2.2). Then $L_{lm}(\tau,\rho)$ satisfy the partial differential equation

$$\sqrt{\frac{r}{2m}}\frac{\partial}{\partial\tau}\left(\sqrt{\frac{2m}{r}}\,r^2\frac{\partial L_{lm}}{\partial\tau}\right)-\sqrt{\frac{r}{2m}}\frac{\partial}{\partial\rho}\left(\sqrt{\frac{r}{2m}}\,r^2\frac{\partial L_{lm}}{\partial\rho}\right)+(M^2r^2+\lambda^2)L_{lm}=0. \tag{3.5.5}$$

From Eqs.(3.4.1), we have

$$\tau_{,r}=-\sqrt{r/2m}=-\rho_{,r}. \tag{3.5.6}$$

Consider an ansatz

$$L_{lm}(\tau,\rho)=\sum_n (2m\,r^3)^{-1/4}\exp(-i\omega\tau)\,G_{lmn\omega}(\rho), \tag{3.5.7}$$

Then by substituting Eqs.(3.5.6) and (3.5.7) into Eq.(3.5.5), $G_{lmn\omega}(\rho)$ satisfy the following differential equation

$$\frac{d^2G_{lmn\omega}(\rho)}{d\rho^2}+\frac{\sqrt{2m/r}}{r}\frac{dG_{lmn\omega}(\rho)}{d\rho}+\{(l^2+m^2+n^2)\frac{2m}{r}$$
$$-\frac{3m}{8r^3}-\frac{2m\lambda^2}{r^3}-\frac{9m^2}{4r^4}\}G_{lmn\omega}(\rho)=0. \tag{3.5.8}$$

This differential equation has been solved numerically (see Appendix C). To obtain $G_{lmn\omega}(\rho)$ from Eq.(3.5.8), we solve this equation over the ψN-hypersurfaces. It was found that the solutions of Eq.(3.5.8) satisfy the orthonormality condition (3.2.1) by replacing $R_{lmn\omega}(u)$ by $G_{lmn\omega}(\rho)$ and r^2du by $d\rho$.

Notice that the mass of the field has no effect on the solutions of Eq.(3.5.8). Also Eq.(3.5.2) we see that for r to be properly defined the range of ρ is $\tau \le \rho < \infty$, where $\rho=\tau$ corresponds to a point on the singularity r =0. It means that for one value of l, m and n there is a unique

solution of Eq.(3.4.8) at each value of τ. These facts did not appear in both the previous both cases. Numerical solutions for $G_{lmn\omega}(\rho)$ are shown in Fig.3.3 for different values of l, m and n over the ψN-hypersurfaces. In all cases these solutions converge to zero as ρ tends to

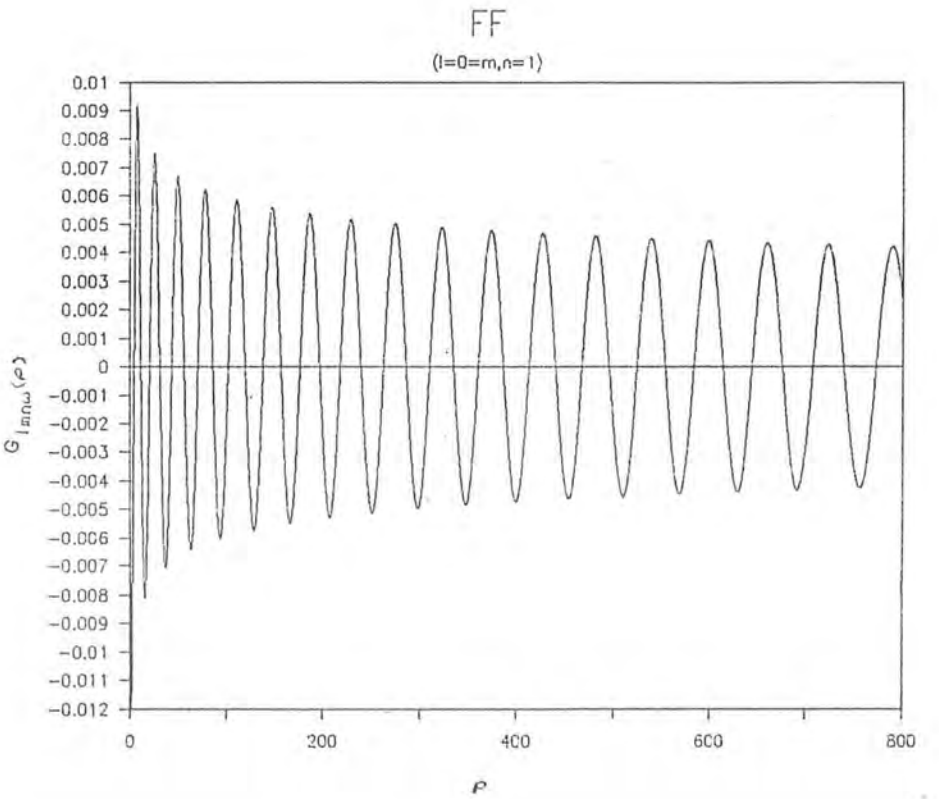

Figure 3.3. The normalised solutions of Eq.(3.4.8) for set of values of l, m and n up to 3 are shown. The convergence does not appear obvious but has been verified.

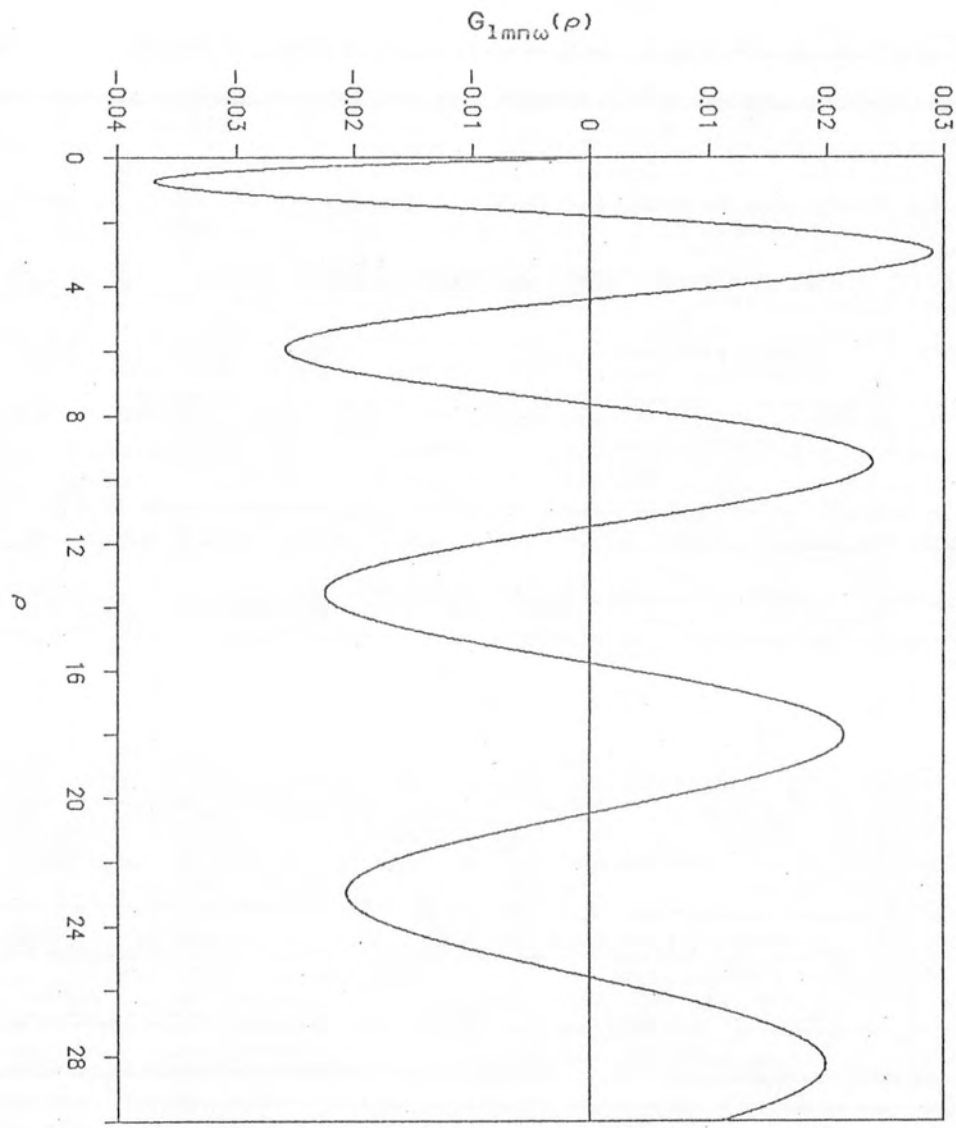
FF
(l=0=m,n=2)
$G_{1mn3}(\rho)$
0.03
0.02
0.01
0
−0.01
−0.02
−0.03
−0.04
0
4
8
12
16
20
24
28
ρ

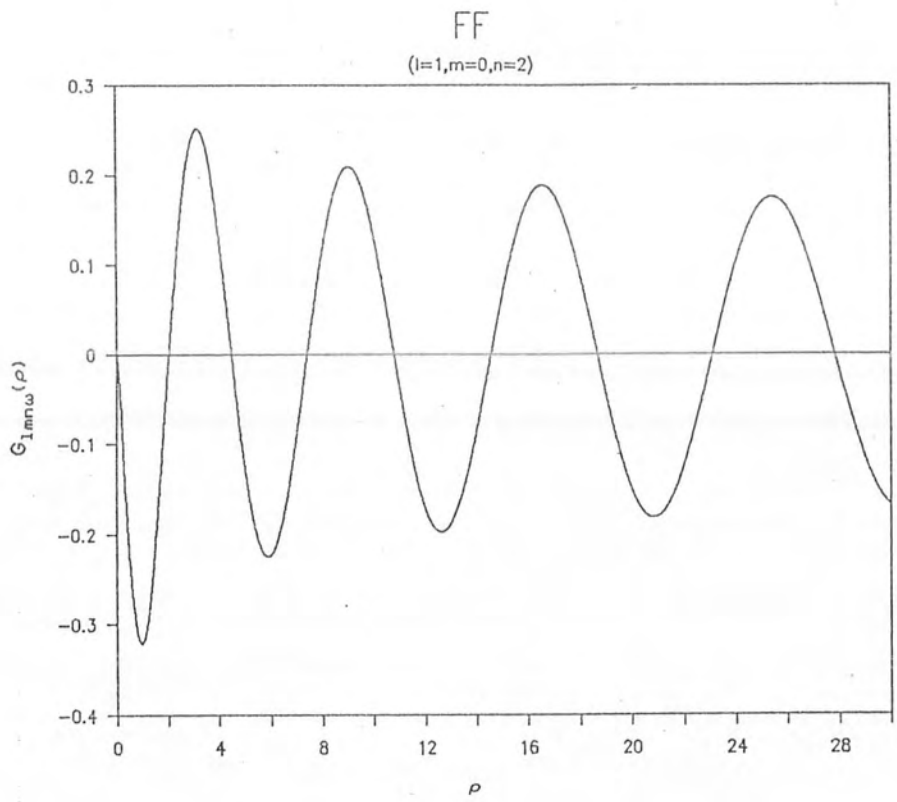
FF
(l=1,m=0,n=2)
0.3
0.2
0.1
0
−0.1
−0.2
−0.3
−0.4
0
4
8
12
16
20
24
28
ρ
$G_{1mn\omega}(\rho)$

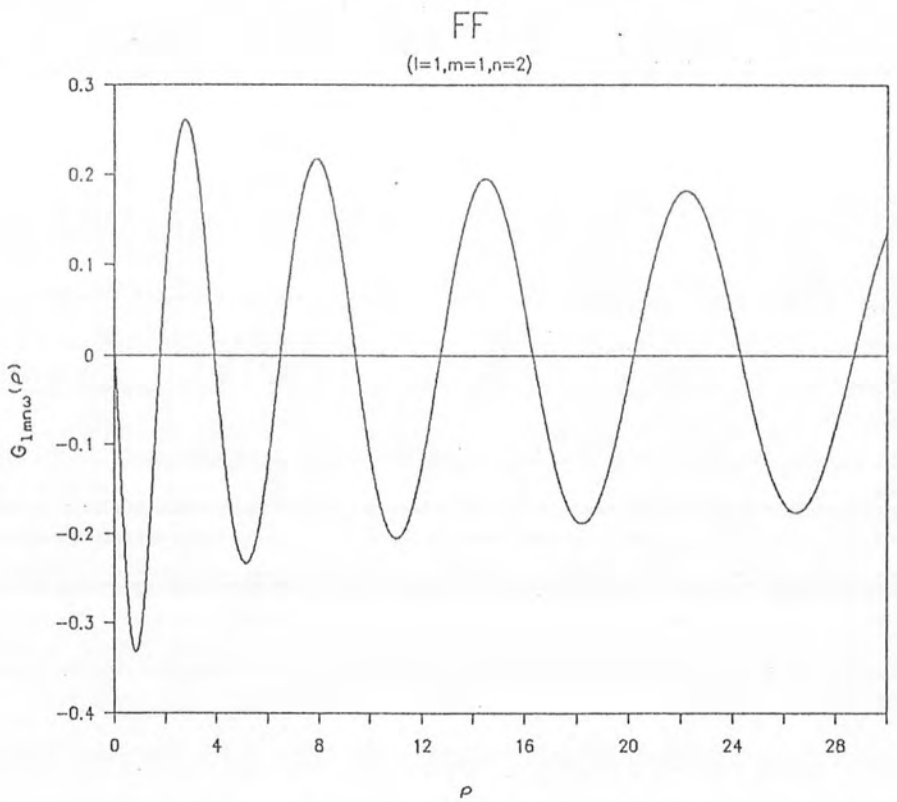
FF
(l=1,m=1,n=2)
0.3
0.2
0.1
0
−0.1
−0.2
−0.3
−0.4
0
4
8
12
16
20
24
28
ρ
$G_{1mn\omega}(\rho)$

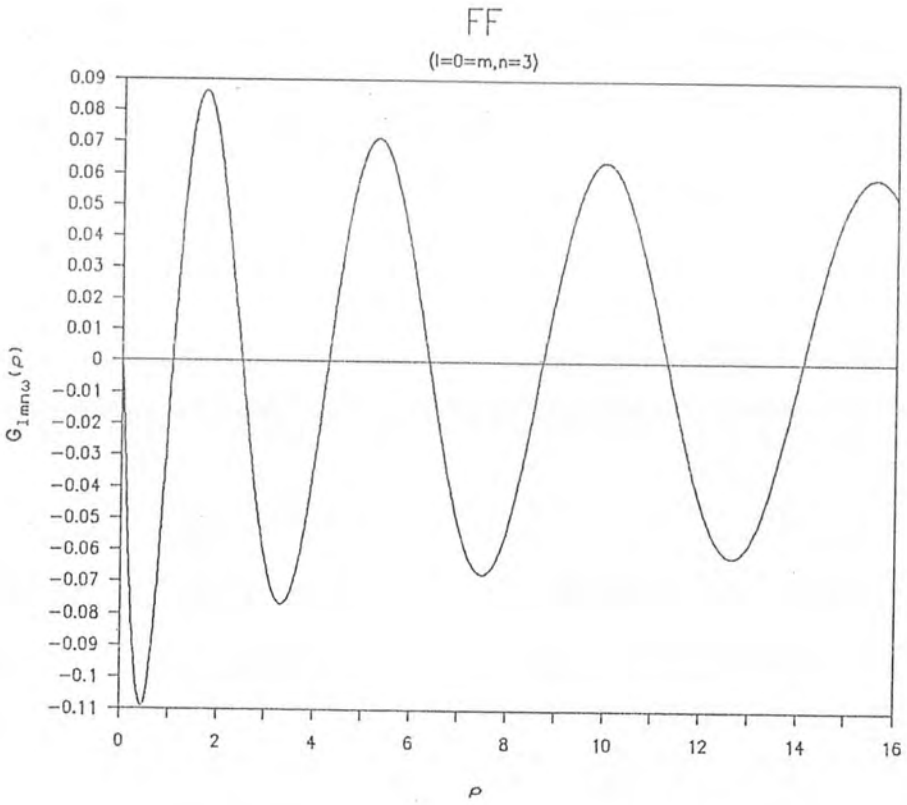
FF
(l=0=m,n=3)
0.09
0.08
0.07
0.06
0.05
0.04
0.03
0.02
0.01
0
−0.01
−0.02
−0.03
−0.04
−0.05
−0.06
−0.07
−0.08
−0.09
−0.1
−0.11
$G_{1mn\omega}(\rho)$
0
2
4
6
8
10
12
14
16
ρ

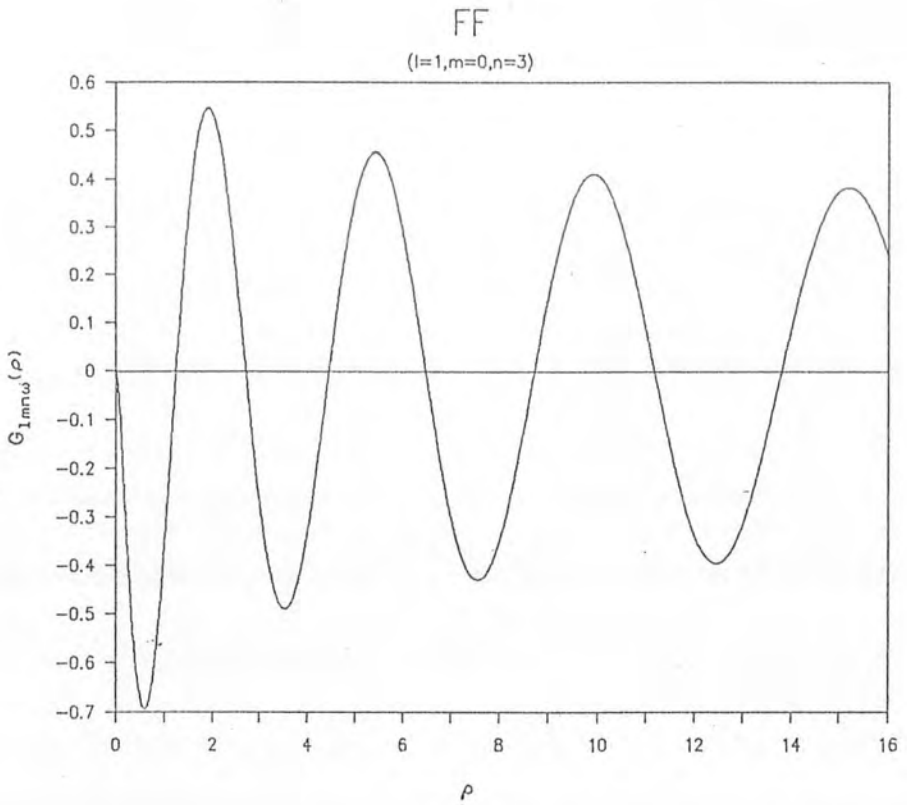
FF
(l=1,m=0,n=3)
0.6
0.5
0.4
0.3
0.2
0.1
0
−0.1
−0.2
−0.3
−0.4
−0.5
−0.6
−0.7
$G_{1mn\omega}(\rho)$
0
2
4
6
8
10
12
14
16
ρ

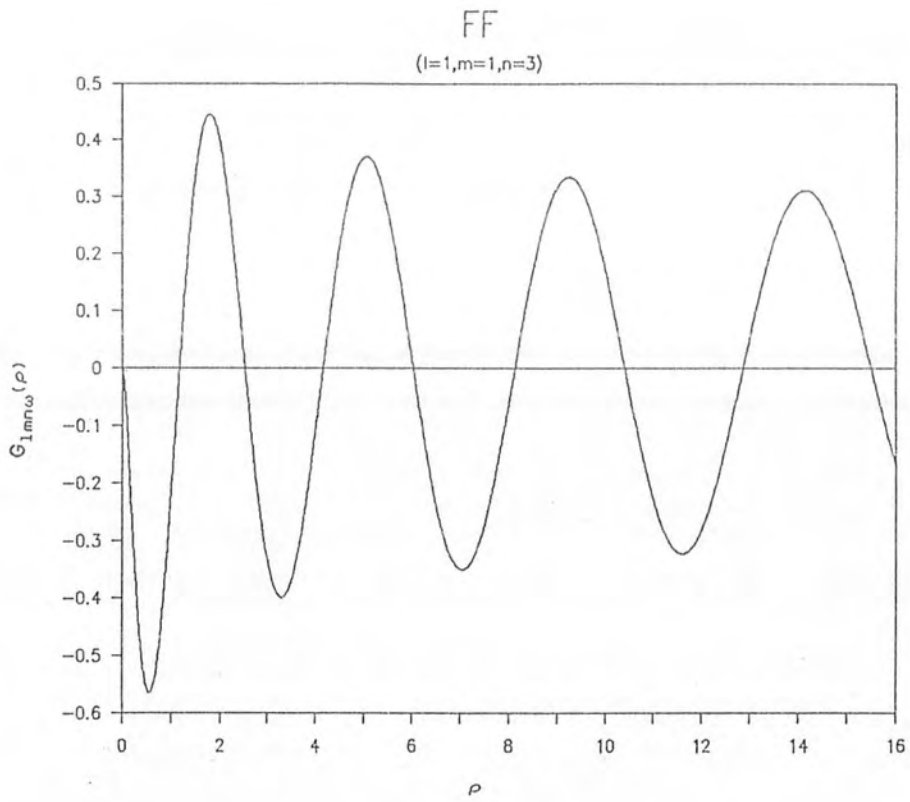
FF
(l=1,m=1,n=3)
0.5
0.4
0.3
0.2
0.1
0
−0.1
−0.2
−0.3
−0.4
−0.5
−0.6
$G_{1mn\omega}(\rho)$
0
2
4
6
8
10
12
14
16
ρ

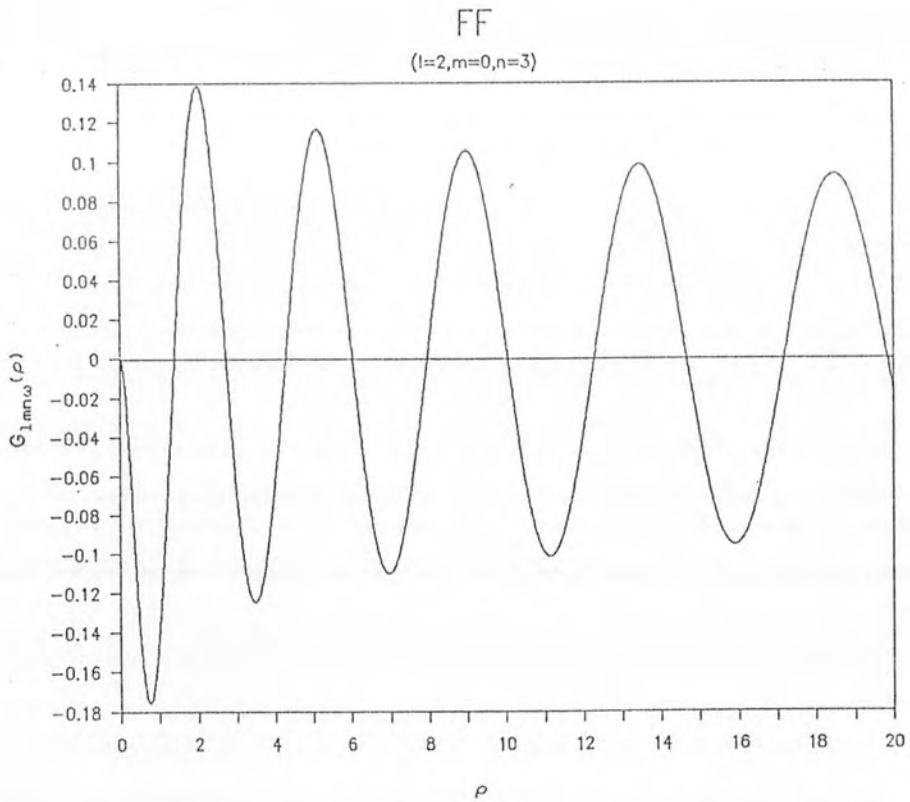
FF
(l=2,m=0,n=3)
0.14
0.12
0.1
0.08
0.06
0.04
0.02
0
−0.02
−0.04
−0.06
−0.08
−0.1
−0.12
−0.14
−0.16
−0.18
$G_{1mn\omega}(\rho)$
0
2
4
6
8
10
12
14
16
18
20
ρ

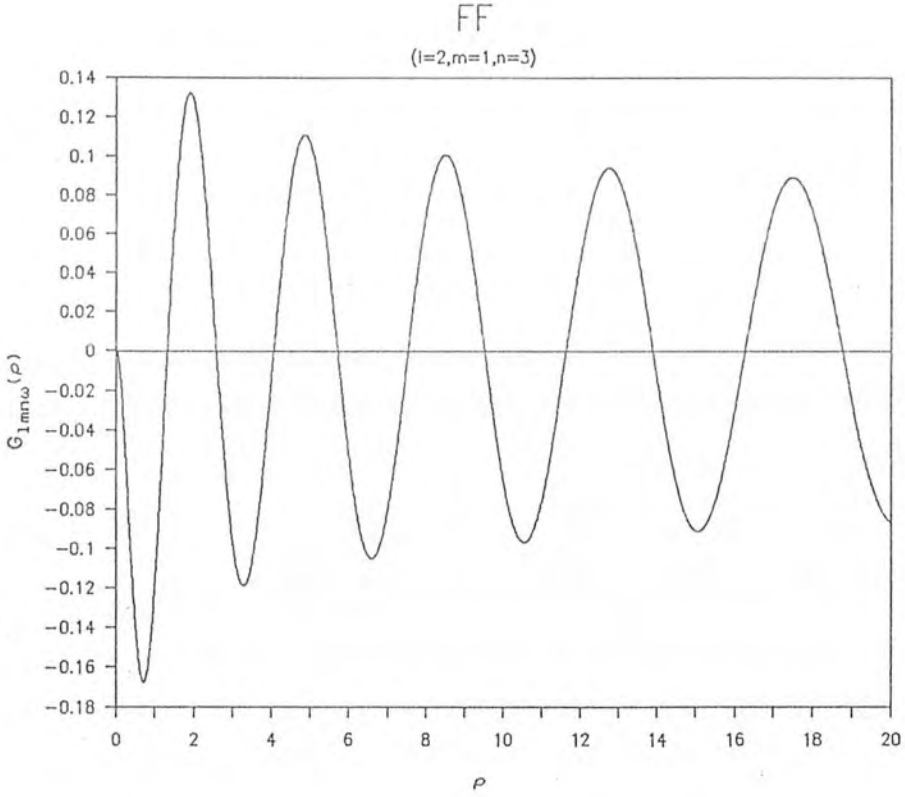
FF
(l=2,m=1,n=3)
0.14
0.12
0.1
0.08
0.06
0.04
0.02
0
−0.02
−0.04
−0.06
−0.08
−0.1
−0.12
−0.14
−0.16
−0.18
$G_{1mn\omega}(\rho)$
0
2
4
6
8
10
12
14
16
18
20
ρ

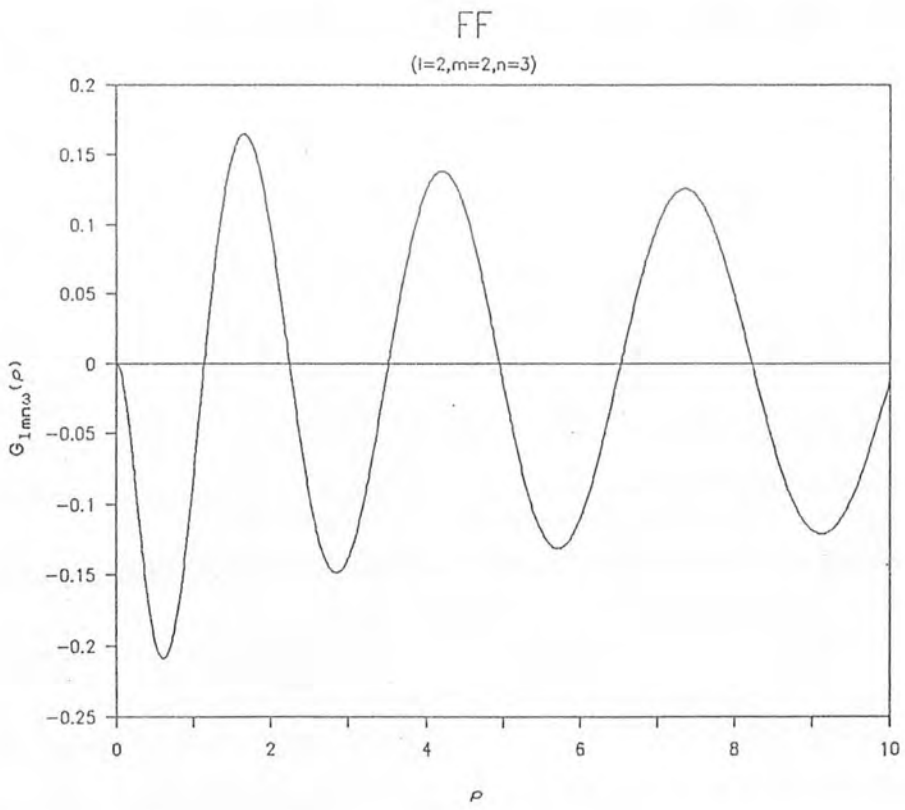
FF
(l=2,m=2,n=3)
0.2
0.15
0.1
0.05
0
−0.05
−0.1
−0.15
−0.2
−0.25
$G_{1mn\omega}(\rho)$
0
2
4
6
8
10
ρ

infinity and the area under the curve is finite (as was true for the CKST and CMEC cases.) As such we normalise the wave function over the ψN-hypersurfaces.

Since $G_{lmn\omega}(\rho)$ with the function $(2mr^3)^{-1/4}exp(-i\omega\tau)$ form a complete orthonormal basis, the solution of the wave equation (1.2.2) over the ψN-hypersurfaces is given by Eq.(3.1.7) by replacing $R_{lmn\omega}(u)$ by $(2mr^3)^{-1/4}G_{lmn\omega}(\rho)$. Due to Eqs.(3.2.1) and (3.2.2) it is clear that the mode solutions satisfy the orthonormality conditions (3.2.3). The canonically conjugate momentum Π can be written as

$$\Pi(\tau,\rho,\theta,\phi)=\sqrt{2m/r}\ r^2 sin\theta\ \frac{\partial\Phi}{\partial\tau}\ . \qquad (3.5.9)$$

Following the canonical quantisation procedure, we find that the VEV of the number operator over the ψN-hypersurfaces is zero. Notice that we are not actually calculating the wave functions on $\mathscr{I}^+$ but only on the interior of the Penrose digram for the Schwarzschild spacetime. In the next chapter we will give a brief discussion of our work and compare the results of the quantisation procedure for the three type of SHs considered.

CHAPTER FOUR

CONCLUSION

In this thesis we have investigated the quantisation of scalar fields with a view to verifying certain conjectures. One is that the VEV of the number operator is unchanged in spacetimes without horizon. The other is that there may be no radiation seen in a freely falling (or possibly a CMEC) frame. To test these conjectures we used the procedure of canonical quantisation of scalar fields on some SH in the background of the Schwarzschild spacetime and found the VEV of the number operator. We considered three different frames corresponding to three different choices of SH. These SHs were: i) CKST; ii) CMEC; and iii) ψN. For the quantisation of scalar fields on SHs it is necessary that the whole spacetime be foliated by them. The foliation procedure of the spacetime by using the KS coordinates (in all cases) were discussed in chapter two while chapter three dealt with the quantisation of scalar fields on these SHs.

The SHs of CKST provide a complete foliation of the spacetime but presented us with an ambiguity. This ambiguity arises from the fact that the hypersurfaces are divided into two parts for $|v_o| > 1$. For $|v_o| < 1$, the SHs

are non-singular while for $|v_o| \geq 1$ they are singular. The region $|v_o| < 1$ contains connected hypersurfaces but for the other region they are disconnected. The connected hypersurfaces do not provide a complete foliation of the spacetime. Notice that all the CKST hypersurfaces pass smoothly through $r = 2m$, so that there is no horizon in these frames.

The Klein-Gordon equation was relatively simple to solve on these hypersurfaces but the ambiguity in the hypersurfaces does not allow us to apply the canonical quantisation procedure for $|v_o| \geq 1$ as we can not unambiguously normalise the wave function for this region. In §.3.3 we quantised the scalar fields on hypersurfaces inside the region $-1 < v_o < 1$, so as to set up the quantisation procedure. For $|v_o| < 1$ it showed that the VEV of the number operator remains zero. However, the result could not be taken as very significant as we were unable to take asymptotic limits. As such we also can not compare our result for CKST hypersurfaces with Hawking's result so as to test the first conjecture. It is worth emphasising that there is no reason to suppose that there *is* radiation in this frame. If we used each separate hypersurface $|v_o| \geq 1$, hitting the singularity, as the whole hypersurface for normalising the wave function, we would get the same result. On the other hand, if we used the two parts

together as forming a disjoint hypersurface, we would *still* get zero VEV of the number operator. The point was only that the ambiguity *can* cast doubt on the interpretation of the asymptotic results.

The foliation of the Schwarzschild spacetime by the CMEC spacelike hypersurfaces (spacelike K-surfaces) was discussed in §.2.2. K-surfaces completely foliate the spacetime. The intrinsic curvature invariants are asymptotically zero for finite values of K and H and they tend to infinity at the singularity. As the K-surfaces pass smoothly through r = 2m. In the frame, corresponding to the K-surfaces, there is no horizon in this "York frame". Further, there is no ambiguity in the K-surfaces such as that which appeared in the hypersurfaces of CKST. The procedure of canonical quantisation of massive scalar fields on K-surfaces, as discussed in §.3.4, showed that the VEV of the number operator remains zero. Also, corresponding to the K-surfaces, we can quantise the scalar fields in the asymptotic limit. This procedure will be used for a more explicit calculation of Hawking radiation in a closed Friedmann model Universe containing a Schwarzschild BH[46].

K-slicing has repeatedly proved useful for talking about cosmological matters. A case in point is the "Suture model" of a Friedmann Universe in which a black hole forms

due to an inhomogeneity[45]. Suffice it to say that this procedure of foliation was used to demonstrate Penrose's conjecture[48] that the black hole singularity forms simultaneously with the Big Crunch singularity in a closed universe[49] for various simpler models and the suture model.

The foliation of the spacetime in a Schwarzschild background by freely falling, ψN, hypersurfaces was discussed in §.2.3. The ψN-hypersurfaces provided a very interesting foliation of the spacetime. No ambiguity appeared here either. Each ψN-hypersurface passes smoothly through r = 2m and hits the singularity. Therefore, there is no horizon in the ψN-frame. The MEC is finite for large r and infinite only at the singularity. Further, the intrinsic curvature invariants are zero as the intrinsic curvature tensor is, itself, zero. This is necessary for the ψN-observer to see a Minkowski spacetime around him. The ψN-hypersurfaces are particularly important as both conjectures are tested by them. The canonical quantisation of massive scalar fields on ψN-hypersurfaces, discussed in §.3.5, showed that the VEV of the number operator remains zero. Also, we quantised scalar fields on the ψN-hypersurfaces with asymptotic limits to compare our result with Hawking's result.

If the VEV of the number operator is taken as the sole indicator, the canonical quantisation procedure in the

York and ψN frames shows that there is no Hawking radiation seen in these frames (while we can not be so sure about the radiation in the CKST frame). It will be necessary to investigate the question of radiation in these frames using the path integral approach and examining the phenomenon of superradiance. As ψN-observers see a Minkowski spacetime it is reasonable to expect that there is no contribution in the ψN-frame by the zero superradiant modes. Hence it can be argued that the conjecture that ψN-observers see no radiation is proved. However, in the York frame one would, presumably, expect to see superradiance. If superradiance is seen here and not in ψN frames, Padmanabhan's argument[7] could be extended to Hawking radiation as well.

APPENDICES

APPENDIX A

Here we give a procedure for obtaining the numerical solutions of the coupled differential Eqs.(3.3.2) and (3.3.3). We solve these differential equations by using Fortran with double precision. There is an arbitrary choice of initial values of $R_{lmn\omega}(u)$ and $\frac{dR_{lmn\omega}(u)}{du}$ for given l, m, and n and the solution generally diverges. We pick only those initial values which lead to a convergent solution. We obtain the area under the curve $r^2|R_{lmn\omega}(u)|^2$ to find the integral $\int r^2|R_{lmn\omega}(u)|^2 du$ over the entire allowable range of u to normalise. Still there are too many solutions, we select one for given l, m and n. To use Eq.(3.2.1), for different values of l, m and n, we select only one orthogonal to this in that $\int r^2 R_{lmn\omega}(u) R^{*}_{l'm'n'\omega'}(u)du = 0$ integrated over the entire SH.

This procedure will be repeated for various values of l, m and n. If there arises a problem in being able to find orthogonal solutions later we go back to first equation and select new initial conditions which maintain the required orthonormality. Hence we obtain an orthonormal set of solutions.

The numerical solutions of Eqs.(3.3.2) and (3.3.3) over the CKST hypersurfaces were obtained by using the following Fortran program:

```
C      PROGRAM ONE
C      NUMERICAL SOLUTION OF DIFFERENTIAL EQUATION(KRUSKAL-
C      SZEKERES) WITH v-CONSTANT HYPERSURFACE BY USING THE
C      RUNGE-KUTTA METHOD m=1/2, MASS OF THE FIELD = D,
C      X = r/2m, Y= real part of R_lmnω(u),
C      YS = imaginary part of R_lmnω(u), Z = dY/du,
C      E = accoracy, H = Step size,
       IMPLICIT DOUBLE PRECISION(A-H,P-Z)
       WRITE(*,*)'E= ,','V= ,','Ui= '
       READ(*,*)E,V,U
       CALL PROG(E,V,U,X,B)
       WRITE(*,*)'D=,','K=,','L=,','M=,','Yi=,','YSi=,','Zi=
      1,','ZSi=,','H= ,','N= '
       READ(*,*)D,K,L,M,Y,YS,Z,ZS,H,N
       DO 20 I=1,N
       W=DSQRT(K*K+L*L+M*M+D*D)
       XS=X*X
       P1=H*Z
       Q1=H*((4.*(D*D+(L*(L+1.))/XS)/(X*B)-W*W)*Y-4.*U*Z/(XS
      1*B)-4.*W* V*YS/(XS*B))
       PS1=H*ZS
       QS1=H*((4.*(D*D+(L*(L+1.))/XS)/(X*B)-W*W)*YS-4.*U*ZS/
      1(XS*B)+4. *W*V*Y/(XS*B))
       U1=U+0.5*H
       Y1=Y+0.5*P1
       YS1=YS+0.5*PS1
       Z1=Z+0.5*Q1
       ZS1=ZS+0.5*QS1
       CALL PROG(E,V,U1,X,B)
       P2=H*Z1
       XS=X*X
       Q2=H*((4.*(D*D+(L*(L+1.))/XS)/(X*B)-W*W)*Y1-4.*U1*Z1
      1/(XS*B)-4.*W*V*YS1/(XS*B))
       PS2=H*ZS1
       QS2=H*((4.*(D*D+(L*(L+1.))/XS)/(X*B)-W*W)*YS1-4.*U1*
      1ZS1/(XS*B)+4.*W*V*Y1/(XS*B))
       U2=U1
       Y2=Y+0.5*P2
       YS2=YS+0.5*PS2
       Z2=Z+0.5*Q2
       ZS2=ZS+0.5*QS2
       CALL PROG(E,V,U2,X,B)
       P3=H*Z2
       XS=X*X
       Q3=H*((4.*(D*D+(L*(L+1.))/XS)/(X*B)-W*W)*Y2-4.*U2*Z2
      1/(XS*B)-4.*W*V*YS2/(XS*B))
       PS3=H*ZS2
       QS3=H*((4.*(D*D+(L*(L+1.))/XS)/(X*B)-W*W)*YS2-4.*U2*
      1ZS2/(XS*B)+4.*W*V*Y2/(XS*B))
       U3=U+H
       Y3=Y+P3
       YS3=Y+PS3
       Z3=Z+Q3
```

```
      ZS3=ZS+QS3
      CALL PROG(E,V,U3,X,B)
      P4=H*Z3
      XS=X*X
      Q4=H*((4.*(D*D+(L*(L+1.))/XS)/(X*B)-W*W)*Y3-4.*U3*Z3
     1/(XS*B)-4.*W*V*YS3/(XS*B))
      PS4=H*ZS3
      QS4=H*((4.*(D*D+(L*(L+1.))/XS)/(X*B)-W*W)*YS3-4.*U3*
     1ZS3/(XS*B)+4.*W*V*Y3/(XS*B))
      U=U+H
      Y=Y+(P1+2.*P2+2.*P3+P4)/6.
      YS=YS+(PS1+2.*PS2+2.*PS3+PS4)/6.
      Z=Z+(Q1+2.*Q2+2.*Q3+Q4)/6.
      ZS=ZS+(QS1+2.*QS2+2.*QS3+QS4)/6.
      CALL PROG(E,V,U,X,B)
      WRITE(*,10)U,Y,YS,Z,ZS
   10 FORMAT(5D14.7)
   20 CONTINUE
      STOP
      END

      SUBROUTINE PROG(A,G,F,R,S)
      IMPLICIT DOUBLE PRECISION(A,G,F,R,S)
      GG=(F*F-G*G)
      IF(GG-2.)50,50,60
   50 R=0.5
      GO TO 100
   60 R=DLOG(GG)
  100 S=DEXP(R)
      SS=(R-1.)*S-GG
      IF(DABS(SS)-A)300,300,200
  200 R=R-1.+1./R+GG/(R*S)
      GO TO 100
  300 RETURN
      END
```

For the orthogonality conditions of the function $R_{lmn\omega}(u)$, the Fortran program was:

```
      PROGRAM TWO
      IMPLICIT DOUBLE PRECISION(B,D,E,H,P-Z)
      WRITE(*,*)'E= ,','V= ,','Ui= '
      READ(*,*)E,V,U
      CALL PROG(E,V,U,X,B)
      WRITE(*,*)'D=,','L= ,','L1=,','M=,','M1=,','K=,','K1
     1=,','Yi=,','YSi=,','YYi=,','YYSi=,','Zi=,','ZSi=,','
     2ZZi=,','ZZSi= ,','H= ,','N= '
      READ(*,*)D,L,L1,M,M1,K,K1,Y,YS,YY,YYS,Z,ZS,ZZ,ZZS,H,N
      DO 20 I=1,N
      W=DSQRT(L*L+M*M+K*K+D*D)
```

```
 W1=DSQRT(L1*L1+M1*M1+K1*K1+D*D)
 AL=L*(L+1.)
 AL1=L1*(L1+1.)
 XS=X*X
 P1=H*Z
 Q1=H*((4.*(D*D+AL/XS)/(X*B)-W*W)*Y-4.*U*Z/(XS*B)-4.*W
1*V*YS/(XS*B))
 PS1=H*ZS
 QS1=H*((4.*(D*D+AL/XS)/(X*B)-W*W)*YS-4.*U*ZS/(XS*B)+4
1*W*V*Y/(XS*B))
 PP1=H*ZZ
 QQ1=H*((4.*(D*D+AL1/XS)/(X*B)-W1*W1)*YY-4.*U*ZZ/(XS*
1B)-4.*W1*V*YYS/(XS*B))
 PPS1=H*ZZS
 QQS1=H*((4.*(D*D+AL1/XS)/(X*B)-W1*W1)*YYS-4.*U*ZZS/(
1XS*B)+4.*W1*V*YY/(XS*B))
 U1=U+0.5*H
 Y1=Y+0.5*P1
 YS1=YS+0.5*PS1
 Z1=Z+0.5*Q1
 ZS1=ZS+0.5*QS1
 YY1=YY+0.5*PP1
 YYS1=YYS+0.5*PPS1
 ZZ1=ZZ+0.5*QQ1
 ZZS1=ZZS+0.5*QQS1
 CALL PROG(E,V,U1,X,B)
 P2=H*Z1
 XS=X*X
 Q2=H*((4.*(D*D+AL/XS)/(X*B)-W*W)*Y1-4.*U1*Z1/(XS*B)-4
1*W*V*YS1/(XS*B))
 PS2=H*ZS1
 QS2=H*((4.*(D*D+AL/XS)/(X*B)-W*W)*YS1-4.*U1*ZS1/(XS*B
1)+4.*W*V*Y1/(XS*B))
 PP2=H*ZZ1
 QQ2=H*((4.*(D*D+AL1/XS)/(X*B)-W1*W1)*YY1-4.*U1*ZZ1/(
1XS* B)-4.*W1*V*YYS1/(XS*B))
 PPS2=H*ZZS1
 QQS2=H*((4.*(D*D+AL1M/XS)/(X*B)-W1*W1)*YYS1-4.*U1*
1ZZS1/(XS*B)+4.*W1*V*YY1/(XS*B))
 U2=U1
 Y2=Y+0.5*P2
 YS2=YS+0.5*PS2
 Z2=Z+0.5*Q2
 ZS2=ZS+0.5*QS2
 YY2=YY+0.5*PP2
 YYS2=YYS+0.5*PPS2
 ZZ2=ZZ+0.5*QQ2
 ZZS2=ZZS+0.5*QQS2
 CALL PROG(E,V,U2,X,B)
 P3=H*Z2
 XS=X*X
 Q3=H*((4.*(D*D+AL/XS)/(X*B)-W*W)*Y2-4.*U2*Z2/(XS*B)-4
1*W*V*YS2/(XS*B))
 PS3=H*ZS2
```

```
      QS3=H*((4.*(D*D+AL/XS)/(X*B)-W*W)*YS2-4.*U2*ZS2/(XS*B
     1)+4.*W*V*Y2/(XS*B))
      PP3=H*ZZ2
      QQ3=H*((4.*(D*D+AL1/XS)/(X*B)-W1*W1)*YY2-4.*U2*ZZ2/(
     1XS*B)-4.*W1*V*YYS2/(XS*B))
      PPS3=H*ZZS2
      QQS3=H*((4.*(D*D+AL1/XS)/(X*B)-W1*W1)*YYS2-4.*U2*
     1ZZS2/(XS*B)+4.*W1*V*YY2/(XS*B))
      U3=U+H
      Y3=Y+P3
      YS3=Y+PS3
      Z3=Z+Q3
      ZS3=ZS+QS3
      YY3=YY+PP3
      YYS3=YY+PPS3
      ZZ3=ZZ+QQ3
      ZZS3=ZZS+QQS3
      CALL PROG(E,V,U3,X,B)
      P4=H*Z3
      XS=X*X
      Q4=H*((4.*(D*D+AL/XS)/(X*B)-W*W)*Y3-4.*U3*Z3/(XS*B)-4
     1*W*V*YS3/(XS*B))
      PS4=H*ZS3
      QS4=H*((4.*(D*D+AL/XS)/(X*B)-W*W)*YS3-4.*U3*ZS3/(XS*B
     1)+4.*W*V*Y3/(XS*B))
      PP4=H*ZZ3
      QQ4=H*((4.*(D*D+AL1/XS)/(X*B)-W1*W1)*YY3-4.*U3*ZZ3/(
     1XS*B)-4.*W1*V*YYS3/(XS*B))
      PPS4=H*ZZS3
      QQS4=H*((4.*(D*D+AL1/XS)/(X*B)-W1*W1)*YYS3-4.*U3*
     1ZZS3/(XS*B)+4.*W1*V*YY3/(XS*B))
      U=U+H
      Y=Y+(P1+2.*P2+2.*P3+P4)/6.
      YS=YS+(PS1+2.*PS2+2.*PS3+PS4)/6.
      Z=Z+(Q1+2.*Q2+2.*Q3+Q4)/6.
      ZS=ZS+(QS1+2.*QS2+2.*QS3+QS4)/6.
      YY=YY+(PP1+2.*PP2+2.*PP3+PP4)/6.
      YYS=YYS+(PPS1+2.*PPS2+2.*PPS3+PPS4)/6.
      ZZ=ZZ+(QQ1+2.*QQ2+2.*QQ3+QQ4)/6.
      ZZS=ZZS+(QQS1+2.*QQS2+2.*QQS3+QQS4)/6.
      CALL PROG(E,V,U,X,B)
      TOA=H*(Y*YY-YS*YYS)
      TOAC=H*(Y*YYS+YS*YY)
20    CONTINUE
      SUM1=SUM+TOA
      SUM2=SUM+TOAC
      WRITE(*,*)SUM1,SUM2
      STOP
      END
```

APPENDIX B

The procedure given in Appendix A was followed for CMEC hypersurfaces, replacing Eqs.(3.3.2) and (3.3.3) by Eqs.(3.4.15). The CMEC hypersurfaces were obtained using the following program to solve Eq.(2.2.22):

```
C      NUMERICAL SOLUTION OF THE DIFFERENTIAL EQUATION WITH
C         KRUSKAL-SZEKERES COORDINATES FOR THE CONSTANT
C      K-SURFACES HERE m=1/2, dv/du = (Av+Eu)/(Au+Ev)
C      E=H-Kr**3/3, A**2 = E**2 + r(r-2m), We use  ES=E, AA=A,
C      HS=H(Hamiltonian constant), CS=K(K-surfaces)
       IMPLICIT DOUBLE PRECISION(A-H,O-Z)
       WRITE(*,*)'E= ,','Vi= ,','Ui= '
       READ(*,*)E,V,U
       CALL PROG(E,V,U,X)
       WRITE(*,*)'H= ,','HS= ,','CS= ,','L= ,','N= ,','M= '
       READ(*,*)H,HS,CS,L,N,M
       DO 20 I=L,N
       DO 9 J=1,M
       ES=HS-CS*X*X*X/3.
       AS=ES*ES+X*X*X*(X-1.)
       AA=DSQRT(AS)
       P1=H*(AA*V+ES*U)/(AA*U+ES*V)
    1  P1=-H*(AA*V+ES*U)/(AA*U+ES*V)
       U1=U+0.5*H
       V1=V+0.5*P1
       IF(DABS(U1).EQ.DABS(V1))GO TO 1
       CALL PROG(E,V1,U1,X)
       ES=HS-CS*X*X*X/3.
       AS=ES*ES+X*X*X*(X-1.)
       AA=DSQRT(AS)
       P2=H*(AA*V1+ES*U1)/(AA*U1+ES*V1)
    2  P2=-H*(AA*V1+ES*U1)/(AA*U1+ES*V1)
       U2=U1
       V2=V+0.5*P2
       IF(DABS(U2).EQ.DABS(V2))GO TO 2
       CALL PROG(E,V2,U2,X)
       ES=HS-CS*X*X*X/3.
       AS=ES*ES+X*X*X*(X-1.)
       AA=DSQRT(AS)
       P3=H*(AA*V2+ES*U2)/(AA*U2+ES*V2)
    3  P3=-H*(AA*V2+ES*U2)/(AA*U2+ES*V2)
       U3=U+H
       V3=V+P3
       IF(DABS(U3).EQ.DABS(V3))GO TO 3
       CALL PROG(E,V3,U3,X)
       ES=HS-CS*X*X*X/3.
```

```
      AS=ES*ES+X*X*X*(X-1.)
      AA=DSQRT(AS)
      P4=H*(AA*V3+ES*U3)/(AA*U3+ES*V3)
    4 P4=-H*(AA*V3+ES*U3)/(AA*U3+ES*V3)
      U=U+H
      V=V+(P1+2.*P2+2.*P3+P4)/6.
      IF(DABS(U).EQ.DABS(V))GO TO 4
      CALL PROG(E,V,U,X)
    9 CONTINUE
      K=M*I+1
      WRITE(*,10)K,U,V,X
   10 FORMAT(I8,E18.10,2X,E18.10,2X,E18.10)
   20 CONTINUE
      STOP
      END
```

The subroutine program was the same as used in, program one, Appendix A.

APPENDIX C

For the quantisation on the γN-hypersurfaces we again used the procedure given in Appendix A to solve Eq.(3.5.9). The modification in the program was that here we solve only one differential equation instead of coupled differential equations. For the one differential equation the program was:

```
C      FREELY FALLING HYPERSURFACES
C      NUMERICAL SOLUTION OF COUPLE DIFFERENTIAL EQUATION
C      (KS) BY USING THE RUNGE-KUTTA METHOD r = R τ = TO
C      m = 1/2, MASS OF THE FIELD = AM, Y = G_lmnω(ρ), X = ρ,
C      Z = dY/dX,
       IMPLICIT DOUBLE PRECISION(A-H,O-Z)
       WRITE(*,*)'TO= ,',',X= '
       READ(*,*)TO,X
       CALL RX(TO,X,R)
       WRITE(*,*)'AM= ,',',L= ,',',M= ,',',K= ,',',Yi= ,',',Zi=
      1,',',H= ,',',N= '
       READ(*,*)AM,L,M,K,Y,Z,H,N
       DO 20 I=1,N
       AT=L*L+M*M+K*K+AM*AM
       W=DSQRT(AT)
       P1=H*Z
       Q1=H*((((AM*AM-W*W)/R)+((L*(L+1.)+(3./16.))/(R*R*R))
      1+((9./16.)/(R*R*R*R)))*Y-((R)**(-3./2.))*Z)
       X1=X+H/2.
       Y1=Y+P1/2.
       Z1=Z+Q1/2.
       CALL RX(TO,X1,R)
       P2=H*Z1
       Q2=H*((((AM*AM-W*W)/R)+((L*(L+1.)+(3./16.))/(R*R*R))
      1+((9./16.)/(R*R*R*R)))*Y1-((R)**(-3./2.))*Z1)
       X2=X1+H
       Y2=Y+P2/2.
       Z2=Z+Q2/2.
       CALL RX(TO,X2,R)
       P3=H*Z2
       Q3=H*((((AM*AM-W*W)/R)+((L*(L+1.)+(3./16.))/(R*R*R))
      1+((9./16.)/(R*R*R*R)))*Y2-((R)**(-3./2.))*Z2)
       X3=X2
       Y3=Y+P3
       Z3=Z+Q3
       CALL RX(TO,X3,R)
       P4=H*Z3
```

```
      Q4=H*((((AM*AM-W*W)/R)+((L*(L+1.)+(3./16.))/(R*R*R))
     1+((9./16.)/(R*R*R*R)))*Y3-((R)**(-3./2.))*Z3)
      X=X+H
      Y=Y+(P1+2.*P2+2.*P3+P4)/6.
      Z=Z+(Q1+2.*Q2+2.*Q3+Q4)/6.
      CALL RX(TO,X,R)
      WRITE(*,10)I,Y
10    FORMAT(1X,I7,1X,D15.8)
20    CONTINUE
      STOP
      END

      SUBROUTINE RX(TO,X,R)
      IMPLICIT DOUBLE PRECISION(A-H,O-Z)
      R1=1.5*(X-TO)
      R=(R1*R1)**(1./3.)
      RETURN
      END
```

REFERENCES

1. A.Pias, *Subtle is the Lord: The Science and Life of Einstein*, (Oxford University Press, 1982).
2. S.A.Fulling, Phys. Rev., *D7*(1973)2850.
3. S.W.Hawking, Nature, London, *248*(1974)30.
4. N.D.Birrell and P.C.W.Davies, *Quantum Fields in curved Space*, (Cambridge Univ. Press, 1982).
5. S.W.Hawking, Commun. Math. Phys., *43*(1975)199.
6. J.D.Bekenstein, Phys. Rev., *D7*(1973)2333.
7. T.Padmanabhan, Class. Quantum Grav., *2*(1985)117.
8. A.Qadir, *Proc. Second Chittagong Conference Math. Phys.*, ed. J.N.Islam, (to appear).
9. W.G.Unruh, Phys. Rev., *D10*(1974)3194.
10. P.A.M.Dirac, Phys. Z. Sowjetunion, *3*(1933)64.
11. R.P.Feynmann, Rev. Mod. Phys., *20*(1948)367.
12. G.Denardo and R.Percacci, Nuovo Cimento, *B48*(1978)81; J.R.Letaw and J.D.Pfautsch, Phys. Rev., *D24*(1981)1491; F.Hussain and A.Qadir, ZAMP, *37*(1986)387.
13. R.Penrose, Nuovo Cimento, *1*(1969)252; R.Floyd and R.Penrose, Nature, *229*(1971)177.
14. H.B.G.Casimir, *Proc. Kon. Ned. Akad. Wetenschap*, 5(1948)793.
15. C.W.Misner, Private Communication to W.Press and S.Teukolsky [see W.Press and S.Teukolsky, Nature, *238*(1972)211].

16. Ya B.Zel'dovich, JEPT, *14*(1971)180.

17. A.A.Starobinsky, JEPT, *37*(1973)28.

18. G.W.Gibbons, Commun. Math. Phys., *44*(1975)245.

19. J.R.Letaw and J.D.Pfautsch, Phys. Rev. *D22*(1980)1345.

20. M.D.Kruskal, Phys. Rev., *119*(1960)1743;
G.Szekeres, Publ. Mat. Debrecen, 7(1960)285.

21. A.Pervez and A.Qadir, *Proc. Fourth Regional Conference Math. Phys.*, eds. F.Ardalan H.Arfaei and S.Rouhani (World Scientific, to appear).

22. D.R.Brill, J.M.Cavallo and J.A.Isenberg, J. Math. Phys., *21*(1980)2789.

23. A.Einstein and R.Rosen, Phys. Rev., *48*(1935)73.

24. J.W.York Jr., Phys. Rev. Lett., *28*(1971)1656.

25. A.Goddard, Ph.D. Thesis, (Oxford University, 1975);
Gen. Rel. Grav., *8*(1977)525; Commun. Math. Phys., *54*(1977)279.

26. A.Pervez and A.Qadir, *Proc. Fifth Regional Conference Math. Phys.*, eds. A.Baran and M.Koca (World Scientific, to appear).

27. A.Qadir, *Third Regional Conference Math. Phys.*, eds. F.Hussain and A.Qadir (World Scientific, 1990).

28. A.Qadir and J.Quamar, Europhys. Lett., *2*(1986)423.

29. A.Pervez, *Mini Workshop G.Rel., Astrophys. and Cosm.*, eds. A.Qadir and M.Sharif (Quaid-i-Azam University, Pakistan, 1991).

30. R.Penrose, *Conformal Treatment of Infinity*: in *Relativity, Groups and Topology*, eds. C.D.DeWitt and B.S.DeWitt (Gordon and Breach, New York, 1964).

31. C.W.Misner, K.S.Thorne and J.A.Wheeler, *Gravitation*, (W.H.Freeman, 1973).

32. L.D.Landau and E.M.Lifshitz, *The Classical Theory of Fields*, (Pergamon Press, 1975).

33. E.C.Titchmarsch, *Eigenfunction Expension Associated with Second Order Differential Equations* (Clarendon Oxford, 1962).

34. W.Rindler, Am. J. Phys., *34*(1966) 1174.

35. J.M.Greif, Junior Thesis, (Princeton University, 1969).

36. B.Carter, Nature, *238*(1972)71.

37. D.Christodoulou, Phys. Rev. Lett., *25*(1970)1596; Ph.D. Thesis, (Princeton University, 1971).

38. S.W.Hawking, Phys. Rev. Lett., *26*(1971)1344.

39. S.W.Hawking and G.F.R.Ellis, *The Large Scale Structure of Space-Time*, (Cambridge University Press, 1973); B.Carter, in *Black Holes*, eds. C.M.DeWitt and B.S.DeWitt, (Gordon and Breach, New York, 1973).

40. B.S.DeWitt, Phys. Rep., *C19*(1975)297; R.Penrose, in *G. Relativity: An Einstein Centenary Survey*, eds. S.W.Hawking and W.Israel (Cambridge University Press, 1979).

41. A.Qadir and W.A.Syed, Phys. Lett. *B84*(1979)189.

42. D.Eardley and L.Smarr, Phys. Rev., *D19*(1979)2239.

43. S.M.Mahajan, A.Qadir and P.M.Valanju, IL Nuovo Cimento, *B17*(1982)265;
A.Qadir and J.Quamar, *Proc. Third Marcel Grossmann Meeting Gen. Rel.*, ed. Hu Ning, (North-Holland, 1983);
J.Quamar, Ph.D. Thesis, (QAU Pakistan, 1983);
A.Qadir, In *M.A.B. Bég, Memorial volume*, eds. by A.Ali and P.Hoodbhoy, (World Scientific, 1991).

44. A.Pervez and A.Qadir, preprints QAUM-93/72

45. A.Qadir and J.A.Wheeler, Nucl. Phys. B, *Proc. Suppl.*, eds. Y.S.Kim and W.W. Zachary, *6*(1989)345-348;
A.Qadir, *Proc. Fifth Marcel Grossman Meeting*, eds D.G.Blair and M.J.Buckinghum, (World Scientific, 1989);
A.Qadir, *Proc. Third National Symposium on Frontiers in Physics*, eds. G.Murtaza and F.Khawaja, (Quaid-i-Azam University, 1990).

46. J.F.Corum, J. Math. Phys. *18*(1977)770; J. Math. Phys. *21*(1980)2260.

47. G.Lemaitre, Ass. Soc. Sci. Bruxelles *A53*(1933)51.

48. R.Penrose, *Confrontation of Cosmological Theories with Observational data*, ed. M.S.Longair (D.Riedel, 1974).

49. A.Qadir and J.A.Wheeler, *From Su(3) to Gravity*, eds. E.S.Gotsman and G.Tanber, (Cambridge University, 1985).